TRACKING PREHISTORIC CASCADIA TSUNAMI DEPOSITS AT NESTUCCA BAY, OREGON

Final Technical Report

U.S. Geological Survey Award No. 08HQGR0076

November 2009

By

Robert C. Witter, Eileen Hemphill-Haley, Roger Hart and Lindsey Gay

Oregon Department of Geology and Mineral Industries
Coastal Field Office, 313 SW 2nd, Suite D
Newport, Oregon 97365

FINAL TECHNICAL REPORT

TRACKING PREHISTORIC CASCADIA TSUNAMI DEPOSITS AT NESTUCCA BAY, OREGON

Recipient:
Oregon Department of Geology and Mineral Industries
800 NE Oregon Street, Suite 965, Portland, OR 97232
Phone: 971-673-1544; Fax: 971-673-1562

Principal Investigator:
Robert C. Witter[1]

With Contributions By:
Eileen Hemphill-Haley[2], Roger Hart[1] and Lindsey Gay[1]

[1]Oregon Department of Geology and Mineral Industries, Newport Field Office
313 SW 2nd Street, Suite D, Newport, Oregon 97365
Phone: 541-574-6642; Fax 541-265-5241
email: rob.witter@dogami.state.or.us

[2]Consulting Micropaleontology
1871 Pickett Road, McKinleyville, CA 95519
Phone: 707-840-9554

Keywords:
Paleoseismology, Tsunamis, Cascadia subduction zone

Program Elements I and II

U.S. Geological Survey
National Earthquake Hazards Reduction Program
Award No. 08HQGR0076

November 4, 2009

Research supported by U.S. Geological Survey (USGS), Department of Interior, under USGS award number 08HQGR0076. The views and conclusions contained in this document are those of the authors and should not be interpreted as necessarily representing the official policies, either expressed or implied, of the U.S. Government.

AWARD NO. 08HQGR0076

TRACKING PREHISTORIC CASCADIA TSUNAMI DEPOSITS AT NESTUCCA BAY, OREGON

Principal Investigator:
Robert C. Witter

With Contributions By:
Eileen Hemphill-Haley, Roger Hart and Lindsey Gay

ABSTRACT

Three tsunamis triggered by great earthquakes on the Cascadia subduction zone have inundated Nestucca Bay, Oregon over the past 2000 years. The primary evidence includes layers of sandy sediment deposited by the waves that bury tidal marshes submerged by earthquake-related subsidence. Additional tsunami evidence includes: the spatial extent of sandy deposits, clear trends in deposit thickness and mean particle size that both decrease with increasing distance inland, the presence of brackish-marine diatoms within the deposit and the observation of normal grading in layers within each deposit. ^{14}C age ranges for the youngest tsunami sand span the date of the most recent Cascadia earthquake and tsunami in 1700. Sediment cores and a single tidal outcrop define the spatial limit of the 1700 tsunami deposit, which extended at least 4.4 km landward from the Pacific Ocean at the present mouth of the bay. The widespread extent of the deposits – over 4.4 km inland – makes storm surges, and waves superimposed on them, an unlikely explanation. Similar physical attributes of beach and dune sand that indicate an ocean-ward source preclude river flooding as another alternative mechanism for sand emplacement.

Two older sandy deposits record tsunamis that inundated the bay about about 1.2 ka and 1.6 ka – times that correspond to widespread evidence for great Cascadia earthquakes and tsunamis recorded regionally. Both deposits meet multiple criteria used to infer a tsunami origin, although the physical properties of the sand resembled sediment from the sandy flats of the Little Nestucca River rather than beach or dune sand over 5.5 km away. The physical characteristics of the sandy layers studied here suggest that tsunami deposits reflect sediment sources along its flow path.

The stratigraphic record of great Cascadia earthquakes and tsunamis at Nestucca Bay over the past 2000 years is probably incomplete. Some less distinctive buried marsh deposits that lack continuous overlying sandy deposits likely reflect small changes in relative sea level that can be explained by a variety of coastal processes.

We recommend using the spatial distribution of the 1700 Cascadia tsunami deposit to empirically validate numerical tsunami simulations used to develop tsunami mitigation products. Comparisons between empirical and model data should account for differences in topography, tide level and other factors where possible to reduce uncertainty. Further investigation of the Martella Ranch site may preserve additional evidence of flooding during the most recent tsunami.

TABLE OF CONTENTS

LIST OF TABLES

LIST OF FIGURES

preferred ages for contacts N1, N3 and N4, rounded to the nearest hundred years, based on calibrated ^{14}C ages in Table 1. Core elevations determined by RTK GPS survey have <2 cm vertical error. We infer compaction of ~0.6 m lowered the north pasture, located behind large engineered levees that bar tidal flooding. MLLW, mean lower low water tidal datum estimated from tide gage data for the Little Nestucca River.

Figure 5 Simplified stratigraphic profile correlating mud-over-peat or sand-over-peat contacts inferred to reflect sudden rises in relative sea level in cores along the "Saltmarsh transect" in the Nestucca Bay Refuge (Fig. 3). Vertical axis depicts depth, in meters, from the surface.

Figure 6 Photographs of 5-cm diameter sediment cores and an outcrop exposure showing sharp lithologic contacts inferred to record the 1700 Cascadia earthquake and tsunami at Nestucca Bay. Scales to right of cores in cm and inches. Stem bases from sharp contacts in both cores and the outcrop limit the time of submergence to <300 years before 1950 (Table 1), which is consistent with regional evidence for the 1700 Cascadia earthquake and tsunami. (A) Sand-over-peaty-mud contact at ~112 cm depth in core ND-B near the "Nestucca Duck" site studied by Darienzo (1991). *T. maritima* stems rooted in the peaty mud below the sharp contact are entombed in the overlying sand, suggesting the plants were killed by sudden burial. Detrital debris layers overlying sandy sediment has been cited as a common attribute of some tsunami deposits (Peters et al., 2007; Witter, 2008). (B) Contact N1 exposed in outcrop at the northern end of the Upton Slough transect (Figs. 3 and 4). Vertical tape in photo is about 0.8 m. (C) Contact N1 lacks a sandy overlying deposit in core 6 and instead is marked by peaty-mud-over-peat at 73.5 cm depth. *T. maritima* stems and rhizomes were rooted in peaty sediment overlying the contact.

Figure 7 Sharp lithologic contacts (contact N4) in six cores from Upton Slough inferred to mark coseismic subsidence and tsunami deposition caused by a Cascadia earthquake that occurred approximately 1.2 ka.

Figure 8 Sharp lithologic contacts (contact N5) in six cores from Upton Slough inferred to mark coseismic subsidence and tsunami deposition caused by a Cascadia earthquake that occurred approximately 1.6 ka.

Figure 9 Intertidal stratigraphic sequences in five cores from the Upton Slough transect shown in Fig. 4. Dashed gray lines correlate sharp mud-over-peat or sand-over-peat contacts, numbered N1 to N7, inferred to reflect sudden episodes of relative sea level rise caused by coseismic subsidence during great Cascadia earthquakes. Sandy sediment overlying peaty tidal deposits are interpreted to record sediment transported by tsunamis. Bold numbers indicate preferred ages for contacts N3 and N4 based on calibrated ^{14}C ages in Table 1. Contacts N3, N6 and N7, evident in core 33, were not observed in all cores. MLLW, mean lower low water tidal datum estimated from tide gage data for the Little Nestucca River.

Figure 10 Frequency of diatom taxa, grouped by inferred paleoenvironment, from analyses of 9 samples from a 5-cm-diameter Russian-type sampler at core 25 along Upton Slough. Diatom frequency

is expressed as a percentage of total diatoms counted in each sample (Appendix A). Numbers in far right column correspond tot characteristics of diatoms in tsunami samples as compared to non-tsunami samples listed in Table 3. The depths of contacts N4 and N5 in the Russian-type core were 10 to 20 mm deeper than contacts observed in gouge cores used to construct Fig. 9. Photograph of Russian-type core at left.

Figure 11 Frequency of diatom taxa, grouped by inferred paleoenvironment, from analyses of 11 samples from a 5-cm-diameter Russian-type sampler at core 33 along Upton Slough. Diatom frequency is expressed as a percentage of total diatoms counted in each sample (Appendix A). Numbers in far right column correspond tot characteristics of diatoms in tsunami samples as compared to non-tsunami samples listed in Table 3. The depth of contacts N4 and N5 in the Russian-type core were approximately 10 mm deeper than the same contacts observed in gouge cores used to construct Fig. 9. Photograph of Russian-type core at left; core lithology as in Fig. 10.

Figure 12 Frequency of diatom taxa, grouped by inferred paleoenvironment, from analyses of 9 samples from a 5-cm-diameter Russian-type sampler at core 33 along Upton Slough. Diatom frequency is expressed as a percentage of total diatoms counted in each sample (Appendix A). Numbers in far right column correspond tot characteristics of diatoms in tsunami samples as compared to non-tsunami samples listed in Table 3. The depths of contacts N6 and N7 in the Russian-type core differed by <20 mm compared to contacts observed in gouge cores used to construct Fig. 9. Photograph of Russian-type core at left; core lithology as in Fig. 10.

Figure 13 Particle size (μm) analyses by volume percent for selected samples of sandy sediment from surface sites and cores in the Nestucca Bay area. (A) Size distributions for sandy deposits overlying contact N1 come from two cores and an outcrop on the western margin of the Little Nestucca River (LN-02). Results indicate mean particle size of the deposits decreases inland. (B) Size distributions for sandy deposits overlying contact N4 come from 5 cores along Upton Slough. (C) Size distributions for sandy deposits overlying contact N5 come from 3 cores along Upton Slough. (D) Particle size analyses for samples of sandy sediment from the beach (NS-1, NESK-P1), dune (NS-2) and the western channel margin of the Little Nestucca River (LN-01) provide a basis for comparison with samples from outcrop and cores. Analyses of mud sampled from core 5 (Upton-05) provide particle size data for sediment deposited in a muddy tidal flat.

Figure 14 (A) Mean particle size versus distance from the Little Nestucca River channel for the N4 and N5 sandy layers. In both cases, sandy layers become finer grained with increasing distance from the river channel. Mean particle size of sandy sediment from the Little Nestucca River channel (open diamond) for comparison. (B) Sand layer thickness versus distance from the Little Nestucca River channel for the N4 and N5 sand layers as revealed in cores at Upton Slough (Fig. 4).

Figure 15 Frequency of constituent grains in sandy sediment from cores, outcrop and surficial deposits around Nestucca Bay. Samples are arranged vertically according to sample site proximity to the beach: samples at the top of the list are beach samples; samples at the bottom of the list are far

from the beach. Analyses of sandy layers from cores are arranged vertically from north (top) to south (bottom). In general, quartz and mica sand components increased with increasing distance from the beach. We found no mica in samples of either beach or dune sand. Beach, dune and river channel sediment had higher components of dark sand grains relative to sandy layers in cores far from the beach.

Figure 16 Selected photographs of sand grains under 3.5x and 10x magnification using a petrographic microscope. (A and B) Examples of well-rounded beach (NS-1) and dune (NS-2) sand. Conspicuous pyroxene (p) and rock fragments (f) are visible in sample NS-2. (C) Sand sampled from the Nestucca River is subrounded. (D) Very fine, predominantly angular sand from the Little Nestucca River channel near Upton Slough contains rare larger (>300 μm) rounded quartz grains (r) probably redeposited by tidal currents. (E and F) Samples of sand above contact N1 from cores close to river channels contain rounded quartz grains (r), although they are more abundant in sample ND-B and rare in sample LN-02. A rounded pyroxene (p) occurs in sample ND-B and a mica (m) grain is visible in sample LN-02. (G) Rare, subrounded (r) quartz grains were identified in sand overlying contact N5 in core 6. (H and I) Sand overlying contact N4 lacks rounded grains and consists of abundant angular quartz grains and rare rock fragments (f). Note change in scale, lower right of photos.

Figure 17 Comparison of calibrated ^{14}C ages and coastal evidence for great Cascadia earthquakes and tsunamis over the last two millennia at seven sites in southwestern Washington and northwestern Oregon (modified from Nelson et al., 2004). Black rectangles represent ages for offshore turbidite deposits inferred to record strong shaking during prehistoric Cascadia earthquakes (Goldfinger et al., 2009). Arrows indicate maximum limiting ^{14}C ages based on dates of detrital plant fossils and herbaceous stems rooted in marsh sediment. Ages for evidence at sites in southwestern Washington are from Atwater et al. (Atwater et al., 2003). Ages from coastal sites in Oregon come from Cannon Beach (Witter, 2008), Netarts Bay (Darienzo et al., 1994; Nelson et al., 1995; Shennan et al., 1998), Salmon River (Nelson et al., 2004; Nelson et al., 1995), and South Slough near Coos Bay (Nelson et al., 1998; Nelson et al., 1996). Local evidence for earthquake-related subsidence is lacking for one or more stratigraphic contacts at Cannon Beach, Netarts Bay and Coos Bay (e.g., Shennan et al., 1998).

LIST OF APPENDICES

INTRODUCTION

Tsunamis excited by future great earthquakes on the Cascadia subduction zone threaten coastal communities, port facilities and lifelines along the Pacific Northwest coast of the U.S. Since the devastating 2004 Indian Ocean tsunami, State and Federal agencies have refocused attention on characterizing tsunami sources capable of producing damaging tsunamis within reach of U.S. shorelines (Tsunami Warning and Education Act, 2006). Paleoseismology has contributed crucial information toward improving earthquake tsunami source models, including estimates on earthquake magnitude, recurrence interval and rupture length (Atwater et al., 2003; Kelsey et al., 2005; Goldfinger et al., 2009), among other key parameters (Fig. 1). Collaborative modeling exercises are underway (e.g., Priest et al., 2009) that use inputs from tsunami source studies to run simulations of potential tsunami inundation for the purpose of mitigating risk to save lives and reduce property losses. Increasingly, studies of paleotsunami evidence are being used to empirically validate the results of numerical tsunami simulations (Witter, 2008).

This investigation examines the evidence for tsunami inundation, generated by great earthquakes on the Cascadia plate boundary, at Nestucca Bay in Tillamook County, Oregon (Fig. 2). We start from observations by Darienzo (1991) who interpreted sandy layers in sediment beneath tidal marshes and pastures along the Little Nestucca River as potential tsunami deposits that extended 3.5 to 4.5 km inland. The focus of earlier investigations often selected sites near the axis of the river valley where strong currents produced by tsunami outflow and daily tidal flooding may have reworked and erased evidence of tsunami inundation. As a result, earlier studies provided only fragmentary evidence of tsunami deposits and the total extent of inundation remained uncertain. The purpose of this study is to evaluate evidence for tsunami deposition and map the landward extent of the deposits. This report summarizes investigations of more protected settings along the distal margins of the bay, far removed from the main trunk channels, where conditions favored the preservation of sandy deposits left by the AD 1700 tsunami and older tsunamis produced by great Cascadia earthquakes within the past 2000 years.

IDENTIFYING CASCADIA TSUNAMI DEPOSITS AT NESTUCCA BAY

Nestucca Bay, an estuary on the north-central Oregon coast covering approximately 445 hectares, lies at the confluence of the Nestucca and Little Nestucca Rivers that together drain a watershed encompassing 834 sq km of rugged Coast Range forests and agricultural land along river valleys. Tidelands, which cover about half of the estuary (Percy et al., 1974), include broad sandy flats and intertidal salt marshes. Rivers deposit about 54,000 tons of sediment into the bay annually, which has reduced the size of the estuary in the late 20th century (Percy et al., 1974). Maps produced by the U.S. Army Corps of Engineers show a few levees placed to create pasture as early as 1939. By 1952 a more extensive system of flood control structures flanked the entire lower tidal section of the Little Nestucca River. Similar maps show that most of the lower Nestucca River was diked by 1971. A system of levees and tide gates on the north bank of the Little Nestucca River, east of Pacific Coast Highway 101 was removed in 2007 by the U.S. Fish & Wildlife Service allowing the restoration of 34 hectares (83 acres) of tidal marsh (“Saltmarsh” area in Fig. 3). As a result of extensive levee construction to create pasture along the rivers, compaction

and oxidation has disturbed the upper 0.5 m of stratigraphic sequences that reflect the historically more extensive intertidal marshes surrounding the bay.

We use multiple techniques to distinguish sandy layers left by Cascadia tsunamis from sand deposited by other high energy fluvial and coastal processes. Usually, a number of key sedimentary characteristics are cited to differentiate tsunami deposits from sand layers that record river floods or storm surges (Peters et al., 2003). For instance, the presence of marine or brackish diatoms in the sand layer has been used to rule out a river source for sand (Hemphill-Haley, 1995a). Evidence of landward-directed flow, distinctive sand composition and texture and geochemical indicators also have been used to infer a marine rather than a river source for sand deposits (e.g., Atwater, 1987; Atwater and Hemphill-Haley, 1997; Benson et al., 1997; Darienzo, 1991). Distinguishing tsunami deposits from storm-related deposits is more difficult because both reflect a marine source. However, geologic studies of deposits resulting from both processes suggest that tsunamis leave deposits over much broader areas than the localized overwash fans deposited by storm surges that overtop barrier spits and dunes (Tuttle et al., 2004). Sedimentary characteristics also differ. Tsunami deposits frequently include multiple, thick (decimeters) normally graded beds of sand deposited out of suspension possibly from successive giant waves; whereas storm deposits often consist of thinner, cross-laminated deposits with bedform structures that reflect entrainment processes (Nelson and Leclair, 2006; Tuttle et al., 2004). Finally, linking a sand layer to evidence of earthquake-related deformation has also been used to build a case for tsunami as the best explanation for sand deposits (Atwater, 1987).

Lithostratigraphy

We examined stratigraphy to evaluate evidence for widespread tsunami deposits overlying buried tidal marsh soils subsided by great Cascadia earthquake at 57 locations across five sites using a hand-driven gouge core (1-m long, 2.5-cm diameter), at 7 sites using a Russian-peat auger (0.5-m long, 5-cm diameter) and at two additional river-bank outcrops (Fig. 2). Field investigations focused on the distal margins of Nestucca Bay with the objective of exploring the lateral extent of buried peaty horizons and sandy layers identified by Darienzo (1991) and Darienzo et al. (1994) and interpreted as evidence for tsunamis generated by Cascadia subduction zone earthquakes. Of the five areas investigated, including Horn Creek, Martella Ranch, the “Nestucca Duck” site studied by Darienzo (1991), a restored “Saltmarsh” east of Highway 101, and Upton Slough (Fig. 2), only the latter two sites contain laterally continuous stratigraphy that warranted closer examination within the scope of this study (Fig. 3). The locations and elevations of closely-spaced (25- to 50-m apart) cores along Upton Slough were surveyed using real-time kinematic (RTK) global positioning system (GPS) referenced to the North American Vertical Datum of 1988 (NAVD 88). Profiles of stratigraphic sequences along Upton Slough (Fig. 4) and beneath the Saltmarsh site (Fig. 5) illustrate the lateral continuity of sharp, sand-over-peat contacts evaluated to assess the inland extent of tsunami inundation.

A key relationship often cited as evidence for tsunami inundation in Oregon estuaries is the coincidence of sandy deposits overlying sharp upper contacts of submerged tidal marsh horizons inferred to reflect regional subsidence during Cascadia earthquakes (Darienzo and Peterson, 1990; Darienzo et al., 1994; Nelson et al., 1996; Witter et al., 2003). Therefore, to substantiate the case for earthquake-related subsidence, we consider four additional criteria when evaluating the process that submerged peaty horizons overlain by sandy or muddy intertidal sediment: the suddenness of submergence; the amount of

submergence; the lateral extent of submerged tidal marsh horizons; and the synchroneity of submergence with regional evidence for earthquakes at widely spaced sites (Nelson et al., 1996). Although 8 submerged tidal marsh horizons (contacts N1-N8) were identified in the Upton Slough profile (Fig. 4), only 3 possessed sharp, laterally continuous upper contacts consistent with coseismic subsidence. Examples of these contacts (N1, N4 and N5) are shown in Figs. 6-8. We classify field descriptions of lithologic contacts as "sharp" (<3 mm), "clear" (3-10 mm), and "gradual" (>10 mm). Stratigraphic sequences correlated in 5 cores along Upton Slough illustrate the thickness, lateral continuity and extent of sandy deposits that sharply overlie buried tidal marshes located over 5.5 km from the present mouth of Nestucca Bay (Fig. 9).

Biostratigraphic Evidence of Submergence and Tsunami Inundation

Vertical deformation during great plate-boundary earthquakes causes regional subsidence of the Cascadia coast, allowing tidal flooding to drown low-lying wetlands and uplands fringing estuaries and rapidly deposit mud or sandy sediment that typically leaves a sharp lithologic contact in the stratigraphic record (Nelson et al., 2004). Because plant communities, including microscopic diatoms, respond to changes in salinity and tidal inundation, regional subsidence that produces sudden and lasting submergence may be recorded by changes in fossil diatom assemblages in marsh stratigraphy (Hemphill-Haley, 1995a). We infer submergence across lithologic contacts from diatom analyses of two cores from Upton Slough.

Fossil diatoms also have been used to infer Cascadia tsunamis as the source of sandy deposits in coastal wetlands and lakes (Hemphill-Haley, 1996). For example, diatoms indicative of sandy intertidal and subtidal sediments identified the source of tsunami-lain sand deposited above a forest soil subsided by the AD 1700 earthquake at the Copalis River in southwestern Washington (Atwater, 1992). Similarly, diatom analyses showed that tsunami deposits studied along the Niawiakum River originated from the sandy tidal flats of Willapa Bay (Hemphill-Haley, 1995a). The superior preservation of the fossils in the sand indicates rapid burial of a modern diatom assemblage that was transported inland rather than reworking of older deposits by the river (Atwater and Hemphill-Haley, 1997). Also, diatoms proved useful for mapping the inland extent of the tsunami deposit by establishing a seaward source for fine-grained sediment where sandy laminae were not observed. Finally, Hemphill-Haley (1996) emphasizes that analysis of fossil diatoms works particularly well in freshwater environments like the fringing marshes of the Nestucca River estuary because brackish-marine diatoms present in the tsunami sand stand out in striking contrast to freshwater diatom assemblages in the host sediment.

Our approach groups fossil diatom taxa into three ecological categories: (1) fresh or fresh-brackish diatoms found in freshwater marshes, swamps, or bogs; (2) brackish-fresh (oligohalobous) diatoms capable of tolerating a wide range of salinities, which include salt marsh taxa capable of withstanding subaerial exposure; and (3) brackish-marine or marine diatoms that include taxa common in lower intertidal and subtidal settings as well as coastal marine environments. Individual taxa included in these groups are listed in Appendix A. Diatom data also are assigned to general paleoenvironmental groups from which we infer the likely depositional setting of each sediment sample (Figs. 10-12). These paleoenvironmental designations are based on published and unpublished empirical data showing the preferences for some taxa to thrive in certain environmental settings in the Pacific Northwest (McIntire and Overton, 1971; Whiting and McIntire, 1985; Hemphill-Haley, 1993a, b; 1995b; 2006; and unpublished data; Nelson and Kashima, 1993; Hemphill-Haley and Lewis, 1995; Nelson et al., 2000;

Sawai and Nagumo, 2003). Six paleoenvironmental groups are identified, including: (1) freshwater marsh or swamp; (2) high salt marsh; (3) low salt marsh; (4) sandy or muddy tidal flat/shallow channel; (5) brackish-marine planktonic or tychoplanktonic; and (6) miscellaneous – not assigned to any empirical group (Appendix A). Sample preparation, diatom identification and counting followed the methods of Hemphill-Haley (1996). More than 100 valves were counted at high magnification (1250x) in addition to the ubiquitous coastal diatom *Paralia sulcata* in each of 20 samples (1 to 2 cc) from core 33 to evaluate the change in paleoenvironment across four sharp contacts (N4-N7) between mud or sandy mud and peat (Figs. 11 and 12). An additional 9 samples were analyzed to examine paleoenvironmental changes across contacts N4 and N5 in core 25 (Fig. 10).

In addition to the high-magnification paleoecological analyses, at least 100 diatoms larger than 40 µm were also counted at low magnification (500x) in mud and sandy mud deposits above mud-over-peat lithologic contacts to identify changes in diatom preservation and occurrences of marine planktonic taxa associated with possible tsunami deposits (Appendix A). Diatom criteria used to differentiate tsunami from non-tsunami deposits include: (1) severe fragmentation of pennate diatoms > 100 µm long; (2) relatively high fragmentation of all diatom valves larger than 40 µm, particularly pennate valves > 40 µm long; (3) relatively higher frequency of coastal marine planktonic and tychoplanktonic taxa; (4) relatively high frequency of exceptionally large (70-150 µm), benthic epipsammic diatoms; (5) relatively high frequency of small epipsammic diatoms, including evidence for enhanced preservation (Figs. 10, 11, 12; Table 3).

Physical Properties of Sandy Sediment

The mineralogy and sedimentary properties of sand can help trace the source and transport path of coastal sediments, including tsunami deposits. The physical attributes of sandy sediments along the Oregon coast – grain mineralogy, particle size distribution, and degree of grain roundness – have been linked to three primary sources: the Columbia River in the north, the many rivers that originate in the Coast Range, and the Klamath Mountains of southern Oregon and northern California (Clemens and Komar, 1988). The present composition of sand on Oregon beaches is considered a relict mixture of multiple sources reflecting longshore transport during the last glacial sea level lowstand. Present-day beach sand compositions do not solely represent the composition of local sources, even though many headlands divide the Oregon coast into independent littoral cells that prevent mixing of different sand sources. Following the methods of Peterson et al. (1982), Darienzo and Peterson (1990) used sand mineralogy and grain roundness to infer a beach source for tsunami deposits discovered at Netarts Bay. Peterson and Darienzo (1996) used similar methods to deduce a marine source for tsunami sand in tidal outcrops of Alsea Bay. In addition to counting the abundance of rounded grains derived from the beach, these studies assessed the relative component of beach versus river sand by determining pyroxene ratios where high hypersthene:augite ratios indicated a prevalence of beach sand and low hypersthene:augite ratios indicated a greater contribution from the river. In a study of patterns of sediment accumulation in Tillamook Bay, Oregon (Komar et al., 2004) used high abundances of quartz and feldspar minerals to infer a beach source versus high percentages of volcanic rock fragments to indicate a river source. The study concluded that the observed increase in the contribution of beach sand with depth reflected sand transported by the AD 1700 tsunami and that tectonic subsidence allowed storm waves to overtop the barrier spit more frequently following the most recent Cascadia earthquake.

In this study we determined particle size distributions for samples of sandy sediment from 7 sediment cores, one river bank outcrop and 5 surface samples from beach, dune and river environments (Fig. 13). We assessed whether or not mean particle size varied as a function of distance from potential sediment sources (Fig. 14). Particle size distributions were determined using a laser diffraction particle size analyzer (Coulter LS 100Q) that measures particle sizes ranging from clay to coarse sand (0.4 to 948 μm). Samples were thoroughly mixed, split and placed in a beaker filled with 40 mL of 30% hydrogen peroxide and 160 mL deionized water. The covered beakers were placed in an oven at 50°C for at least four hours to digest organic material. After digestion, 10 mL of dispersant (Calgon) was added to the sample and allowed to sit overnight. Samples were thoroughly mixed using a reversing-agitator mixer that suspended the sediment in water; aliquots were transferred to the instrument with a wide-bore pipet until obscuration reached 8 to 12%. A minimum of two aliquots were measured for each sample with two analyses for each aliquot to verify reproducible results. The frequency of particles >850 μm was <<1% for the coarsest sands analyzed.

Grains of sandy sediment processed for particle size analysis were dried, mounted on slides and examined with a petrographic microscope at 3.5x and 10x magnification. Analyses counted between 400 and 600 grains per sample to determine the abundance of the following constituents: quartz, white opaque grains (including feldspar), mica, translucent dark grains, translucent green grains, dark opaque grains, and rock fragments. In addition, a significant number (4 to 27%) of grains were coated with iron-oxide staining that precluded a definitive identification, particularly for samples from cores subjected to weathering within the soil profile. The samples were reanalyzed after treatment with a solution of lactic and gluconic acids and surfactants to remove rust, which removed iron-oxide staining principally from quartz grains. Summary plots showing variations in grain mineralogy for all samples are shown in Fig. 15. Selected photographs of magnified grains provide a qualitative assessment of the variation in grain roundness (Fig. 16).

Synchroneity with Regional Earthquake Records Inferred From ^{14}C Ages

Conifer needles, moss, herbaceous seeds and other identifiable plant remains entombed in sandy deposits were submitted to Beta Analytic Inc. for radiocarbon dating using the accelerator mass spectrometry (AMS) technique (Table 1). The plant fossils were sieved using a 1-mm mesh, cleaned of all sediment and young rootlets, rinsed with water and air dried. With the exception of three samples discussed below, the detrital material dated likely died before deposition. Therefore, lab-reported conventional radiocarbon ages on detrital plant fossils, calibrated using the computer program Calib Rev 5.0.1 (Stuiver and Reimer, 1993) and the IntCal04 calibration dataset of Reimer et al. (2004), provide maximum-limiting estimates of the time of sand deposition (Table 1). Three samples came from plants rooted in peaty sediment below contact N1 and buried by overlying sand, including two woody stem bases from *T. maritima*, that probably provide a closely-limiting event age.

Despite the care with which samples have been selected and the relatively narrow ranges (±35 to ±150 years) of the calibrated ^{14}C ages reported here, correlations with Cascadia earthquake chronologies at other sites remain uncertain (Fig. 17). With the exception of the January 26, 1700 Cascadia earthquake and tsunami (Satake et al., 1996; Satake et al., 2003), broadly overlapping ages for older events leave open the possibility that a series of earthquakes ruptured the subduction zone within decades – a time interval too short to resolve with AMS or tree-ring based ^{14}C ages (Nelson, 1992; Nelson et al., 1995).

However, if earthquakes release strain accrued over hundreds of years rupturing patches of the plate-boundary hundreds of kilometers in length, then precisely dated paleoseismic evidence limits alternative correlations (e.g.,Nelson et al., 2004; Nelson et al., 2006; Witter et al., 2003).

YOUNGEST SANDY DEPOSIT

The youngest sand-over-peat contact preserved beneath tidal marshes surrounding Nestucca Bay was first examined by Darienzo (1991) at a site named "Nestucca Duck," which is located northeast of the bay, landward of the widest part of Nestucca Spit (Fig. 2). According to Darienzo et al. (1994), the site possessed "the most convincing evidence for coseismic subsidence [and] tsunami deposition." Some of the evidence supporting their interpretation included: (1) rapid transition from peat to overlying sand and mud; (2) the presence of *T. maritima* rhizomes implying submergence; (3) an increase in the component of beach sand across the contact; (4) lateral continuity of the contact over 300 m; and (5) a radiocarbon date of 400 ± 60 radiocarbon years before 1950, which overlaps ages of the youngest event at other estuaries. In 2009 we revisited the "Nestucca Duck" site (core ND-B; Fig. 2) to verify the age of the contact, examine the stratigraphic context of the youngest sand layer (Fig. 6) and collect sand samples for particle size and mineralogy analyses. Of the four other sites we investigated in the bay's upper reaches, only one, an outcrop 2.4 km to the south near Upton Slough (LN-2; Figs. 2 and 6), preserved a sandy deposit with sufficient evidence to support correlation with the youngest sand layer identified by Darienzo (1991).

Evidence for Sudden Change over a Wide Area

Contact N1 separates peaty sediment from overlying sandy sediment at the "Nestucca Duck" site and in an outcrop investigated near Upton Sough (Fig. 6) and exhibits two of the key criteria consistent with coseismic subsidence during a great Cascadia subduction zone earthquake (Nelson et al., 1996). In most cores we examined and at outcrop LN-2 contact N1 is sharp (<3 mm). Our observations corroborate the description by Darienzo et al. (1994) of a "rapid transition" between peat and overlying sand. In addition, at both the "Nestucca Duck" site and the outcrop *Triglochin maritima* stems rooted in peaty sediment were smothered by overlying sand suggesting rapid burial (Fig. 6A and B). In contrast, the contact is clear (3-10 mm) in core 6 near Upton Slough between very fine sandy mud that buries peat (Fig. 6C).

Extensive levees have modified and obscure tidal outcrops preventing a more thorough survey of the extent of the N1 sand deposit. Darienzo (1991) established the minimum extent of the contact encountered in cores spanning 300 m at the "Nestucca Duck" site. If the "Nestucca Duck" sand layer correlates with sandy mud above contact N1 at the LN-2 outcrop, then the minimum lateral extent increases to 2.5 km. The actual extent of the youngest contact may have been greater prior to diking to create pasture in the early-to-mid-20th century. Levees have impeded daily tidal inundation and annual river flooding and reduced silt deposition on the pastures. In addition, cattle grazing, plowing, excavation of ditches and farm machinery have compacted, dewatered and oxidized the soils. As a result, the elevation of pastures has dropped by as much as 0.6 m (Fig. 4) and stratigraphic sequences with the upper 0.5 m have been severely altered or in some places destroyed. Faint soil A-horizons and discontinuous sandy lamina within this zone of disturbance, shown in Fig. 4, lacked sharp contacts and other distinctive features needed to extend correlation of contact N1 further south.

Lithologic Evidence of Submergence

Sparsely rooted mud overlying contact N1 at the "Nestucca Duck" site implies sudden submergence, but this study collected little data to substantiate a precise estimate of the amount of sea level rise. If the abundant stems and rhizomes of growth position *Triglochin maritima* in peaty mud below the contact reflect low marsh conditions (Fig. 6A) then the transition to overlying mud suggests submergence to the elevation of a tidal flat. Similar lithologic changes at the LN-2 outcrop indicate sudden submergence but do not necessarily support 1 to 1.5 m of subsidence estimated by Darienzo et al. (1994) on the basis of the presence of *Triglochin maritima* in tidal flat mud overlying low to high marsh peat. Fortunately, Hawkes et al. (2008) estimated 0.8 ± 0.3 m of submergence using a statistical transfer function derived from changes in fossil foraminifera across the sharp upper contact of a buried, high-marsh peat correlative with contact N1 at the Nestucca Duck site.

Physical Properties of Sandy Sediment

The physical properties of the youngest sand layer preserved at Nestucca Bay suggest an oceanward source. Using the ratio of hypersthene to augite minerals, Darienzo (1991) inferred an increase in the beach component of sand deposited on contact N1 at the "Nestucca Duck" site. We also identified several attributes of the sand sampled from core ND-B that are similar to beach and dune sand on Nestucca Spit. Particle size analyses indicate the deposit consists chiefly of fine to medium sand (200 to 300 μm; sample ND-B; Fig. 13A), which overlaps the fine tail of the grain size distributions for both beach and dune sand from the Nestucca Spit (Fig. 13D). From visual inspection of cores at the "Nestucca Duck" site sediment grain size appeared to fine upward suggesting the deposit is normally graded. Also, like beach and dune sand, sample ND-B contained a moderate abundance of subrounded to rounded quartz and pyroxene grains (Fig. 16F). The sand is depleted in mica and contains >10% dark grains, also consistent with the mineralogy of beach and dune sands.

In contrast, sandy deposits above contact N1 further inland are predominantly very fine to fine sand (Fig. 13A) and display particle size distributions that more closely resemble the texture of channel sediment from the Little Nestucca River (Fig. 13D). Mineral abundances in the sand samples also were similar to river channel sediment, notably the presence of mica (Fig. 15). Although N1 sand from core 6 and outcrop LN-2 contained some subrounded quartz grains (Fig. 16E and 16G) so, too, did sand from the river channel (Fig. 16F). More striking was the preponderance of subangular to angular grains in these samples. Finally, the mean particle size of the N1 sand decreases inland from 169 μm at "Nestucca Duck" to <50 μm at core 6, 2.4 km to the south (Table 2).

Synchroneity with Regional Earthquake Chronologies

Three ages on herbaceous stem bases rooted in peaty sediment below contact N1 provide nearly identical estimates of the time of marsh submergence <300 cal yr BP (Table 1). The woody stems of *Triglochin maritima* submitted for ^{14}C dating were rooted within a few centimeters below the contact at both the "Nestucca Duck" site and outcrop LN-2. The plants likely were killed by submergence. A stem base or rhizome from an unidentified vascular plant rooted in peat a few centimeters below contact N1 in core 6 also may be the fossil remains of a plant killed by the event. All three ages are consistent with regional

evidence for the most recent Cascadia earthquake and tsunami, which has been precisely dated to January 26, 1700 from tsunami records in Japan (Satake et al., 1996; Satake et al., 2003).

OLDER SANDY DEPOSITS

Investigations along Upton Slough and at the "Saltmarsh" site (Figs. 4 and 5) identified seven older sharp contacts (N2-N8) placing mud or sandy sediment over peaty horizons. Darienzo (1991) identified an even longer sequence of 12 peaty marsh horizons buried within the last 5700 years at a site on the north bank of the Nestucca River. This section describes two laterally continuous sandy layers overlying contacts N4 and N5 (Figs. 7 and 8) that extend ~5.5 km inland from the point where the present estuary reaches the Pacific Ocean. Ample evidence suggests there are other sharp contacts beneath wetlands surrounding Nestucca Bay that predate the 1700 event, but these contacts are less continuous and generally lack distinctive sandy deposits that aid in mapping tsunami inundation.

Evidence for Sudden Change over a Wide Area

The distinct lithologic contrast and continuity of contacts N4 and N5 satisfy two criteria used to infer submergence caused by Cascadia plate-boundary earthquakes. Most often sandy layers buried peaty sediment across sharp (<3 mm), well-defined contacts indicating a sudden change in depositional environment. A few contacts were clear (3-10 mm) or rarer gradual (>10 mm), but allowed correlation among cores 25 to 50 m apart based on lithology and depth. In addition, both contacts could be correlated in the subsurface for over 1 km along the Upton Slough transect (Fig. 4), which extends over 5.5 km from the present mouth of Nestucca Bay. At the "Saltmarsh" site contacts N4 and N5 were discontinuous, less distinctive and lacked sandy sediment above sharp to clear lower contacts. Buried peaty intervals in cores studied by Darienzo (1991) located on the south bank of the Little Nestucca River east of Highway 101 may correlate with peat layers below contacts N4 and N5; however, there are no intermediately spaced cores to establish a stratigraphic connection. ^{14}C ages reported by Darienzo et al. (1994) further inhibit correlation because the ages are unexpectedly old and in reversed stratigraphic order. However, we believe that further investigations along the south side of the Little Nestucca River valley may reveal buried marshes overlain by sandy deposits that extend further toward the east.

Diatom Evidence of Submergence

Changes in fossil diatom assemblages across contacts N4 and N5 imply that high marsh and fresh water wetland environments dropped to tidal flat or shallow subtidal elevations as a result of sudden submergence. Fossil diatom abundances were analyzed across contacts N4 and N5 in two cores along the Upton Slough transect: core 25 (Fig. 10) and core 33 (Fig. 11). We also examined fossil diatoms in samples across contacts N6 and N7 in core 33 (Fig. 12). This section summarizes the diatom analyses for contacts N4 and N5 that provide evidence of sudden changes in paleoenvironment that suggest submergence as well as deposition by tsunamis. We refer to results from previous studies at Netarts Bay (Shennan et al., 1998) and the Salmon River (Nelson et al., 2004) to infer preliminary estimates of the amount of submergence. Changes in species assemblages across two older contacts (N6 and N7 in core 33) are equivocal making inferences about the amount and suddenness of submergence less conclusive. The complete report for diatom analyses, including taxonomy and frequency data, is attached in Appendix A.

Changes in Diatom Assemblages Across Contact N4

Fossil diatoms present in samples from core 25 indicate a gradual transition upward from a tidal flat environment, to a low marsh environment and finally grading upward into a high marsh environment in the peat below contact N4 (Fig. 10). Lower intertidal taxa, also prominent in the peat, suggest tidal inundation regularly flooded the salt marsh.

Diatoms in the sandy mud and mud above contact N4 in core 25 suggest a transition from a high salt marsh to a tidal flat (Fig. 10). Evidence that the sandy mud was emplaced by a tsunami is supported by 4 of the 5 diatom criteria for differentiating possible tsunami from non-tsunami deposits (Table 3). In addition to severe fragmentation of elongate taxa > 100 µm long, and overall poorer preservation of all taxa larger than 40 µm, relatively abundant and unusually well-preserved benthic tidal flat diatoms in sandy sediment directly above the contact, including diverse small epipsammic species, offer supporting evidence to infer transport and deposition by a tsunami. In addition to abundant occurrences and good preservation of small epipsammic taxa, prominent occurrences of large, robust epipsammic taxa also suggest up-estuary transport from a coastal source.

Fossil diatom assemblages in peat and peaty mud below contact N4 in core 33 also indicate a gradual change from a low salt marsh to a fresh-brackish marsh removed from tidal inundation followed by a shift to a high salt marsh environment (Fig. 11). Diatoms in the peaty mud between 80 and 90 cm depth imply lower intertidal conditions consistent with a low marsh or colonizing tidal flat, but include reworked high marsh material. However, peat sampled at 70 cm in core 33 contains diatoms indicative of a fresh-brackish wetland protected from the influx of salt water. In contrast, diatoms from peat sample directly below contact N4 contains diatoms that can tolerate fluctuating salinities in an estuarine environment, suggesting high salt marsh conditions.

Diatoms in the sandy mud and mud above contact N4 suggest submergence from a high salt marsh to a tidal flat (Fig. 11). Tsunami deposition for the sandy mud above the buried soil is supported by the same 4 diatom criteria as for core 25 (Table 3). In addition, a possible 5th criteria is evidenced by the relatively greater frequency of large planktonic and tychoplanktonic diatoms in the sandy mud, supporting incursion from a marine source.

Changes in Diatom Assemblages Across Contact N5

Evidence for submergence is complicated by the sparse preservation of diatoms in the peat below contact N5 in core 25, but consistent with a change from high salt marsh to a low marsh or tidal flat (Fig. 10). A single sample from the peat contains remnants of brackish diatoms, but unlike typical buried marsh peat, even the sturdier diatom valves are strongly dissolved. Despite sparse preservation (the relative % is based on a total of only 15 diatoms), the few species identified support a brackish rather than freshwater environment, as no freshwater taxa were observed. The unusual condition of the thanatocoenosis (with obviously dissolved, rather than fragmented, diatom valves) indicates that the biogenic silica was leached away. Diatoms will start to dissolve in settings that are undersaturated in silica (interstitial water, lake water, etc.), as well as in alkaline conditions. Andrejko and Cohen (1984) worked on diatoms in peat deposits from the Okefenoke wetlands and found that the activity of organisms will strip the system of available silica, especially for peats that have limited “minerogenic inputs,” but rather only have

atmospheric exposure. We postulate that the sparse preservation of diatoms and apparent dissolution of valves in this sample is a result of silica undersaturation. If this condition is accurate it also suggests that the peat may have been at an elevation above mean higher high water (with infrequent tidal inundation) by the time burial occurred.

The diatom data support tsunami deposition for the sandy mud overlying contact N5 in core 25 (Fig 10; Table 3). In addition to excellent preservation of dominant epipsammic taxa, which suggests rapid redeposition and burial of a modern assemblage (Hemphill-Haley, 1995a, 1996; Sawai et al., 2009), there is evidence for severe fragmentation of larger benthic diatoms and frequent occurrences of large planktonic taxa, which supports turbulent redeposition of material from a marine source, rather than *in situ* accumulation on a sandy tidal flat.

In core 33 (Fig. 11), peat below contact N5 contains fossil diatoms with affinities toward a wet freshwater marsh or swamp. Prominent diatoms include species of *Pinnularia*, *Eunotia*, and *Gomphonema* which are not found in saline environments. A sudden change in environment is indicated by a diatom assemblage consisting dominantly of brackish-marine tidal flat species in the mud capping the peat (Fig. 11). Diatoms in the mud immediately above the peat are diverse but relatively rare, and not well preserved (fragmentation is severe). Species typical of tidal flats and shallow channels are evident, including *Delphineis surirella*, *Synedra fasciculata*, and *Planothidium delicatulum*. Comparable to contact N5 in core 25, the diatom data strongly support tsunami deposition for mud above the peat contact samples at 92.5-93.5 cm and 91-92 cm (Fig. 11, Table 3). Epipsammic diatoms are not as pristine in the muddy deposit in core 33 as in the sandy deposit in core 25, but overall the two deposits can be well correlated based on diatom characteristics.

Changes in Diatom Assemblages Across Contacts N6 and N7

Sharp to clear transitions across contacts N6 and N7 also suggest submergence in cores at the south end of the Upton Slough transect (Fig. 4), although diatom assemblages in the overlying muddy sediment are not as common and well preserved as for contacts N4 and N5.

Diatoms in peat below contact N6 include taxa typical of high marshes (*Cosmioneis pusilla*, *Pinnularia lagerstedtii*), but also include common valves of *Luticola mutica*. *L. mutica* is only moderately helpful as an ecological indicator because it can tolerate a very wide range of salinities, and is often found in fresh as well as brackish areas of estuaries, and on both high and low marshes. Because *L. mutica* is an epiphyte it is often quite abundant on riverbanks and, unlike *C. pusilla* and *P. lagerstedtii*, does not tolerate dry aerophile conditions (in high marshes above MHHW). Together, these diatoms suggest a salt marsh environment regularly inundated by brackish water.

Diatoms in mud at 152 and 150 cm above contact N6 show a transition to a lower intertidal/subtidal brackish marine deposit (Fig. 12). Pertinent taxa include species common on tidal flats (*Nitzschia sigma*, *N. fasciculata*, *Scoliotropis tumida*, *Gyrosigma peisonis*, *Tryblionella* spp.) as well as coastal planktonic/tychoplanktonic species (*Actinoptychus senarius*, *Coscinodiscus* spp., *Thalassionema nitzschioides*). In addition, large valves of *Paralia sulcata* are particularly prominent in this sample (Appendix 1), which further supports a brackish-marine environmental setting.

There is no supporting diatom evidence for tsunami deposition for the mud above contact N6 based on the diatom criteria evident for contacts N4 and N5 (Fig. 12, Table 3; Appendix A). Small epipsammic diatoms are present but not abundant, and there is no evidence for enhanced preservation of small valves from rapid burial (Appendix 1). Further, the occurrences of large, elongate diatom valves (*Gyrosigma)* in the mud are consistent with accumulation on a tidal flat or shallow subtidal zone, but inconsistent with turbulent flow by a tsunami.

Peat below contact N7 contains fossil diatoms indicative of a high marsh environment (Fig. 12). Pertinent taxa include well preserved valves of *Cosmioneis pusilla*, *Nitzschia terrestris*, and *Diadesmis contenta*, all of which reflect aerophile conditions in high salt marshes. Mud with woody debris that buries the peat contains rare large marine planktonic diatoms, and large poorly preserved valves of pennate (benthic) taxa. The assemblages indicate a change from a dry, high marsh to a brackish-marine setting, but the assemblages dominated by relatively large valves are different from typical tidal flat assemblages, and may reflect the effects of winnowing. Weak but possible evidence for the mud sample at 179.5-180.5 cm having been emplaced by a tsunami includes greater fragmentation of pennate diatoms larger than 40 µm and more prominent occurrences of large planktonic marine taxa as compared to samples of mud higher in the core (Table 3).

Peaty mud near 170 cm depth (Fig. 12) contains poorly preserved, fragmented diatoms valves primarily of the same dominant marsh species that comprise the assemblage in peat N6 (*Luticola mutica*, *Cosmioneis pusilla*, and *Pinnulaira lagerstedtii*). Significantly, whereas the marsh diatoms are well preserved in peat N6, the diatoms in the peaty mud and mud are poorly preserved with fragmented valves. The diatom data show that there is a lack of evidence for a stable marsh horizon (with well-preserved, *in situ* diatoms) giving way to a lower intertidal/shallow subtidal environment. Instead, both samples appear to be composed of reworked marsh material.

Physical Properties of Sandy Sediment

Sandy layers overlying contacts N4 and N5 at Upton Slough can be traced in the subsurface for more than 1 km. The physical properties of sandy deposits alone are not diagnostic but when combined with supporting evidence they can be used to build a case for or against a tsunami origin. The physical properties of the sand layers include sediment texture, grading, deposit thickness, lateral extent, grain shape and mineralogy.

The textures of sandy layers overlying contacts N4 and N5 consist of mixtures of fine- to very-fine sand and mud (silt and clay). Mean particle size of sandy deposits on the N4 contact ranged from 89.8 to 41.2 μm (Table 1), in all cases finer than beach, dune and river sediment, but coarser than mud from core 5, which is inferred to represent muddy tidal flat sediment (Fig. 13). Samples of sandy mud overlying contact N5 possessed finer textures with mean particle sizes that ranged from 44.7 to 27.4 (Table 1). Mean particle size of both sandy layers decreased with increasing distance from the Little Nestucca River channel (Fig. 14A). The thickness of the deposits varied greatly in cores along Upton Slough (Fig. 14B) and in some cases no sand was apparent directly above the two contacts. However, in both cases the thickest sandy deposits occurred close to the river channel: an 11-cm-thick layer was observed above contact N4 in core 5 and a 15-cm-thick layer was observed over contact N5 in core 6. Normally graded

layers within sandy deposits were observed in samples above contact N4 in cores 5 and 19 and above contact N5 in core 6 (Table 1).

Mineralogical analyses of the constituent grains in each sample indicate the sandy layers above contacts N4 and N5 have distinctively different compositions from beach, dune and river sand (Fig. 15). In general, the presence of mica, higher quartz abundances and lower numbers of dark grains (e.g., heavy minerals) distinguished the sandy layers in cores along Upton Slough from beach and dune sand. Although samples of channel sand from the Little Nestucca and Nestucca Rivers contained small quantities of mica (<2 %), higher abundances of dark minerals (>12%) differentiated the river samples from sandy deposits overlying sharp contacts in cores. Notably absent or very rare (e.g., Fig. 16I) in nearly all samples were identifiable rock fragments,which were used to differentiate river versus beach sediment sources in a study of Tillamook Bay (Komar et al., 2004).

Other physical properties, including grain shape, evidence of an eroded lower contact, and the presence of rip-up clasts, were not characteristic traits of the N4 and N5 sandy layers. For example, sub rounded grains were rare or absent from most samples with the exception of the N5 sandy layer in core 6 (Fig. 16G). Other samples were dominated by angular to sub-angular grains (e.g., Fig. 16H and 16I). Both contacts appeared to be conformable between mud or sandy-mud over peat without obvious evidence of erosion. Although none were found, all sandy layers deposited above sharp lithologic contacts were examined for the presence of clasts of material that may reflect erosive flows that plucked or ripped up muddy or peaty sediment and incorporated them as clasts in the sandy deposit.

Synchroneity with Regional Earthquake Chronologies

^{14}C age estimates for contacts N4 and N5 come from detrital plant macrofossils picked from sandy beds overlying the contacts or the upper few millimeters of underlying peaty sediment in cores from Upton Slough (Fig. 4). Because the materials selected for dating are detrital – often including conifer needles or cones, moss stems or seeds of herbaceous plants – and likely died before deposition of the sand layer, ^{14}C ages provide a maximum constraint on the time of the event that formed the contact. Assuming stratigraphic correlations are correct, we selected the youngest ^{14}C age from multiple detrital ages on the same contact as the preferred age estimate because the youngest ^{14}C ages probably reflect plant death nearer to the time of the event compared to older ages. For example, the preferred ^{14}C age for contact N4 is 1270-1060 cal yr BP based on analyses of 6 spruce needle fragments, a single herbaceous seed and a delicate moss stem (Table 1). We infer these fossils were deposited within several decades, or probably not more than one hundred years before sandy mud buried marsh peat forming contact N4. Older age estimates for contact N4 on similar materials (Table 1) probably reflect plant death hundreds of years before the event. Similar reasoning supports a preferred age of 1690-1430 cal yr BP for contact N5. The preferred ^{14}C age ranges for contacts N4 and N5 overlap age estimates for great Cascadia earthquakes and tsunamis around 1.2 ka and 1.6 ka inferred from evidence at five other estuaries in southwestern Washington and northwestern Oregon and in submarine channel turbidites (Fig. 17).

A single ^{14}C age from core G shown in the Saltmarsh profile (Fig. 5) provides an estimate for contact N3 of 960-790 cal yr BP. The material dated consisted of twelve, well-preserved conifer needles deposited horizontally on the sharp upper contact of dark brown peaty sediment buried by mud. Although evidence for extensive submergence of peaty horizons with coincident overlying sand deposits is limited in the

stratigraphy beneath the Saltmarsh site, the age for contact N3 overlaps the ranges of age estimates for a great earthquake around 0.8 ka based on evidence at other estuaries in Washington and Oregon and the marine turbidite record (Fig. 17).

HISTORY OF TSUNAMI INUNDATION AT NESTUCCA BAY

Multiple lines of evidence satisfy criteria supporting the interpretation that at least three sandy layers identified in wetland stratigraphic sequences at Nestucca Bay were deposited by tsunamis generated by great plate-boundary earthquakes on the Cascadia subduction zone (Table 4). Although, none of the sandy deposits met all the criteria consistent with a tsunami origin, the preponderance of the evidence favors a tsunami explanation over alternative processes like storm waves, storm surges and river flooding. From the complexity and the limited extent of some lithologic contacts examined in this study, stratigraphic sequences beneath what once were extensive intertidal marshes around Nestucca Bay – now largely converted to pastures – probably represent an incomplete late Holocene record of Cascadia earthquakes and tsunamis. The spatial variability in the extent of sharp lithologic contacts and differences in the physical attributes of sandy deposits suggest a variety of thresholds (e.g.,Nelson et al., 2006) may control the preservation of evidence that records vertical deformation and tsunami flooding that often attends great Cascadia earthquakes.

Youngest Sandy Deposit

The 1700 tsunami reached at least 4.4 km inland, measured from the present mouth of Nestucca Bay, leaving as its trace a clean, fine-to-medium grained sand deposit that buried *Triglochin maritima* growing in lower intertidal marshes. The physical attributes of the sand, including particle size, grain shape and mineralogy, are similar to characteristics exhibited by beach and dune sand directly west of the site. In addition, limited data indicate the texture of the deposit becomes finer in the landward direction based on the mean particle sizes of the three sand samples analyzed (Table 2). These traits suggest the source of the sand came from the direction of the ocean obviating an alternative explanation involving river flooding. The lateral extent of the deposit, which spans at least 2.5 km, rules out storm surges and waves as a viable mechanism for sand deposition (Nelson and Leclair, 2006; Tuttle et al., 2004).

Evidence that the sand was deposited shortly after a Cascadia earthquake is supported by sharp sand-over-peaty mud contacts and evidence for rapid submergence that can be correlated between cores and outcrops over hundreds of meters. The sharp lithologic contacts attest to the suddenness of change in depositional environment. Biostratigraphic data imply that regional subsidence during a Cascadia earthquake raised sea level by 0.8 ± 0.3 m and submerged high salt marshes along the margin of the bay (Hawkes et al., 2008). Three new ^{14}C age estimates for the time of submergence and sand deposition represented by contact N1 are concurrant (<300 cal yr BP) and encompass the time of the most recent Cascadia earthquake and tsunami in 1700.

Older Sandy Deposits

Older tsunamis probably inundated 5.5 km inland or more, but without knowing the configuration of Nestucca Bay at the time of these earlier events it is difficult to accurately reconstruct the extent of inundation. Sandy beds deposited by two tsunamis are associated with sharp, laterally continuous

lithologic contacts (N4 and N5) at Upton Slough that formed about 1.2 ka and 1.6 ka (Fig. 4). The physical attributes of the sandy deposits supporting a tsunami origin include normally graded layers within the deposits (Table 2) and decreases in the thickness and mean particle size of the sandy layers with increasing distance from the probable source: the Little Nestucca River channel. Diatom evidence consistent with tsunami deposition points to a marine or lower estuary source for the sandy layers and rules out river flooding (Table 3). The extensive preservation of sandy layers spanning more than a kilometer along Upton Slough and reaching ~5.5 km inland challenges storm surges and waves as reasonable alternative depositional mechanisms to tsunamis.

Despite a number of features that are consistent with tsunami deposits recognized in other sites along the Cascadia coast (Peters et al., 2007), sandy layers above contacts N4 and N5 lack a few key attributes typical of many tsunami sand layers. For instance, unlike the youngest sand the mineralogy of older sandy layers lends less support for a tsunami origin because the presence of mica, higher abundance of quartz and lower numbers of dark grains clearly differentiate the deposits from beach and dune sand. In addition, samples of the older sand layers rarely included grains with rounded or subrounded shapes like the abundant frosted and rounded particles evident in beach and dune sand. Instead, the N4 and N5 sand grains were typically angular and shared mineralogy more similar to sand from the Little Nestucca River channel (Fig. 15). We did not observe rip up clasts incorporated in the deposits nor did we note the presence of eroded lower contacts, both attributes identified for other Cascadia tsunami deposits (Kelsey et al., 2005; Peters et al., 2007).

From changes in diatom assemblages we infer that submergence caused by coseismic subsidence dropped marshes into lower intertidal environments, but we cannot estimate the precise amount of vertical change caused by earthquakes around 1.2 and 1.6 ka. Without extensive outcrops to examine changes in fossil plant communities above and below older contacts and knowledge of the local tidal range and elevational ranges of ecological zones (Hemphill-Haley, 1995a), estimates of the amount of submergence have uncertainties greater than 0.5 m (Peterson et al., 2000). Through comparisons with correlative lithologic contacts at adjacent estuaries where more quantitative biostratigraphic estimates of submergence have been reported, a range in submergence amounts offers the best estimate for older contacts at Nestucca Bay. For example, changes in pollen assemblages across sharp contacts in a core from the Salmon River, located 20 km south of Nestucca Bay, were interpreted to indicate <0.5 m of sudden submergence caused by earthquakes 1.2 ka and 1.6 ka (Nelson et al., 2004). At Netarts Bay, 20 km to the north, changes in fossil pollen and diatom indicate submergence of a high marsh to a low marsh amounting to probably no more than 0.5 m (Shennan et al., 1998).

However, placed within a regional context, ^{14}C age estimates for the sandy deposits on contacts N4 and N5 overlap with age ranges for evidence of two earthquakes and accompanying tsunamis 1.2 ka an d1.6 ka (Fig. 17). Although the older sandy deposits at Nestucca Bay do not meet all the criteria listed in Table 4, the preponderance of evidence supports tsunamis as the most likely depositional mechanism.

Thresholds Controlling Preservation of Tsunami Deposits in Oregon Estuaries

Mapping the extent of Cascadia tsunami deposits gives a minimum estimate of past inundation – indeed, flooding may have continued inland with little or no sand transported leaving no lithologic evidence of the maximum penetration of the wave. The processes that control the creation and preservation of tsunami

evidence must exceed certain thresholds before the event becomes recorded in the landscape, stratigraphy or fossil record (Nelson et al., 2006). For example, to exceed the creation threshold for a tsunami deposit, sand layers, changes in fossil assemblages or other evidence must be distinct from similar features that might be produced by other coastal processes (e.g., river flooding or storm surges and waves). To exceed the preservation threshold, competing processes of erosion, bioturbation, soil formation must allow diagnostic evidence of tsunami inundation to endure in the geologic record. We infer that the creation and preservation thresholds for tsunami evidence at Nestucca Bay were exceeded at least three times producing a geologic archive that records the 1700 Cascadia tsunami and two earlier tsunamis around 1.2 ka and 1.6 ka. From well-documented examples throughout the Pacific Northwest region of other Cascadia earthquakes and tsunamis not evident at Nestucca Bay, we infer either one of two explanations: (1) only three tsunamis inundated Nestucca Bay in the past ca. 2000 years; or (2) additional tsunamis may have occurred but the creation and preservation thresholds for tsunami evidence were not exceeded.

Specific creation thresholds may influence the spatial extent of tsunami evidence observed at Nestucca Bay. For instance, differences in the extent of tsunami deposits that record individual Cascadia tsunamis generated by different plate boundary earthquakes may be explained by a number of factors, including: (1) variation in tsunami size between events; (2) variation in the amount of coseismic subsidence produced by different earthquakes; (3) spatial and temporal changes in the hydrography of the estuary; or (4) variation in tidal or atmospheric conditions through the duration of the tsunami. Therefore, when using paleoseismic data as empirical evidence with which to check the validity of numerical tsunami simulations it is important to consider the range of thresholds that likely influenced the creation of the tsunami evidence.

A recent tsunami hazard assessment for Cannon Beach, Oregon illustrates one approach used to consider coastal processes when evaluating tsunami modeling results. Priest et al. (2009) considered hindcast tidal predictions for January 26, 2009 (Mofjeld et al., 1997) to estimate the variation in tide level during the 1700 tsunami. In addition to tide data, numerical simulations of prehistoric tsunamis at Cannon Beach used reconstructions of the paleotopography to account for coastal erosion, alluvial sedimentation in the coastal valley and artificial fill placed for urban development. By considering these creation thresholds in their evaluation of numerical tsunami simulations, Priest et al. (2009) were able to directly compare model inundation results with the spatial distribution of sand deposited by the 1700 Cascadia tsunami and older events.

Paleotopography and late Holocene sea level rise become increasingly important controls on inundation estimates when investigating evidence for older tsunamis in the geologic record. The limited stratigraphic data presented here suggests that Nestucca Bay was a much larger estuary in the past and that shoaling and progradation of a transgressive estuarine delta has shifted intertidal environments westward over the past 2000 years. Understanding the transient and sometimes ephemeral nature of changing depositional environments through time becomes critical to identifying preservation thresholds that may influence the spatial variability of tsunami evidence. At Nestucca Bay, for instance, older sandy sediment left by tsunamis 1.2 ka and 1.6 ka extend more than a kilometer farther inland than the 1700 tsunami deposit. Despite these clear differences in the spatial distribution of the tsunami deposits, we have too little information about past configurations of the estuary to conjecture about the differences in relative size of one tsunami versus another.

CONCLUSIONS AND RECOMMENDATIONS

At least three tsunamis generated by great plate-boundary earthquakes on the Cascadia subduction zone inundated Nestucca Bay in the past 2000 years. The primary evidence includes layers of sandy sediment that bury tidal marshes submerged by earthquake-related subsidence. Additional evidence supporting a tsunami origin for the sand layers includes: the spatial extent of the deposits, clear trends in deposit thickness and mean particle size that decrease with increasing distance inland, the presence of brackish-marine diatoms within the deposit and the observation of normal grading in layers within each deposit. ^{14}C age ranges for the youngest tsunami sand span the date of the most recent Cascadia earthquake and tsunami in 1700. Sediment cores and a single tidal outcrop define the spatial limit of the 1700 tsunami deposit, which extended at least 4.4 km landward from the Pacific Ocean at the present mouth of the bay. The widespread extent of the deposits makes storm surges and waves an unlikely process to deposit sand so far from the ocean. The 1700 tsunami deposit shares the physical attributes of beach and dune sand indicating an oceanward source and ruling out river flooding as alternative mechanism for sand emplacement.

Older sandy deposits evidence tsunamis that inundated Nestucca Bay about 1.2 ka and 1.6 ka, in both cases overlapping ^{14}C age estimates for widespread upheaval and inundation affected by great Cascadia earthquakes and attendant tsunamis documented at multiple sites along the Pacific Northwest coast and in the offshore record of submarine turbidites (Fig. 17). Although both deposits meet multiple criteria consistent with tsunami origin (Table 4) and extend 5.5 km or more inland, farther than the 1700 tsunami deposit, the sand lacked the physical characteristics of beach and dune sand and instead more closely resembled sediment from the nearby sandy flats along the Little Nestucca River channel. Such a finding does not rule out a tsunami as a source, but instead suggests that deposits left by tsunamis may reflect the source of sand along its flow path (Sato et al., 1995).

Stratigraphic sequences of intertidal facies beneath the margins of Nestucca Bay archive a history of relative sea level change in response to the earthquake deformation cycle as well as the effects of tsunamis, but they may not capture a complete record of great Cascadia earthquakes and tsunamis at Nestucca Bay over the past 2000 years. This inference is supported by equivocal evidence for one or two peaty horizons buried between the times of the 1.2 ka and1700 tsunamis. These buried marsh deposits that largely lack distinctive, laterally continuous sandy deposits, probably reflect small changes in relative sea level that may have been caused by a number of processes, including earthquakes, climate variation and changes in the configuration of the estuary (Nelson et al., 1996). In addition, older sharp lithologic contacts recognized in stratigrphic sequences along Upton Slough lack the lateral continuity and biostratigraphic evidence necessary to confidently attribute them to Cascadia events. Therefore, the evidence we have uncovered at Nestucca Bay stresses the importance of understanding the variability of creation and preservation thresholds that control whether a particular site holds complete or incomplete geologic record of great Cascadia earthquakes and tsunamis.

In light of these findings, we make the following recommendations:

Because the 1700 tsunami deposit represents the most recent Cascadia tsunami to inundate Nestucca Bay, we recommend using its spatial distribution to empirically validate numerical tsunami simulations used to design tsunami mitigation measures. When testing the simulations, models must account for differences in topography, tide level and other factors where possible to reduce error by reconstructing, as accurately as possible, the thresholds that control the creation of the 1700 tsunami evidence.

We feel that environmental factors controlling the spatial extent of older tsunami deposits are too poorly constrained to be useful for testing the validity of tsunami simulations. However, further investigation of these deposits is warranted to provide accurate estimates of Cascadia tsunami recurrence intervals and to increase our understanding of the evolution of the estuary.

We found evidence for the 1700 Cascadia tsunami to be restricted to tidal marshes in the central and southern part of Nestucca Bay. However, reconnaissance coring during this study identified at least one additional site that may contain evidence of the most recent tsunami deposit. Therefore we recommend additional investigations to assess whether or not the 1700 tsunami inundated the area behind Pacific City on the Martella Ranch, which is now part of the Nestucca Bay Wildlife Refuge.

ACKNOWLEDGMENTS

George Priest encouraged us to pursue an investigation of tsunami deposits near Pacific City to provide an empirical check on tsunami inundation modeling. T. Manning of the Tillamook County Sheriff's Office and the Tillamook County Board of Commissioners endorsed the study. We thank R. Lowe and K. White for access to the Nestucca Bay National Wildlife Refuge. We also owe thanks to S. Martella and R. Hurliman for access to private land. C. Folger and T. DeWitt trained Witter in particle size analysis and the U.S. Environmental Protection Agency at Hatfield Marine Science Center provided use of its laser particle size analyzer at no cost to this project. R. Van Hoy provided tide gage data for the Little Nestucca River. This study was funded by a grant from the U.S. Geological Survey's National Earthquake Hazard Reduction Program, award number 08HQGR0076.

REFERENCES

Andrejko, M.J. and Cohen, A.D., 1984. Scanning electron microscopy of silicophytoliths from the Okefenoke swamp-marsh complex. In: A.D. Cohen, D.J. Casagrande, M.J. Andrejko and G.R. Best (Editors), The Okefenokee Swamp: Its natural history, geology and geochemistry. Wetland Surveys, Los Alamos, pp. 466-491.

Atwater, B.F., 1987. Evidence for great Holocene earthquakes along the outer coast of Washington state. Science, 236: 942-944.

Atwater, B.F., 1992. Geologic evidence for eartqhuakes during the past 2000 years along the Copalis River, southern coastal Washington. Journal of Geophysical Research, 97(B2): 1901-1919.

Atwater, B.F. and Hemphill-Haley, E., 1997. Recurrence intervals for great earthquakes of the past 3500 years at northeastern Willapa Bay, Washington. U.S. Geological Survey Professional Paper 1576, 108 pp.

Atwater, B.F. et al., 2005. The orphan tsunami of 1700-Japanese clues to a parent earthquake in North America. U.S. Geological Survey Professional Paper 1576, 144 pp.

Atwater, B.F. et al., 2003. Earthquake recurrence inferred from paleoseismology. In: A.R. Gillespie, S.C. Porter and B.F. Atwater (Editors), The Quaternary Period in the United States, Developments in Quaternary Science. Elsevier, New York, pp. 331-350.

Benson, B.E., Grimm, K.A. and Clague, J.J., 1997. Tsunami deposits beneath tidal marshes on northwestern Vancouver Island, British Columbia. Quaternary Research, 48: 192-204.

Clemens, K.E. and Komar, P.D., 1988. Oregon beach-sands compositions produced by the mixing of sediments under a transgressing sea. Journal of Sedimentary Petrology, 58(3): 519-529.

Darienzo, M.E., 1991. Late Holocene paleoseismicity along the northern Oregon coast. Ph.D Thesis, Portland State University, Portland, Oregon, 176 pp.

Darienzo, M.E. and Peterson, C.D., 1990. Episodic tectonic subsidence of late Holocene salt marshes, northern Oregon central Cascadia margin. Tectonics, 9(1): 1-22.

Darienzo, M.E., Peterson, C.D. and Clough, C., 1994. Stratigraphic evidence for great subduction-zone earthquakes at four estuaries in northern Oregon, U.S.A. Journal of Coastal Research, 10: 850-876.

Goldfinger, C. et al., 2009. Turbidite event history: methods and implications for Holocene paleosesimicity of the Cascadia subduction zone. U. S. Geological Survey, Professional Paper 1661-F,

Hawkes, A.D., Horton, B.P., Nelson, A.R. and Grand Pre, C., 2008. Late Holocene coseismic deformation at the Cascadia subduction zone, Oregon, USA. Eos Trans. AGU, 89(53): Fall Meet. Suppl., Abstract T53B-1937.

Hemphill-Haley, E., 1993a, Occurrences of recent and Holocene intertidal diatoms (Bacillariophyta) in northern Willapa Bay, Washington: U.S. Geological Survey Open-File Report 93-284, 94 p.

Hemphill-Haley, E., 1993b, Taxonomy of recent and fossil (Holocene) diatoms (Bacillariophyta) from northern Willapa Bay, Washington: U.S. Geological Survey Open-File Report 93-289, 151 p.

Hemphill-Haley, E., 1995a. Diatom evidence for earthquake-induced subsidence and tsunami 300 yr ago in southern coastal Washington. Geological Society of America Bulletin, 107: 367-378.

Hemphill-Haley, E., 1995b. Intertidal diatoms from Willapa Bay, Washington: Application to studies of small-scale sea-level changes. Northwest Science, 69 (1): 29-45.

Hemphill-Haley, E., 1996. Diatoms as an aid in identigying late-Holocene tsunami deposits. The Holocene, 6: 439-448.

Hemphill-Haley, E., 2006, Diatoms (Bacillariophyta) from salt marshes and intertidal flats of Tomales Bay, California. A report to the National Park Service Tomales Bay Biodiversity Inventory (TBBI), 30 pp., 17 plates. Available from: http://www.tomalesbaylife.org

Hemphill-Haley, E., and Lewis, R.C., 1995, Distribution and taxonomy of diatoms (Bacillariophyta) in surface samples and a two-meter core from Winslow Marsh, Bainbridge Island, Washington: U.S. Geological Survey Open-File Report 95-833, 103 p.

Hemphill-Haley, E., and Lewis, R.C., 2003, Diatom data from Bradley Lake, Oregon: Downcore analyses: U.S. Geological Survey Open-File Report 03-190, 138 p.

Kelsey, H.M., Nelson, A.R., Hemphill-Haley, E. and Witter, R.C., 2005. Tsunami history of an Oregon coastal lake reveals a 4600 yr record of great earthquakes on the Cascadia subduction zone. Geological Society of America Bulletin, 117(7/8): 1009-1032.

Komar, P.D., McManus, J. and Styllas, M., 2004. Sediment accumulation in Tillamook Bay, Oregon: Natural processes versus human impacts. Journal of Geology, 112: 455-469.

McIntire, C.D., and Overton, W.S., 1971, Distributional patterns in assemblages f attached diatoms from Yaquina Estuary, Oregon: Ecology, v. 52, no. 5, p. 758-777.

Mofjeld, H., Foreman, M.G.G. and A, R., 1997. West coast tides during Cascadia subduction zone tsunamis. Geophysical Research Letters, 24(17): 2215-2218.

Nelson, A.R., 1992. Discordant ^{14}C ages from buried tidal-marsh soils in the Cascadia subduction zone, southern Oregon coast. Quaternary Research, 38: 74-90.

Nelson, A.R., Aspuith, A.C. and Grant, W.C., 2004. Great earthquakes and tsunamis of the past 2000 years at the Salmon River estuary, central Oregon coast, USA. Bulletin of the Seismological Society of America, 94: 1276-1292.

Nelson, A.R. et al., 1995. Radiocarbon evidence for extensive plate-boundary rupture about 300 years ago at the Cascadia subduction zone. Nature, 378(23): 371-374.

Nelson, Alan R., Jennings, Anne E., Gerson, Linda D., Sherrod, Brian L., 2000, Differences in great-earthquake rupture extent inferred from tsunami-laid sand and foraminiferal assemblages beneath tidal marshes at Alsea Bay, Oregon: Geological Society of America Abstracts with Programs, v. 32, no. 7.

Nelson, A.R., and Kashima, K., 1993, Diatom zonation in southern Oregon tidal marshes relative to vascular plants, Foraminifera, and sea level: Journal of Coastal Research, v. 9, no. 3, p. 673-697.

Nelson, A.R., Kelsey, H.M., Hemphill-Haley, E. and Witter, R.C., 2006. Great earthquakes of variable magnitude at the Cascadia subduction zone. Quaternary Research, 65: 354-365.

Nelson, A.R., Ota, Y., Umitsu, M., Kashima, K. and Matshushima, Y., 1998. Seismic or hydrodynamic control of rapid late-Holocene sea-level rise in southern coastal Oregon, USA? The Holocene, 8: 287-299.

Nelson, A.R., Shennan, I. and Long, A.J., 1996. Identifying coseismic subsidence in tidal-wetland stratigraphic sequences at the Cascadia subduction zone of western North America. Journal of Geophysical Research, 101(B3): 6115-6135.

Nelson, S.A. and Leclair, S.F., 2006. Katrina's unique splay deposits in a New Orleans neighborhood. GSA Today, 16: 4-10.

Olmstead, D., 2003. Development in Oregon's Tsunami Inundation Zone: Information Guide for Developers and Local Government. Oregon Department of Geology and Mineral Industries, Open-File-Report O-03-05, Portland, Oregon, 20 pp.

Percy, K.L., Sutterlin, C., Bella, D.A. and Klingeman, P.C., 1974. Oregon's Estuaries. Oregon State University Sea Grant College Program, Corvallis, Oregon, 294 pp.

Peters, R., Jaffe, B. and Gelfenbaum, G., 2007. Distribution and sedimentary characteristics of tsunami deposits along the Cascadia margin of western North America. Sedimentary Geology, 200: 372-386.

Peters, R., Jaffe, B., Gelfenbaum, G. and Peterson, C.D., 2003. Cascadia tsunami deposit database. U.S. Geological Survey, Open-File Report 03-13, 24 pp.

Peterson, C., Scheidegger, K. and Komar, P., 1982. Sand-dispersal patterns in an active-margin estuary of the northwestern United States as indicated by sand composition, texture and bedforms. Marine Geology, 50: 77-96.

Peterson, C.D. and Darienzo, M.E., 1996. Discrimination of climatic, oceanic, and tectonic mechanisms of cyclic marsh burial, Alsea Bay, Oregon. U.S. Geological Survey, 115-146 pp.

Peterson, C.D., Doyle, D.L. and Barnett, E.T., 2000. Coastal flooding and beach retreat from coseismic subsidence in the Central Cascadia Margin, USA. Environmental and Engineering Geoscience, 6(3): 255-269.

Priest, G.R., 1995. Explanation of mapping methods and use of the tsunami hazard maps of the Oregon coast. Oregon Department of Geology and Mineral Industries, Open-File-Report O-95-67, Portland, Oregon, 100 pp.

Priest, G.R. et al., 2009. Tsunami hazard assessment of the northern Oregon coast: A multi-deterministic approach tested at Cannon Beach, Clatsop County, Oregon. Oregon Department of Geology and Mineral Industries, Special Paper 41., Portland, Oregon,

Reimer, P. J., and others, 2004, IntCal04 atmospheric radiocarbon age calibration, 26-0 ka BP: Radiocarbon, v. 46, p. 1029–1058.

Satake, K., Shemazaki, K., Yoshinobu, T. and Ueda, K., 1996. Time and size of a giant earthquake in Cascadia inferred from Japanese tsunami records of January 1700. Nature, 379(6562): 246-249.

Satake, K., Wang, K.L. and Atwater, B.F., 2003. Fault slip and seismic moment of the 1700 Cascadia earthquake inferred from Japanese tsunami descriptions. Journal of Geophysical Research.

Sato, H., Shimamoto, T., Tsutsumi, A. and Kawamoto, E., 1995. Onshore tsunami deposits caused by the 1993 southwest Hokkaido and 1983 Japan Sea earthquakes. PAGEOPH, 144(3/4): 693-717.

Sawai, Y., Jankaew, K., Martin, M.E., Prendergast, A., Choowong, M., Charoentitirat, T., 2009. Diatom assemblages in tsunami deposits associated with the 2004 Indian Ocean tsunami at Phra Thong Island, Thailand. Marine Micropaleontology, 73: 70-79.

Sawai, Y., and Nagumo, T., 2003. Diatoms from Alsea Bay, Oregon. Diatom, 19: 33-46.

Schlicker, H.G., Deacon, R.J., Beaulieu, J.D. and Olcott, G.W., 1972. Environmental geology of the coastal region of Tillamook & Clatsop Counties, Oregon. Oregon Department of Geology and Mineral Industries, Bulletin 74, Portland, Oregon, 164 p., 18 maps pp.

Shennan, I. et al., 1998. Tidal marsh stratigraphy, sea-level change and large earthquakes, II: submergence events during the last 3500 years at Netarts Bay, Oregon, USA. Quaternary Science Reviews, 17: 365-393.

Snavely, P.D. and Vokes, H.E., 1949. The coastal area between Cape Kiwanda and Cape Foulweather, Oregon: U.S. Geological Survey map OM 97.

Stuiver, M., and Reimer, P. J. ,1993, Extended 14C data base and revised CALIB 3.0 14C age calibration program: Radiocarbon, v. 35, p. 215–230.

Tsunami Warning and Education Act, 2006, Public Law 109-424 available at: http://frwebgate.access.gpo.gov/cgi-bin/getdoc.cgi?dbname=109_cong_public_laws&docid=f:publ424.109.pdf

Tuttle, M.P., Ruffman, A., Anderson, T. and Jeter, H., 2004. Distinguishing tsunami from storm deposits in eastern North America: The 1929 Grand Banks tsunami versus the 1991 Halloween storm. Seismological Research Letters, 75: 17-131.

Witter, R.C., 2008. Prehistoric Cascadia tsunami inundation and runup at Cannon Beach, Clatsop County, Oregon. Oregon Department of Geology and Mineral Industries, Open-file-report O-08-12, Portland, Oregon,

Witter, R.C., Kelsey, H.M. and Hemphill-Haley, E., 2003. Great Cascadia earthquakes and tsunamis of the past 6700 years, Coquille River estuary, southern coastal Oregon. Geological Society of America Bulletin, 115: 1289-1306.

Table 1 Calibrated age estimates of sand sheets in the Nestucca Bay area derived from AMS radiocarbon dates on plant macrofossils

Sand/peat contact*	Analytical lab number[#]	Core Number[†]	Sample depth in core (m)	Material dated	$\delta^{13}C$ (‰)	Lab-reported age (^{14}C yr BP at 1σ)[§]	Calibrated age (cal yr BP at 2σ)**
N1	261985	Uptn-6	69-74	Herb stem base	-23.0	110 ± 40	280-0
N1	261984	LN-02	45	Woody stem of *T. maritima*	-23.9	110 ± 40	280-0
N1	261986	ND-B	116.5-122	Woody stem of *T. maritima*	-26.2	180 ± 40	300-0
N3	258578	Saltmsh-G	86-87.3	12 conifer needles	-27.1	980 ± 40	960-790
N4	258570	Uptn-33	62.5-64	Seeds, needles, moss	-27.5	1220 ± 40	1270-1060
N4	258569	Uptn-5C	74-76.5	Seeds, needles, cone fragment	NA	1370 ± 40	1340-1260
N4	258573	Uptn-4	96-98.2	Herb stems	-27.1	1380 ± 40	1340-1270
N4	258571	Uptn-34	81-83	Needles, seeds, moss, cone	-27.7	1390 ± 40	1350-1270
N4	258572	Uptn-19	75-82	Needles, wood, stems, seeds	-26.8	1550 ± 40	1530-1350
N5	258577	Uptn-23	101.5-104.5	Moss stems	-23.0	1660 ± 40	1690-1430
N5	258576	Uptn-25-104.5	104.5-105.5	15 conifer needles	-29.0	1690 ± 40	1700-1520
N5	258575	Uptn-23	104.5-106	12 conifer needles	-26.9	1780 ± 40	1820-1600
N5	258574	Uptn-33	92-93.5	15 conifer needles	-28.4	1890 ± 40	1920-1720

*Radiocarbon age data grouped by sand/peat or mud/peat contact number interpreted from stratigraphic correlations shown in Figs. 4 and 5. Contact numbers increase with age.

[#]Lab number reported by Beta Analytic, Inc., Miami, Florida.

[†]Core number designates locality and specific core identified by number. The localities are abbreviated as follows: Uptn, Upton Slough; LN, Little Nestucca River outcrop; ND-B, core B at "Nestucca Duck" locality studied by Darienzo (1991); Saltmsh, Restored saltmarsh in wildlife refuge east of Highway 101.

[§]Conventional ages reported by radiocarbon laboratory based on the Libby half life (5570) for ^{14}C.

**Calibrated age ranges before AD 1950 reported to the nearest decade, computed by Beta Analytic, Inc. using the INTCAL98 radiocarbon calibration dataset of Stuiver et al. (1998) with a lab error multiplier of 1.0 and reported to 2σ.

Table 2 Grain size characteristics and statistics for samples of sandy sediment deposited in Nestucca Bay, Oregon.

Sample ID*	Sample Interval (cm)	Sample Interval (cm)	Sand (%)	Silt (%)	Clay (%)	Mean Grain Size (μm)	Skew-ness	Kurtosis	Field Description
LN-01 [0]	†sfc	0-5	62.283	32.962	4.755	92.011	0.228	-1.018	Sandy mud from the Little Nestucca River channel.
LN-02 [8]	27-45	43-45	52.603	42.232	5.166	80.165	0.536	-0.784	Lower 2 cm of sandy mud deposited on a clear contact (5 mm; contact N1) over peaty mud with abundant stems and rhizomes of *Triglochin maritima* in growth position.
UPT-6 [54]	71-74	71-74	32.650	59.828	7.523	46.007	0.591	-0.869	Lower 3 cm of grey peaty mud deposited on a clear contact (5 mm; contact N1) over dark brown woody peat.
	162-172	162-165	24.485	69.376	6.139	38.918	0.637	-0.773	Upper and lower layers of sandy mud deposited on a sharp (~1 mm) contact (N5) over dark brown peat.
		168-172	29.023	65.461	5.516	44.772	0.821	-0.257	
UPT-5 [282]	63-66	63-66	3.986	81.018	14.996	21.405	1.129	0.492	Grey mud overlying sandy deposit.
	69-78	69-72	62.385	33.060	4.556	85.384	0.218	-0.842	Upper, middle and lower layer of sand deposited on a sharp (~1 mm) contact (N4) over dark brown peat.
		72-74	52.809	41.490	5.702	68.200	0.210	-0.957	
		74-78	62.197	33.194	4.609	89.815	0.199	-1.013	
UPT-19 [736]	77-84	77-79	37.438	55.912	6.651	50.449	0.343	-1.052	Upper, middle and lower layer of sandy mud deposited on a sharp (~1 mm) contact (N4) over dark brown peat.
		79-81	44.106	50.345	5.548	59.766	0.470	-0.685	
		81-84	57.965	38.196	3.838	81.695	0.308	-0.909	
	116-118	116-118	14.240	80.651	5.109	29.490	1.325	0.832	Lower 2 cm of mud sharply (1-2 mm; contact N5) overlying brown peat.
UPT-24 [860]	57-59.5	57-59.5	34.708	58.872	6.420	48.579	0.488	-0.902	Lower 2.5 cm of sandy mud deposited on a sharp (~1 mm) contact (N4) over dark brown peat.
	96-98	96-98	12.159	81.067	6.774	27.455	1.061	0.055	Lower 2 cm of mud deposited on a clear (3-5 mm) contact (N5) overlying dark brown peat.

Table 2 (Continued.)

Sample ID*	Sample Interval (cm)	Sample Interval (cm)	% Sand	% Silt	% Clay	Mean Grain Size (µm)	Skew-ness	Kurtosis	Field Description
UPT-25 [885]	73-77	73-77	34.295	58.260	7.445	48.188	0.581	-0.628	A 4-cm thick sandy deposit with sharp (~1 mm) lower contact (N4) overlying dark brown peat.
UPT-34 [1262]	81-84	81-84	26.949	68.821	4.230	41.205	0.680	-0.793	A ~3-cm thick sandy mud deposit with sharp sharp (~1 mm) lower contact (N4) overlying dark brown peat.
ND-B [na]	107-110	107-110	72.938	24.186	2.876	168.732	-0.339	-1.517	Sand sharply (~1 mm; contact N1) deposited over peaty mud with abundant stems and rhizomes of *Triglochin maritima* in growth position.
NS-1 [na]	†sfc	0-5	100	0	0	513.473	0.575	-0.132	Beach sand sampled from the beach surface at about 1 m NAVD 88 (below wet-dry sand line).
NS-2 [na]	†sfc	0-5	100	0	0	358.64	0.582	0.021	Dune sand sample from wave erosion scarp in foredune at the beach-dune junction.
NESK-P1 [na]	†sfc	0-5	100	0	0	463.614	0.852	0.357	Beach sand sampled from the beach surface at Neskowin, Oregon.
NR-1 [na]#	†sfc	0-5	2.271	75.838	21.892	20.543	0.924	-0.439	Sandy mud from the Nestucca River channel.

* Sample ID includes abbreviated site name: LN, Little Nestucca River; UPT, Upton Slough; ND, Nestucca Duck; NR, Nestucca River; NESK, Neskowin Beach. Values in brackets represent distance in meters from core site to the Little Nestucca River channel.

† Sfc indicates grab samples of approximately beach and river sand from upper 5 cm of deposit. Dune sand was sampled from wave cut scarp at the junction between the beach and dune.

Visual comparisons of NR-1 with other sand samples indicate that the particle size distribution determined for NR-1 is inaccurate. We suspect this error is related to the method used to transfer sediment to the laser particle size analyzer that may result in incomplete mixing of the suspended sample.

Table 3 Diatom evidence used to differentiate tsunami and non-tsunami deposits above lithologic contacts N4-N7.

Lithologic contact ID	Core ID	Depth in core (cm)	[1] % intact pennate diatom valves > 100 µm long	[2] % intact pennate diatom valves > 40 µm long	[3] % coastal marine diatoms (planktonic + tychoplanktonic species)	[4] # of large epipsammic taxa observed in 10 traverses (400 mm^2 area of slide)	[5] % well-preserved epipsammic diatoms (high mag counts)	Lithology	Evidence for tsunami
Contact N4	**25**	68-69	31.7%	70.8%	7.5%	4	3.6%	Mud	–
		69-70	1.0%	50.0%	7.7%	9	48.1%	Sandy mud	1, 2, 4, 5
	33	61-62	20.2%	71.6%	1.8%	9	44.2%	Mud	–
		63-64	4.9%	30.4%	9.8%	19	69.1%	Sandy mud	1, 2, (3), 4, 5
Contact N5	**25**	102-103	23.8%	52.4%	14.3%	4	54.7%	Mud	–
		103.5-104.5	2.9%	27.2%	31.1%	9	74.5%	Sandy mud	1, 2, 3, 4, 5
	33	87-88	23.3%	65.8%	4.8%	1	9.9%	Peaty mud	–
		91-92	0.8%	41.7%	30.8%	12	62.4%	Mud	1, 2, 3, 4, 5
		92.5-93.5	0.0%	39.3%	29.9%	8	55.9%	Mud	1, 2, 3, 4, 5
Contact N6	**33**	150-151	21.7%	51.7%	5.8%	1	7.4%	Mud	–
		152-153	13.9%	51.1%	8.0%	1	11.1%	Mud	–
Contact N7	**33**	177-178	1.0%	43.8%	7.6%	0	2.8%	Mud	–
		179.5-180.5	3.0%	26.7%	19.8%	0	2.7%	Mud	2, 3

Characteristics of diatoms in tsunami samples as compared to non-tsunami samples:

[1] Severe fragmentation of large, narrow pennate diatoms > 100 µm long.

[2] Fewer intact specimens of all diatom valves > 40 µm long.

[3] Greater frequency of coastal marine planktonic and tychoplanktonic taxa.

[4] Greater frequency of exceptionally large, robust epipsammic diatoms (*Cerataulus turgidus*, *Campylodiscus echeneis*).

[5] Greater frequency of small epipsammic diatoms, including evidence for enhanced preservation.

Table 4 Summary of evidence for sandy layers deposited at Nestucca Bay that satisfy criteria for a Cascadia tsunami origin.

Sand layer	Deposit has attributes of beach/dune sand*	Diatom evidence for marine incursion[†]	Deposit thins/grain size fines landward	Normally-graded beds observed	Ripup clasts present in deposit	Sharp or eroded lower contact	Organic debris layer associated with sandy deposit	Extent of deposit (km)[§]	Deposit overlies submerged tidal marsh sediment	Age overlaps with evidence for regional Cascadia event[#]
N1	✓	**I**	✓	✓	no	✓	✓	4.4	✓	✓
N4	no	✓	✓	✓	no	✓	✓	5.6	✓	✓
N5	no	✓	✓	✓	no	✓	✓	5.5	✓	✓

Note: check (✓) indicates the evidence was observed at multiple sites; **I**, data are insufficient to provide conclusive evidence; "no" indicates the absence of evidence.

*Beach sand component interpreted from sand mineralogy and grain size.

[†]Diatom evidence for inundation by marine water summarized in Table 3.

[§] Landward extent of deposit measured from mouth of Nestucca Bay to core site furthest inland where sand sheet was observed. Only tsunamis or high-stream flow could explain such widespread deposits in the lower valley, ruling out storm waves superimposed on extreme ocean levels as an alternative explanation.

[#]Correlations based on regional geologic records of Cascadia earthquakes and tsunamis shown on Fig. 17.

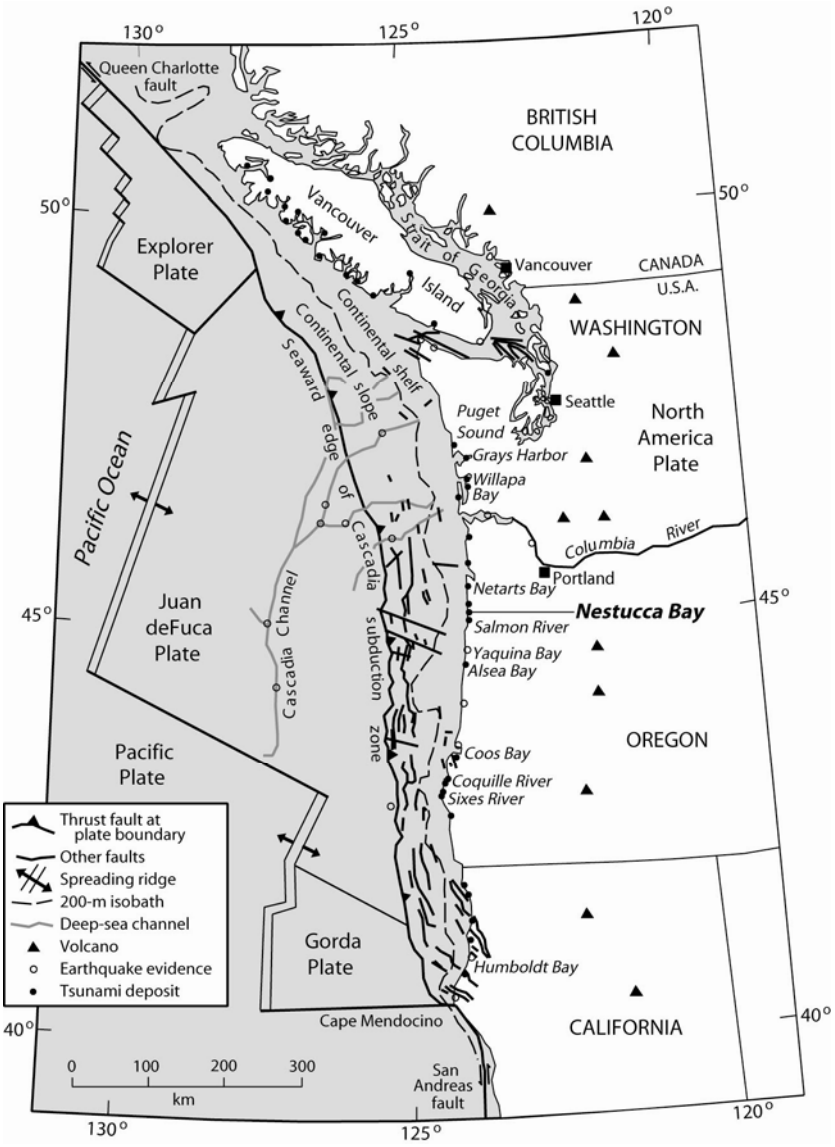

Figure 1 Tectonic setting of the Pacific northwestern U.S. showing the Cascadia subduction zone and other plate boundaries, Quaternary faults in the North American plate, and the location of the study site at Nestucca Bay in northwestern Oregon (modified from Nelson et al., 2004). The deformation front (barbed line) is defined by bathymetry where the abyssal plain meets the continental slope and is inferred to represent the surface projection of the Cascadia thrust fault. Open and closed circles represent sites with evidence for prehistoric Cascadia earthquakes and tsunamis. Closed circles mark sites with deposits interpreted to record tsunami inundation caused by a M9 Cascadia earthquake on January 26, 1700 (Satake et al., 1996).

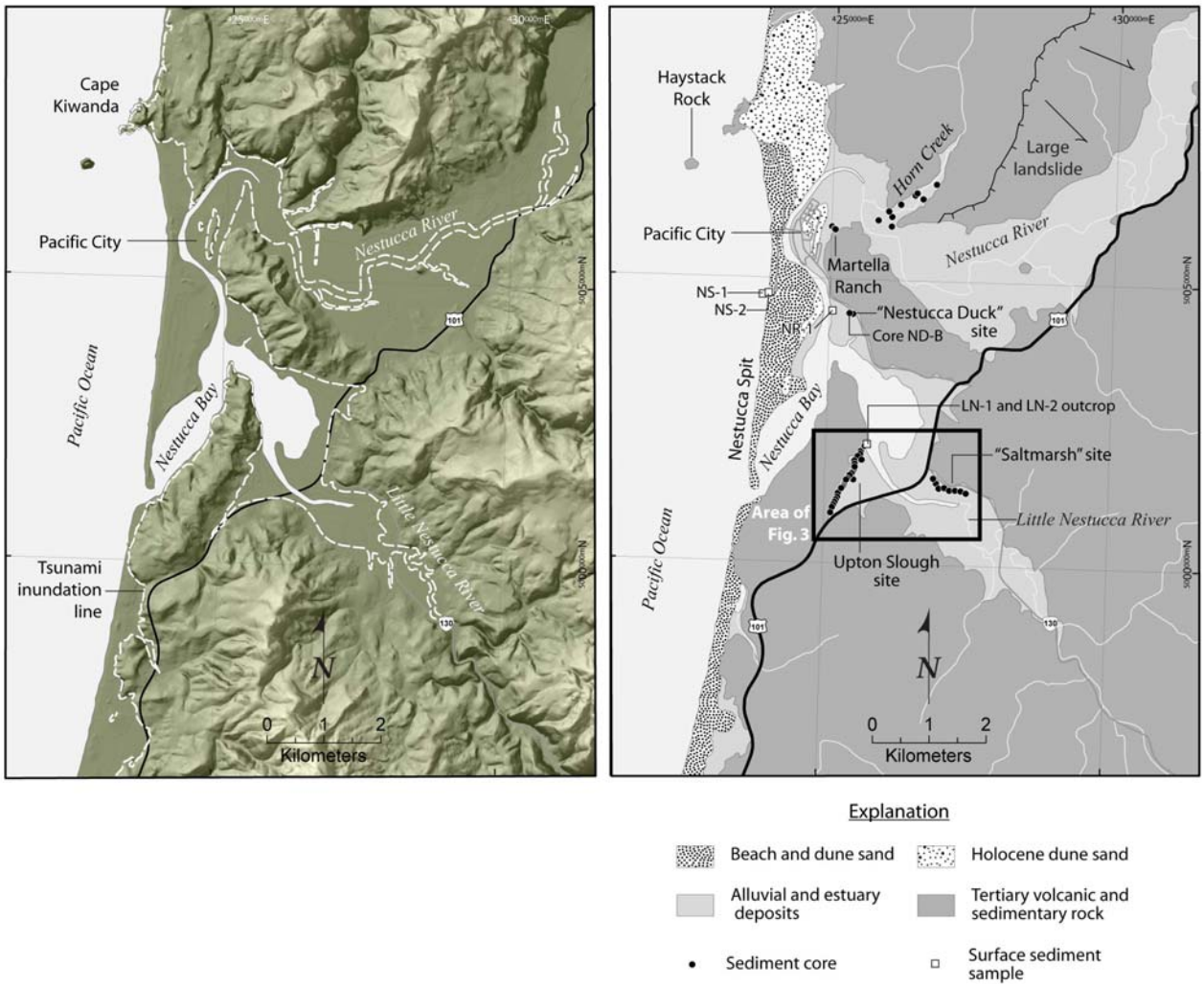

Figure 2 Map of Nestucca Bay estuary and surrounding uplands showing the locations of 57 sediment cores examined for evidence of sand layers deposited by tsunamis or river floods. (Left) Topographic hillshade (USGS 10 m DEM) of the Nestucca Bay area showing the Oregon tsunami inundation line used to restrict new development along the coast (Olmstead, 2003; Priest, 1995). (Right) Simplified geologic map of the Nestucca Bay area showing core sites (black dots) and sites sampled for sandy surface sediment (white squares). West and northwest of the bay, active and Holocene dunes deflect the Nestucca River to the south and provide a barrier protecting the bay. Uplands surrounding the estuary are composed of Tertiary volcanic and sedimentary rocks mapped by Snavely and Vokes (1949) and Schlicker et al. (1972).

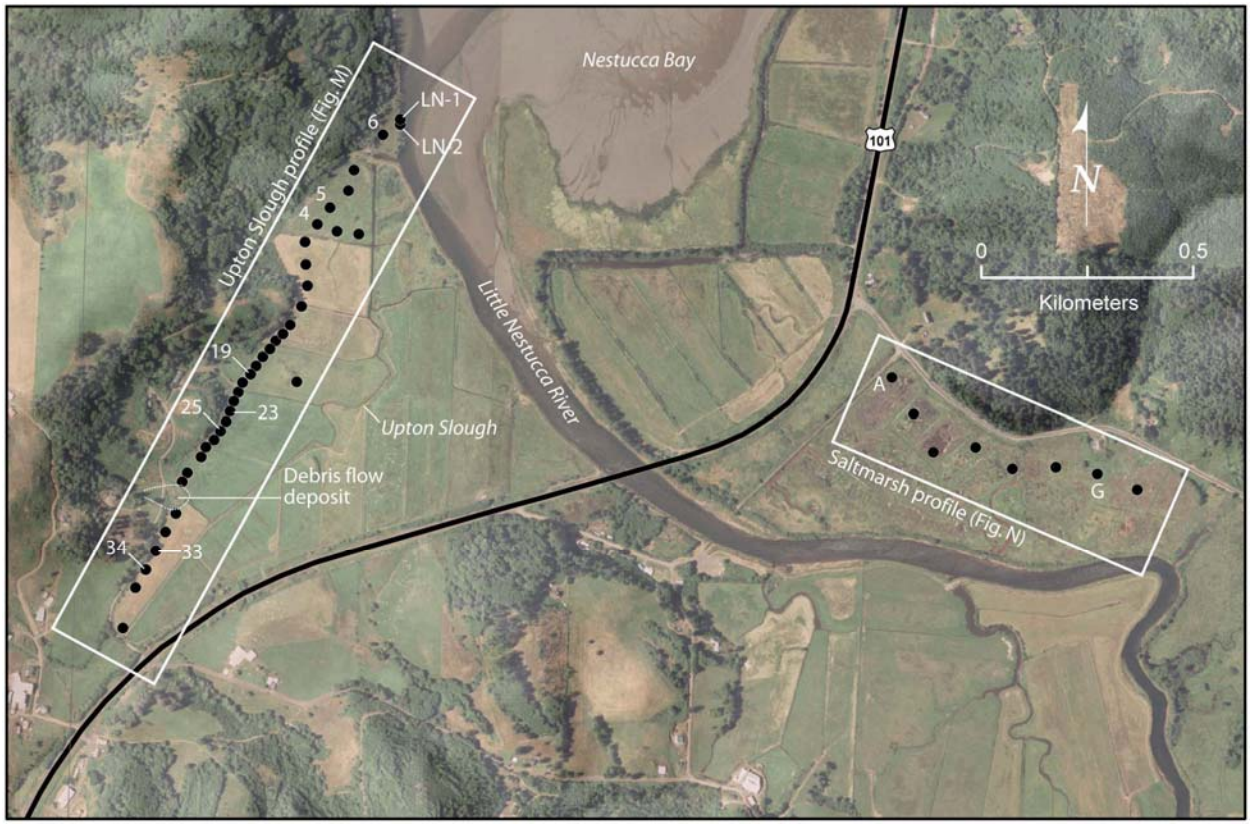

Figure 3 Map covering part of the Nestucca Bay National Wildlife Refuge and the Little Nestucca River showing core locations along two transects: one along Upton Slough and another within a saltmarsh east of Highway 101 restored by the U.S. Fish & Wildlife Service.

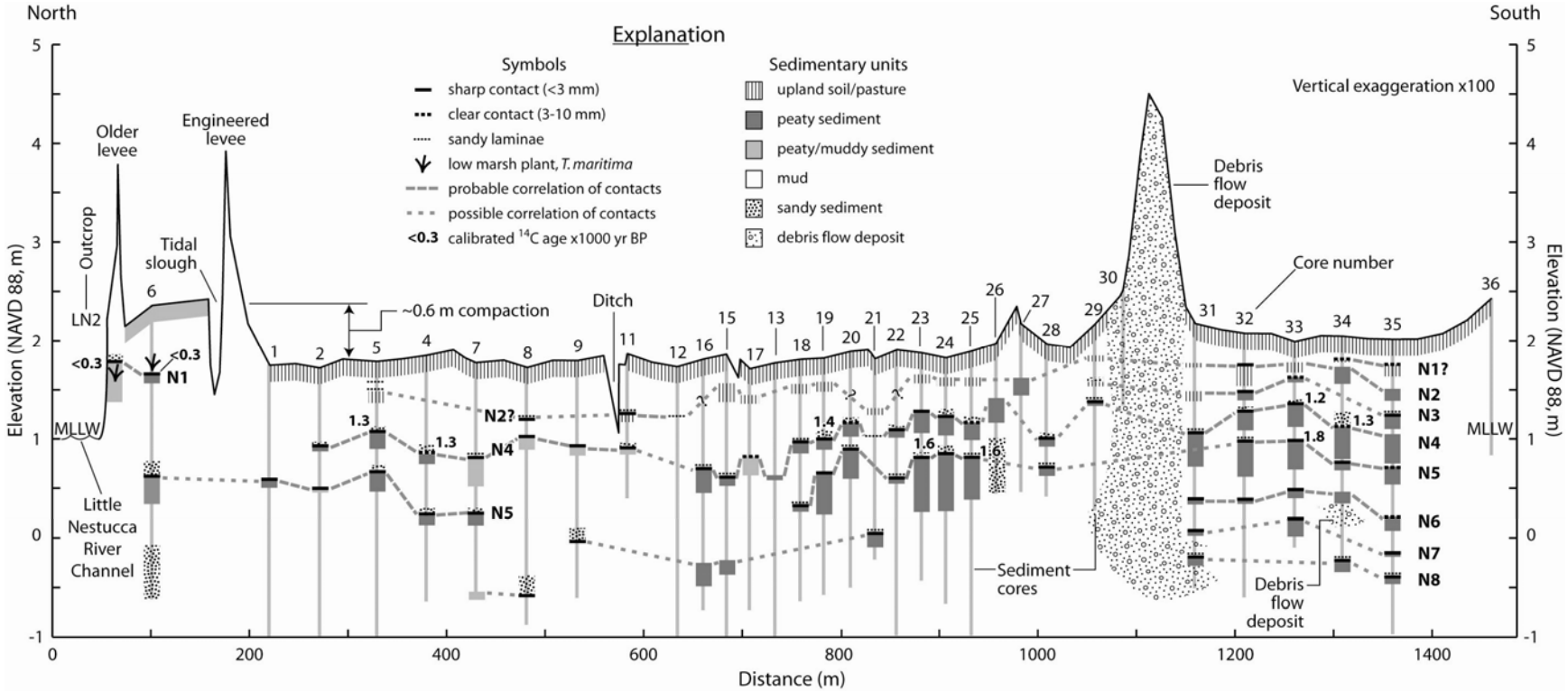

Figure 4 Simplified stratigraphic profile correlating mud-over-peat or sand-over-peat contacts inferred to reflect sudden rises in relative sea level in cores along Upton Slough (Fig. 3). Solid and dashed black lines mark sharp (<3 mm) and clear (3-10 mm) lithologic contacts, respectively. Gradual lithologic contacts lack either line symbol. Gray dashed lines labeled N1 through N8 correlate contacts inferred to record sudden episodes of relative-sea level rise. Bold numbers indicate preferred ages for contacts N1, N3 and N4, rounded to the nearest hundred years, based on calibrated ^{14}C ages in Table 1. Core elevations determined by RTK GPS survey have <2 cm vertical error. We infer compaction of ~0.6 m lowered the north pasture, located behind large engineered levees that bar tidal flooding. MLLW, mean lower low water tidal datum estimated from tide gage data for the Little Nestucca River.

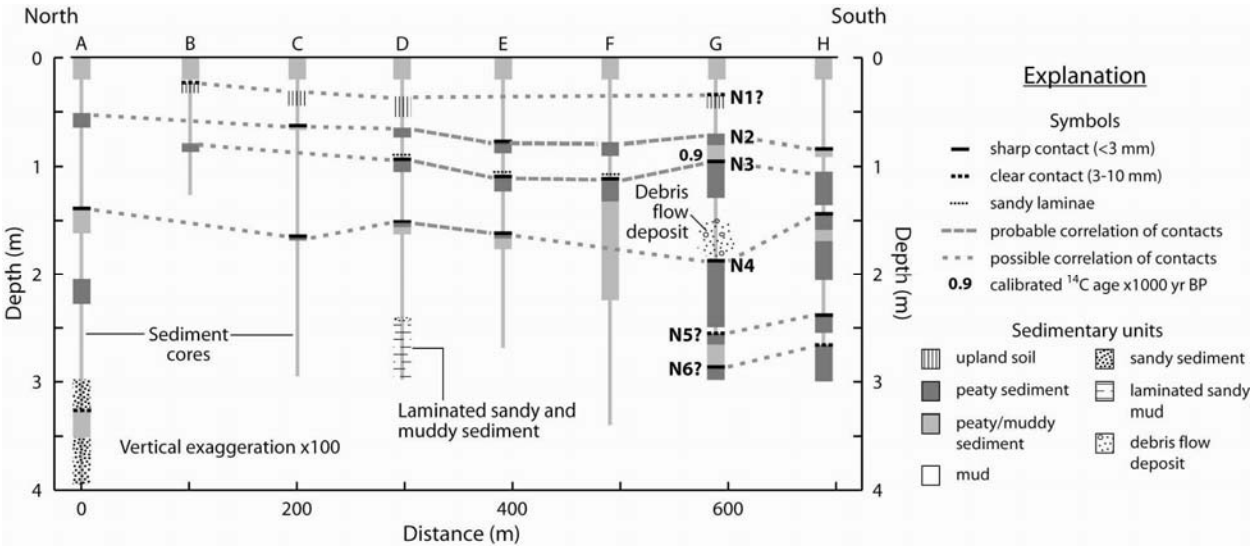

Figure 5 Simplified stratigraphic profile correlating mud-over-peat or sand-over-peat contacts inferred to reflect sudden rises in relative sea level in cores along the "Saltmarsh transect" in the Nestucca Bay Refuge (Fig. 3). Vertical axis depicts depth, in meters, from the surface.

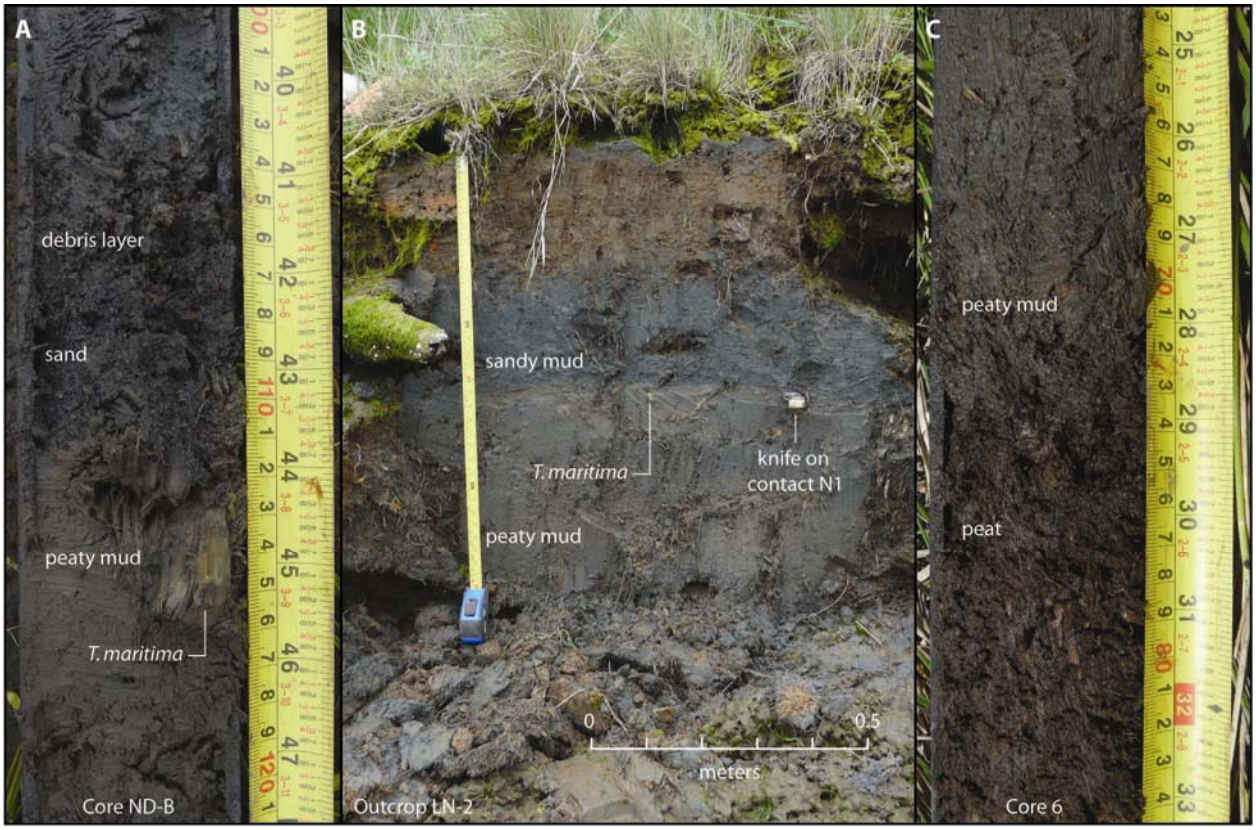

Figure 6 Photographs of 5-cm diameter sediment cores and an outcrop exposure showing sharp lithologic contacts inferred to record the 1700 Cascadia earthquake and tsunami at Nestucca Bay. Scales to right of cores in cm and inches. Stem bases from sharp contacts in both cores and the outcrop limit the time of submergence to <300 years before 1950 (Table 1), which is consistent with regional evidence for the 1700 Cascadia earthquake and tsunami. (A) Sand-over-peaty-mud contact at ~112 cm depth in core ND-B near the "Nestucca Duck" site studied by Darienzo (1991). *T. maritima* stems rooted in the peaty mud below the sharp contact are entombed in the overlying sand, suggesting the plants were killed by sudden burial. Detrital debris layers overlying sandy sediment has been cited as a common attribute of some tsunami deposits (Peters et al., 2007; Witter, 2008). (B) Contact N1 exposed in outcrop at the northern end of the Upton Slough transect (Figs. 3 and 4). Vertical tape in photo is about 0.8 m. (C) Contact N1 lacks a sandy overlying deposit in core 6 and instead is marked by peaty-mud-over-peat at 73.5 cm depth. *T. maritima* stems and rhizomes were rooted in peaty sediment overlying the contact.

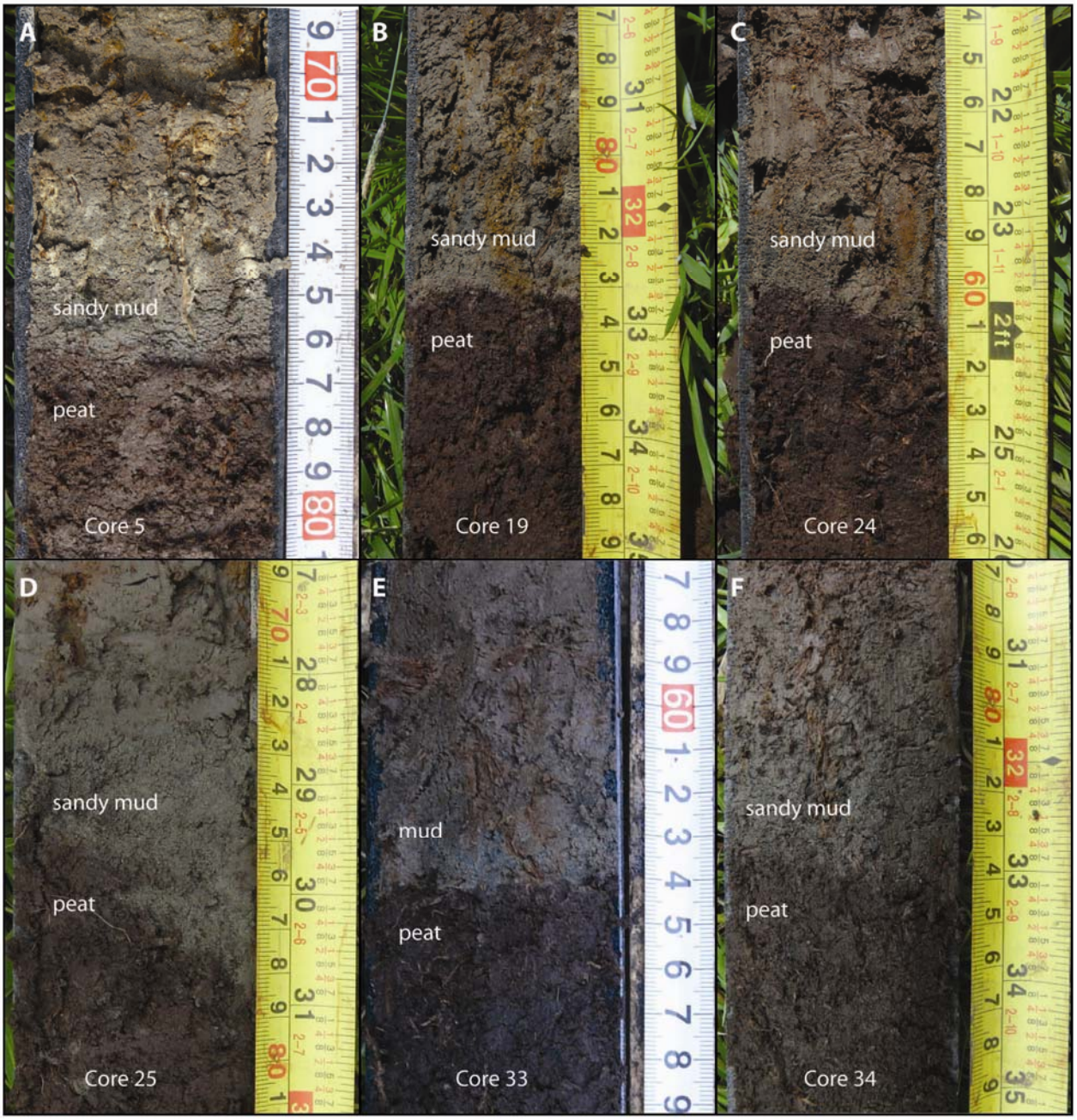

Figure 7 Sharp lithologic contacts (contact N4) in six cores from Upton Slough inferred to mark coseismic subsidence and tsunami deposition caused by a Cascadia earthquake that occurred approximately 1.3 ka.

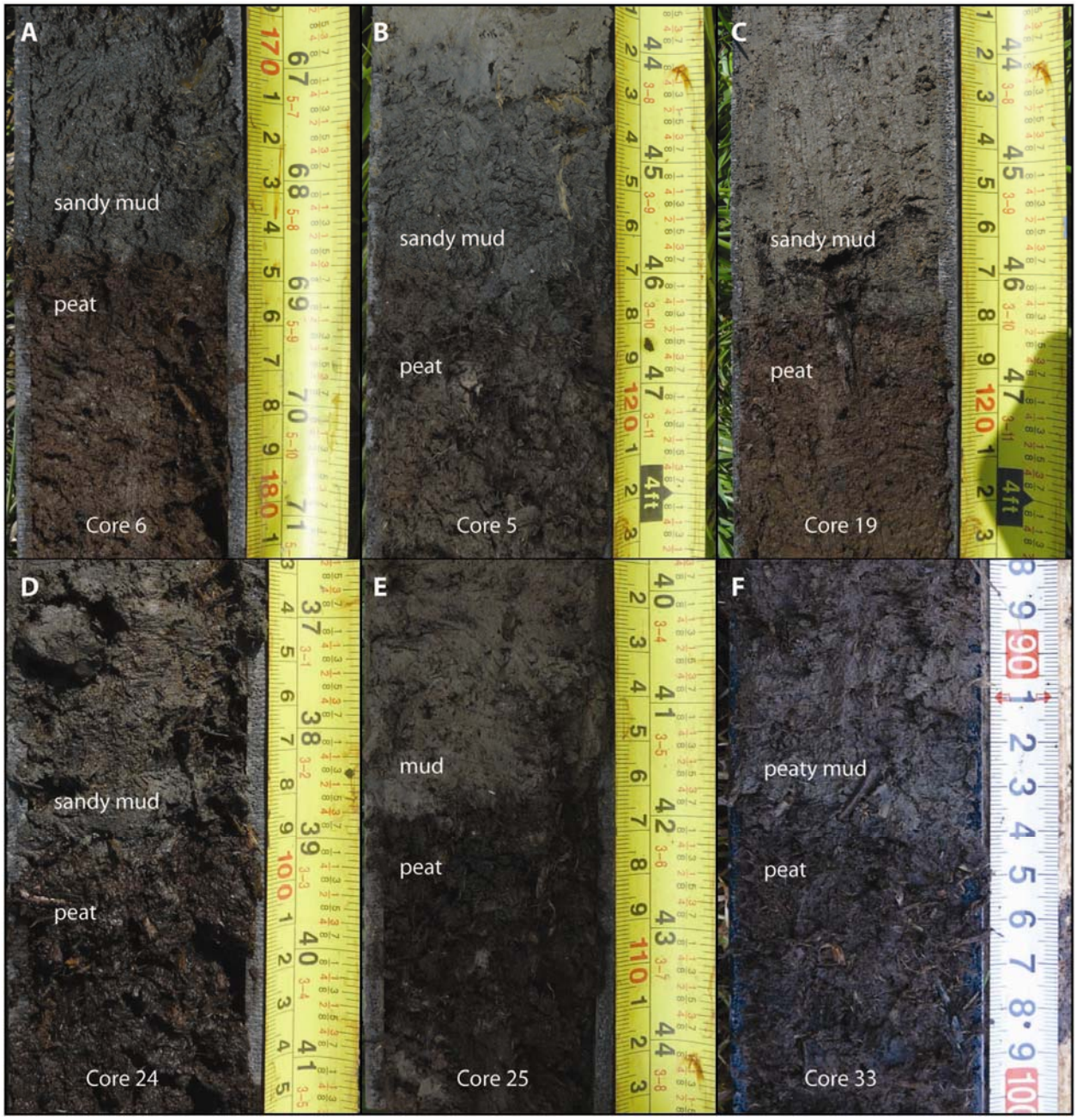

Figure 8 Sharp lithologic contacts (contact N5) in six cores from Upton Slough inferred to mark coseismic subsidence and tsunami deposition caused by a Cascadia earthquake that occurred approximately 1.6 ka.

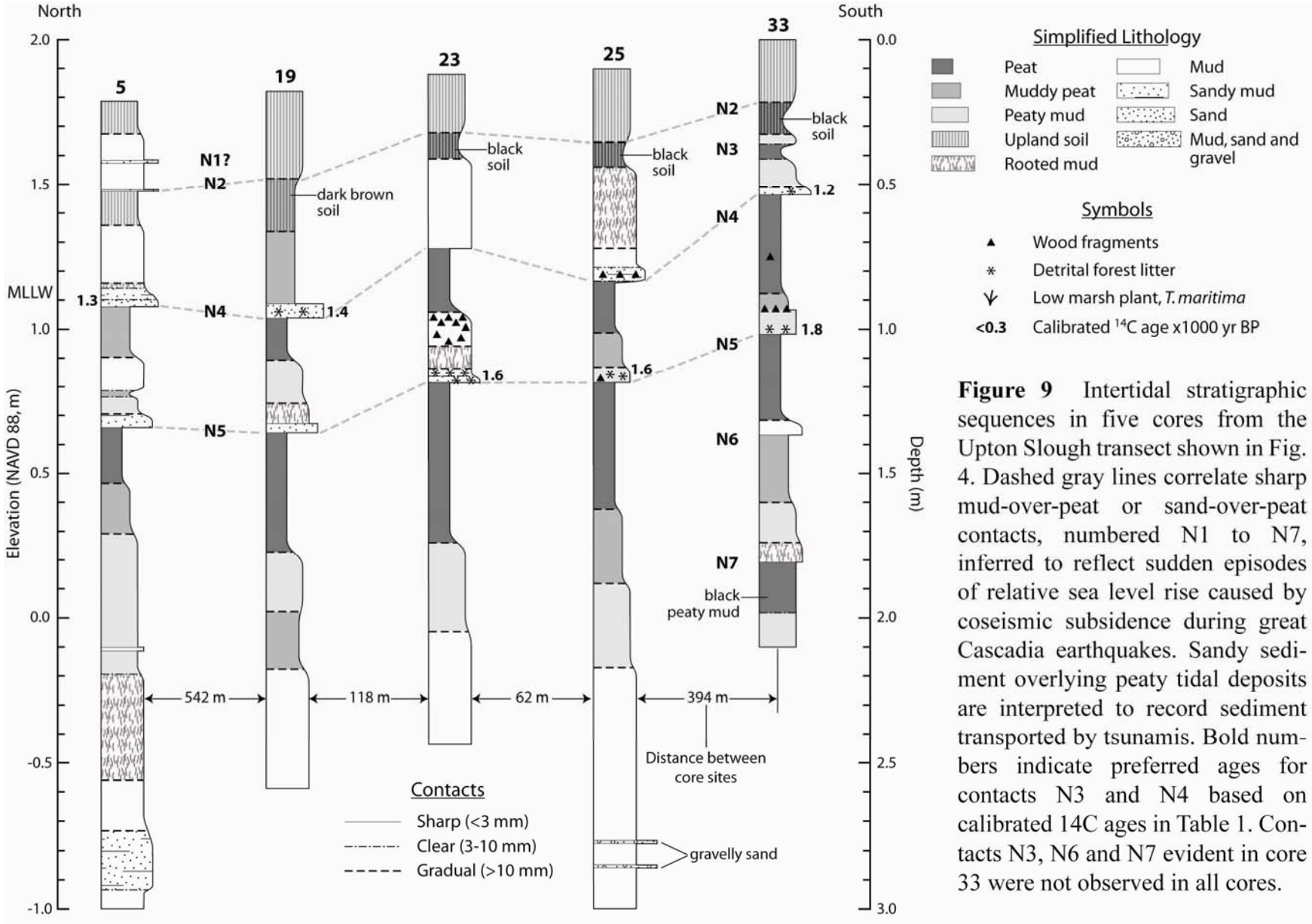

Figure 9 Intertidal stratigraphic sequences in five cores from the Upton Slough transect shown in Fig. 4. Dashed gray lines correlate sharp mud-over-peat or sand-over-peat contacts, numbered N1 to N7, inferred to reflect sudden episodes of relative sea level rise caused by coseismic subsidence during great Cascadia earthquakes. Sandy sediment overlying peaty tidal deposits are interpreted to record sediment transported by tsunamis. Bold numbers indicate preferred ages for contacts N3 and N4 based on calibrated 14C ages in Table 1. Contacts N3, N6 and N7 evident in core 33 were not observed in all cores.

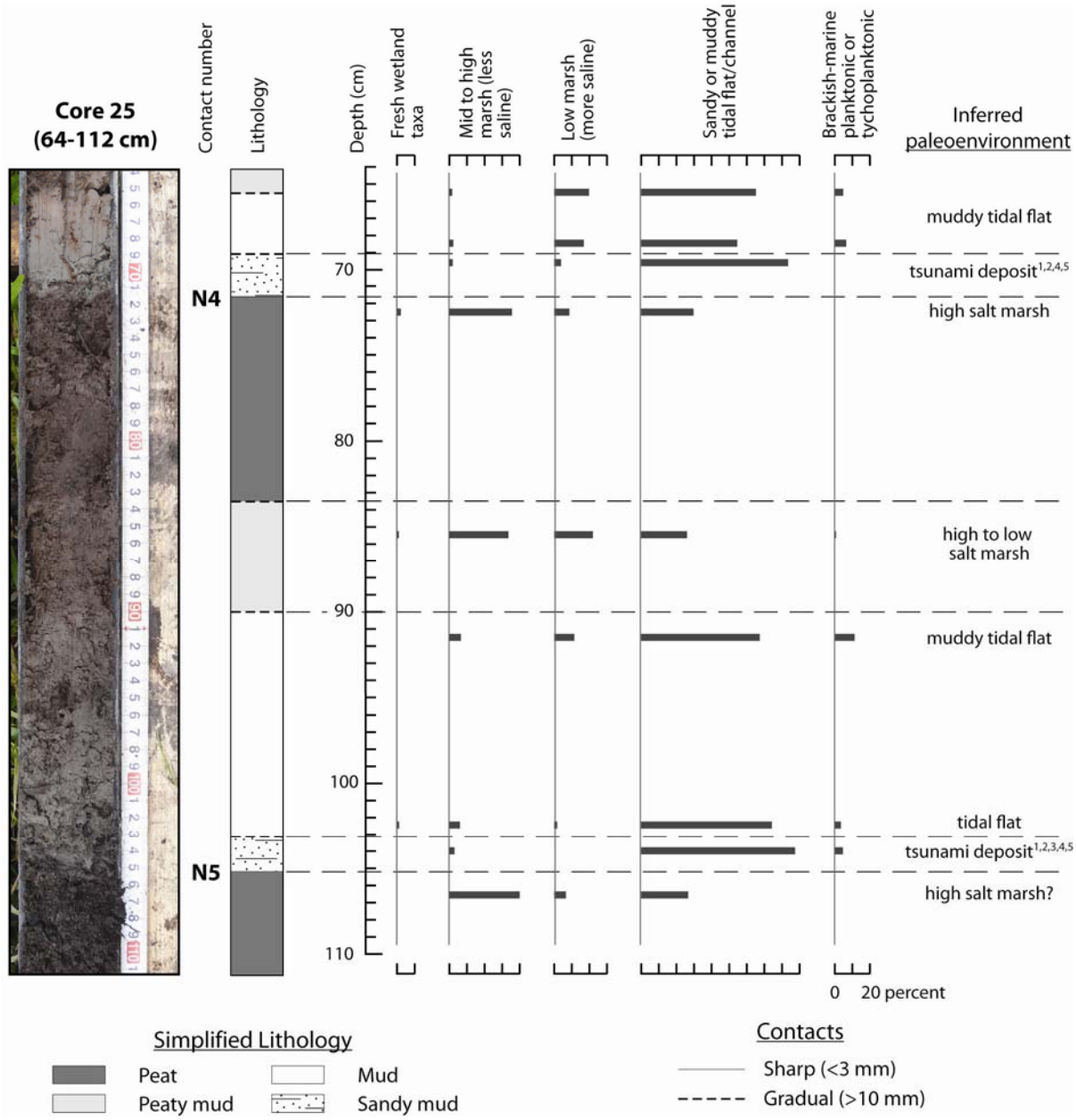

Figure 10 Frequency of diatom taxa, grouped by inferred paleoenvironment, from analyses of 9 samples from a 5-cm-diameter Russian-type sampler at core 25 along Upton Slough. Diatom frequency is expressed as a percentage of total diatoms counted in each sample (Appendix A). Numbers in far right column correspond tot characteristics of diatoms in tsunami samples as compared to non-tsunami samples listed in Table 3. The depths of contacts N4 and N5 in the Russian-type core were 10 to 20 mm deeper than contacts observed in gouge cores used to construct Fig. 9. Photograph of Russian-type core at left.

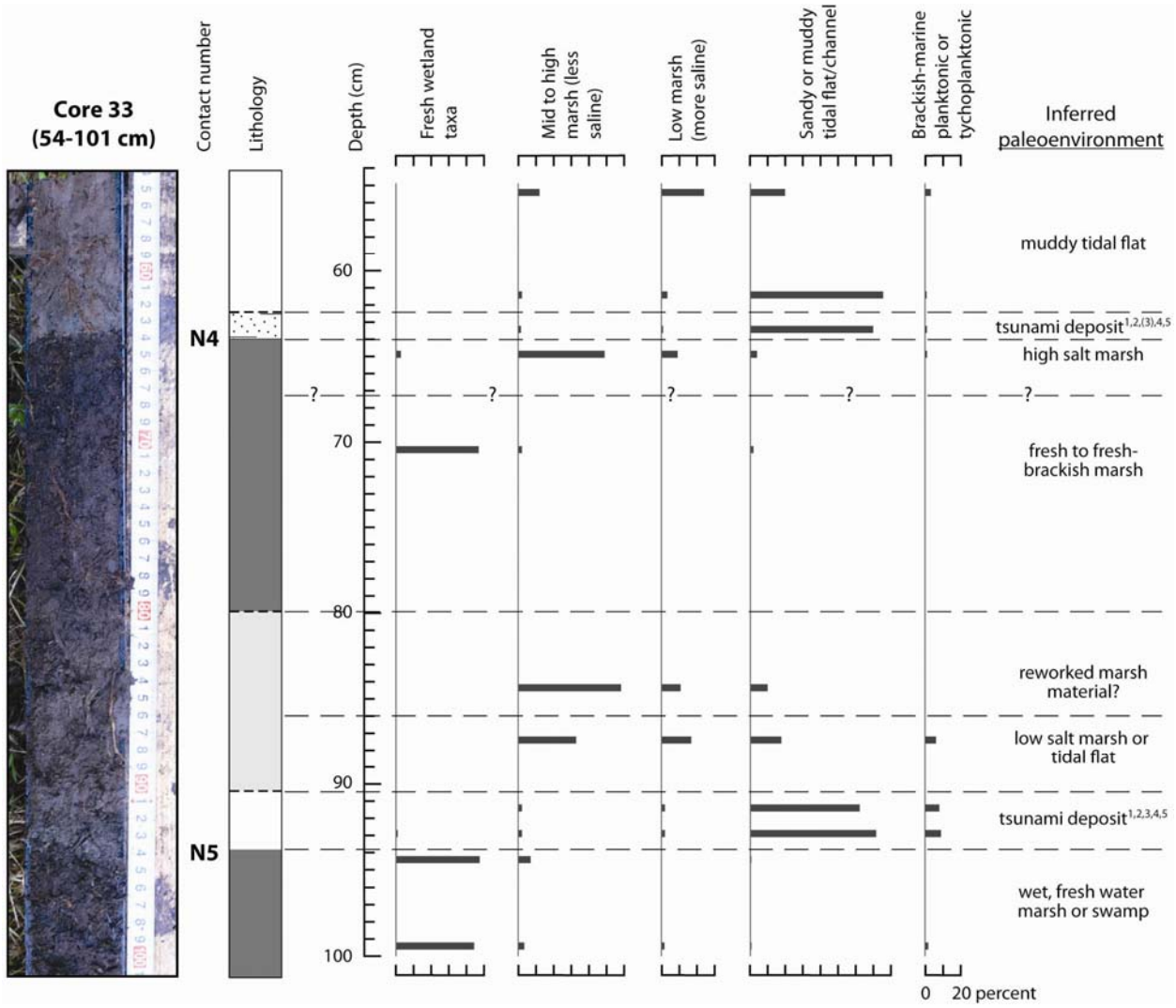

Figure 11 Frequency of diatom taxa, grouped by inferred paleoenvironment, from analyses of 11 samples from a 5-cm-diameter Russian-type sampler at core 33 along Upton Slough. Diatom frequency is expressed as a percentage of total diatoms counted in each sample (Appendix A). Numbers in far right column correspond tot characteristics of diatoms in tsunami samples as compared to non-tsunami samples listed in Table 3. The depth of contacts N4 and N5 in the Russian-type core were approximately 10 mm deeper than the same contacts observed in gouge cores used to construct Fig. 9. Photograph of Russian-type core at left; core lithology as in Fig. 10.

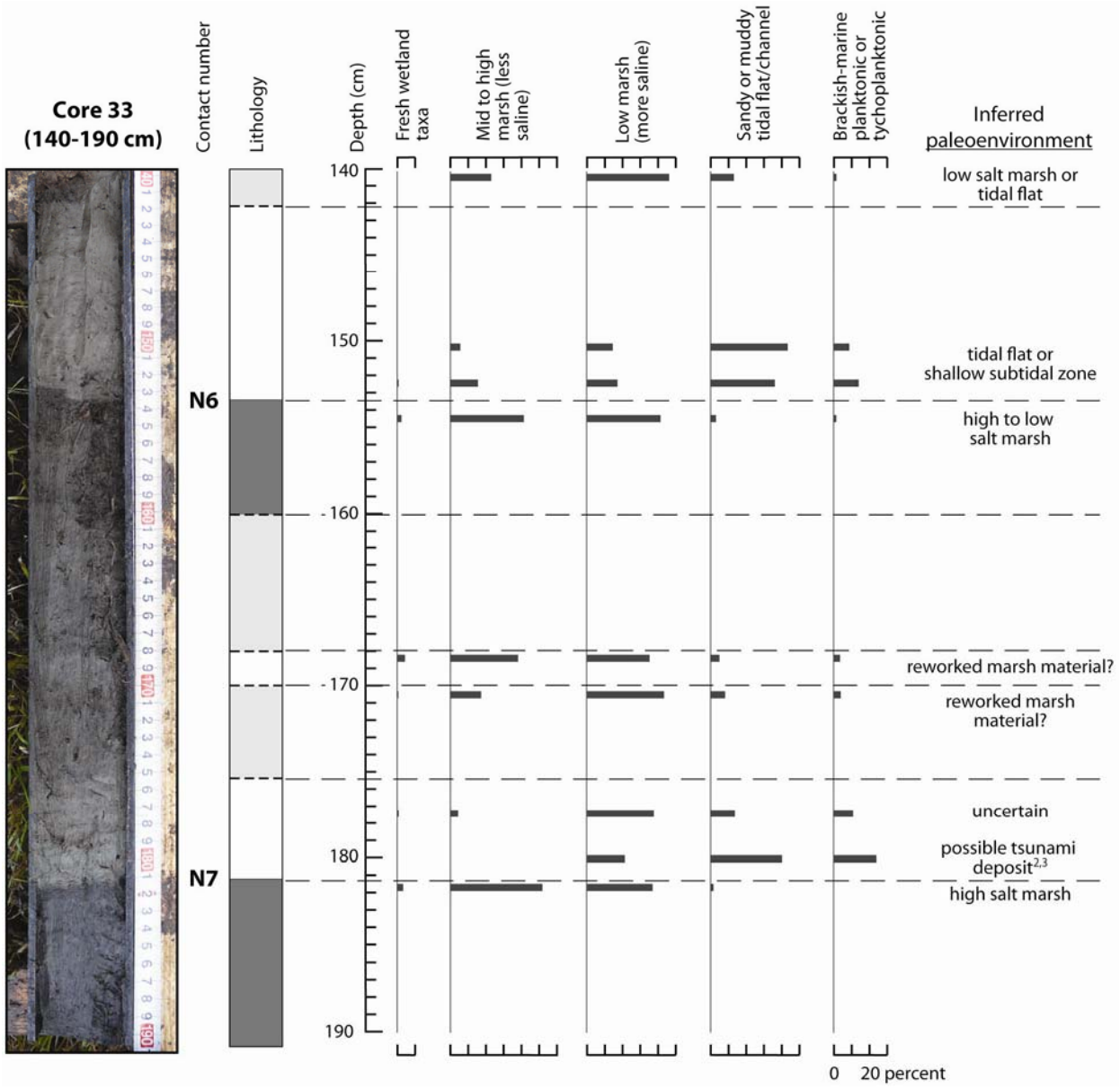

Figure 12 Frequency of diatom taxa, grouped by inferred paleoenvironment, from analyses of 9 samples from a 5-cm-diameter Russian-type sampler at core 33 along Upton Slough. Diatom frequency is expressed as a percentage of total diatoms counted in each sample (Appendix A). Numbers in far right column correspond tot characteristics of diatoms in tsunami samples as compared to non-tsunami samples listed in Table 3. The depths of contacts N6 and N7 in the Russian-type core differed by <20 mm compared to contacts observed in gouge cores used to construct Fig. 9. Photograph of Russian-type core at left; core lithology as in Fig. 10.

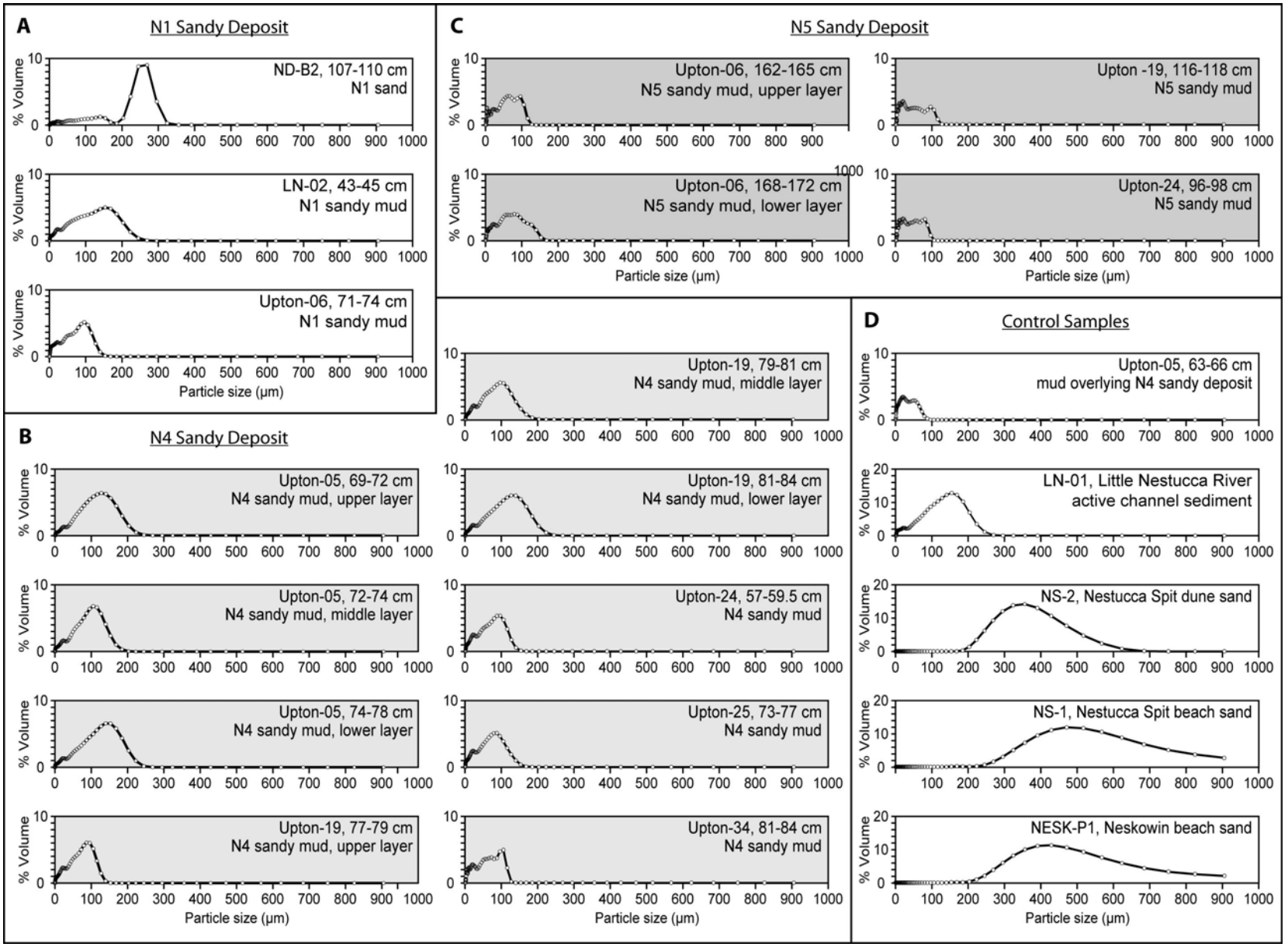
A
N1 Sandy Deposit
ND-B2, 107-110 cm
N1 sand
LN-02, 43-45 cm
N1 sandy mud
Upton-06, 71-74 cm
N1 sandy mud
B
N4 Sandy Deposit
Upton-05, 69-72 cm
N4 sandy mud, upper layer
Upton-05, 72-74 cm
N4 sandy mud, middle layer
Upton-05, 74-78 cm
N4 sandy mud, lower layer
Upton-19, 77-79 cm
N4 sandy mud, upper layer
Upton-19, 79-81 cm
N4 sandy mud, middle layer
Upton-19, 81-84 cm
N4 sandy mud, lower layer
Upton-24, 57-59.5 cm
N4 sandy mud
Upton-25, 73-77 cm
N4 sandy mud
Upton-34, 81-84 cm
N4 sandy mud
C
N5 Sandy Deposit
Upton-06, 162-165 cm
N5 sandy mud, upper layer
Upton -19, 116-118 cm
N5 sandy mud
Upton-06, 168-172 cm
N5 sandy mud, lower layer
Upton-24, 96-98 cm
N5 sandy mud
D
Control Samples
Upton-05, 63-66 cm
mud overlying N4 sandy deposit
LN-01, Little Nestucca River
active channel sediment
NS-2, Nestucca Spit dune sand
NS-1, Nestucca Spit beach sand
NESK-P1, Neskowin beach sand
% Volume
Particle size (µm)

Figure 13 (Opposite page) Particle size (μm) analyses by volume percent for selected samples of sandy sediment from surface sites and cores in the Nestucca Bay area. (A) Size distributions for sandy deposits overlying contact N1 come from two cores and an outcrop on the western margin of the Little Nestucca River (LN-02). (B) Size distributions for sandy deposits overlying contact N4 come from 5 cores along Upton Slough. (C) Size distributions for sandy deposits overlying contact N5 come from 3 cores along Upton Slough. (D) Particle size analyses for samples of sandy sediment from the beach (NS-1, NESK-P1), dune (NS-2) and the western channel margin of the Little Nestucca River (LN-01) provide a basis for comparison with samples from outcrop and cores. Analyses of mud sampled from core 5 (Upton-05) provide particle size data for sediment deposited in a muddy tidal flat.

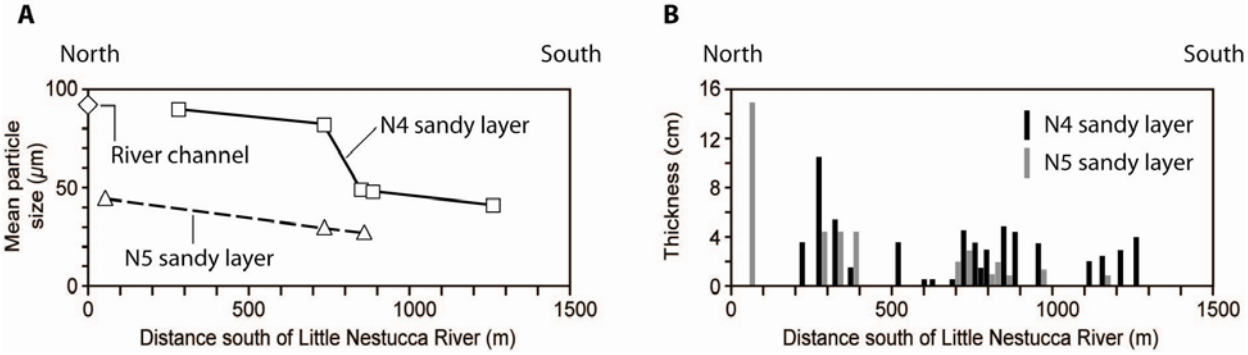

Figure 14 (A) Mean particle size versus distance from the Little Nestucca River channel for the N4 and N5 sandy layers. In both cases, sandy layers become finer grained with increasing distance from the river channel. Mean particle size of sandy sediment from the Little Nestucca River channel (open diamond) for comparison. (B) Sand layer thickness versus distance from the Little Nestucca River channel for the N4 and N5 sand layers as revealed in cores at Upton Slough (Fig. 4).

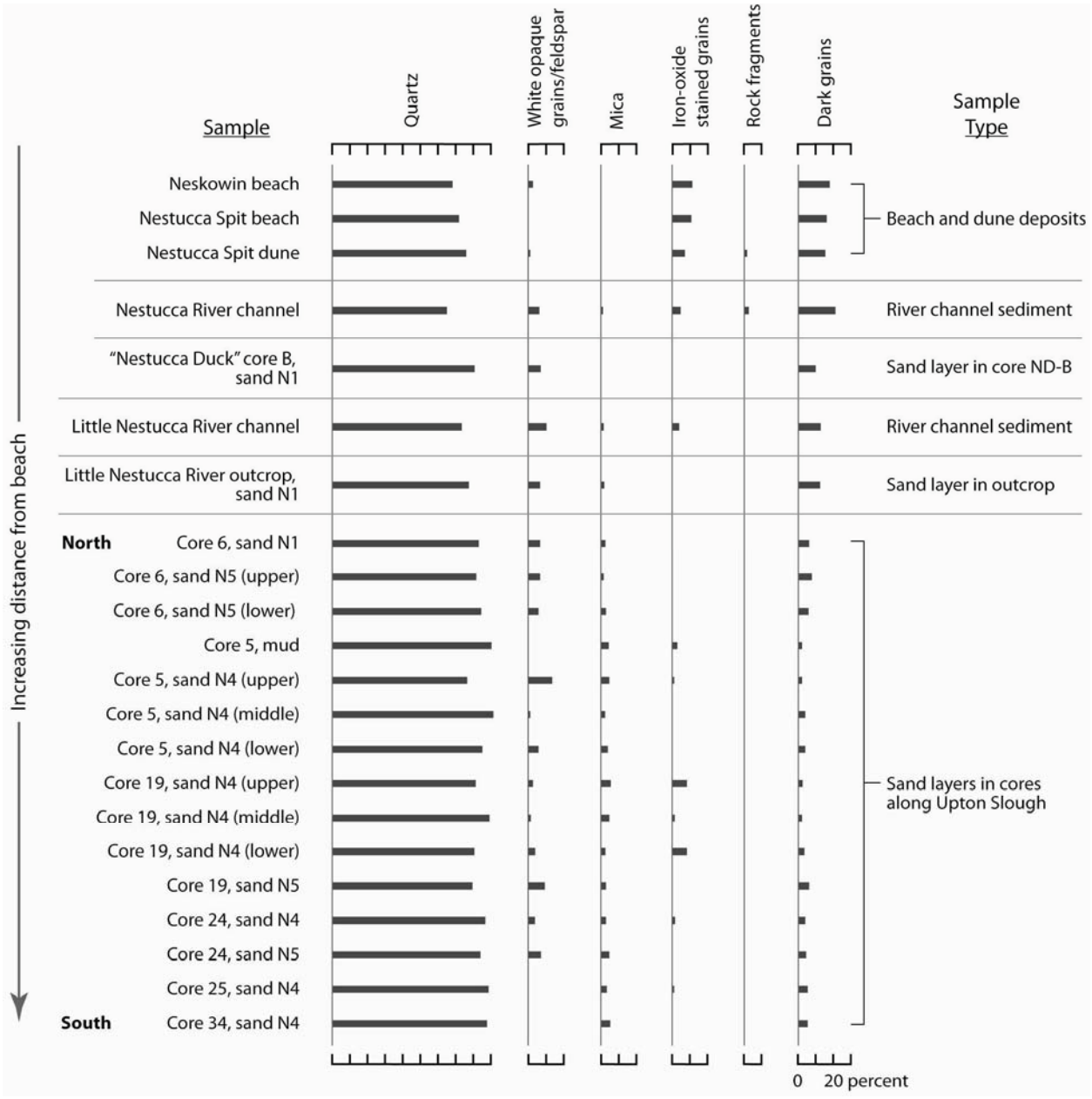

Figure 15 Frequency of constituent grains in sandy sediment from cores, outcrop and surficial deposits around Nestucca Bay. Samples are arranged vertically according to sample site proximity to the beach: samples at the top of the list are beach samples; samples at the bottom of the list are far from the beach. Analyses of sandy layers from cores are arranged vertically from north (top) to south (bottom). In general, quartz and mica sand components increased with increasing distance from the beach. We found no mica in samples of either beach or dune sand. Beach, dune and river channel sediment had higher components of dark sand grains relative to sandy layers in cores far from the beach.

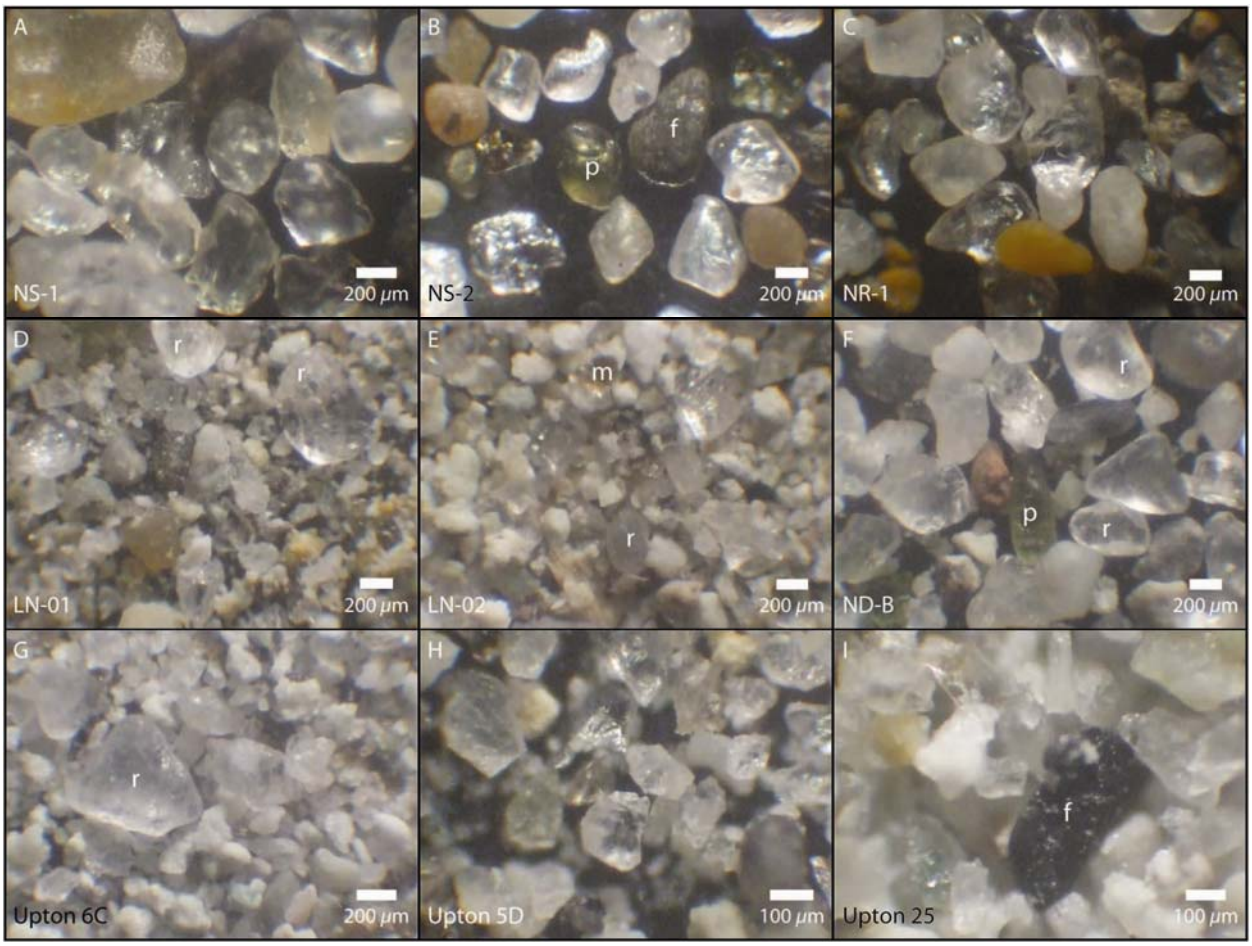

Figure 16 Selected photographs of sand grains under 3.5x and 10x magnification using a petrographic microscope. (A and B) Examples of well-rounded beach (NS-1) and dune (NS-2) sand. Conspicuous pyroxene (p) and rock fragments (f) are visible in sample NS-2. (C) Sand sampled from the Nestucca River is subrounded. (D) Very fine, predominantly angular sand from the Little Nestucca River channel near Upton Slough contains rare larger (>300 μm) rounded quartz grains (r) probably transported inland from the beach by tidal currents. (E and F) Samples of sand above contact N1 from cores close to river channels contain rounded quartz grains (r), although they are more abundant in sample ND-B and rare in sample LN-02. A rounded pyroxene (p) occurs in sample ND-B and a mica (m) grain is visible in sample LN-02. (G) Rare, subrounded (r) quartz grains were identified in sand overlying contact N5 in core 6. (H and I) Sand overlying contact N4 lacks rounded grains and consists of abundant angular quartz grains and rare rock fragments (f). Note change in scale, lower right of photos.

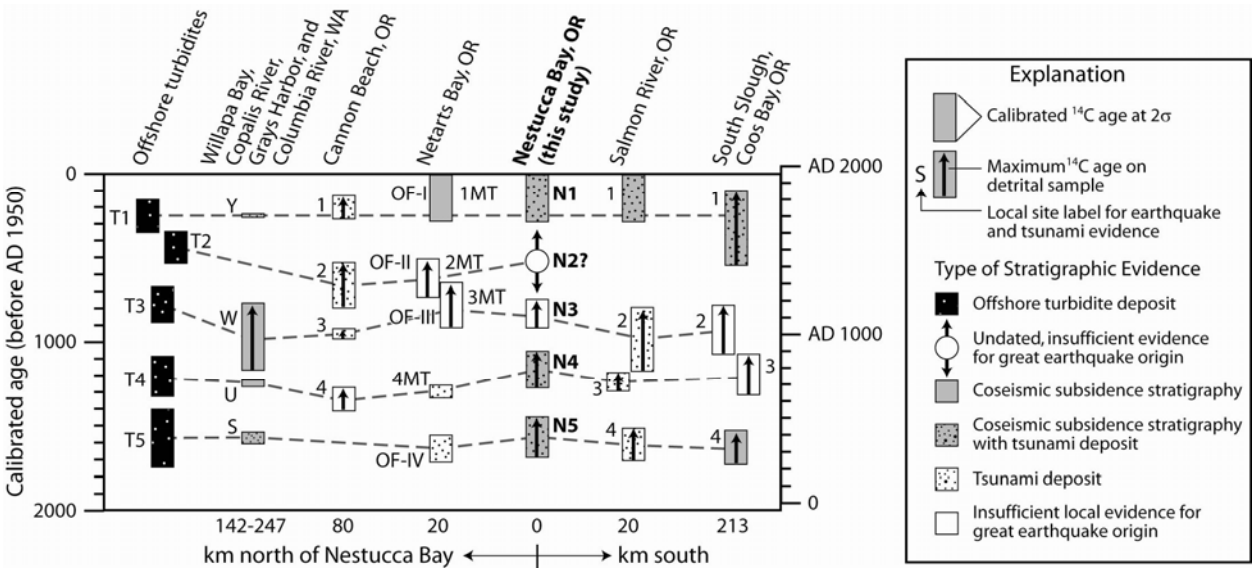

Figure 17 Comparison of calibrated ^{14}C ages and coastal evidence for great Cascadia earthquakes and tsunamis over the last two millennia at seven sites in southwestern Washington and northwestern Oregon (modified from Nelson et al., 2004). Black rectangles represent ages for offshore turbidite deposits inferred to record strong shaking during prehistoric Cascadia earthquakes (Goldfinger et al., 2009). Arrows indicate maximum limiting ^{14}C ages based on dates of detrital plant fossils and herbaceous stems rooted in marsh sediment. Ages for evidence at sites in southwestern Washington are from Atwater et al. (Atwater et al., 2003). Ages from coastal sites in Oregon come from Ecola Creek (Witter, 2008), Netarts Bay (Darienzo et al., 1994; Nelson et al., 1995; Shennan et al., 1998), Salmon River (Nelson et al., 2004; Nelson et al., 1995), and South Slough near Coos Bay (Nelson et al., 1998; Nelson et al., 1996). Local evidence for earthquake-related subsidence is lacking for one or more stratigraphic contacts at Ecola Creek, Netarts Bay and Coos Bay (e.g., Shennan et al., 1998).

APPENDIX A

UPTON SLOUGH DIATOM ANALYSES

UPTON SLOUGH DIATOM ANALYSES
For CORES 25 and 33A/33B
FINAL REPORT

October 2009

CONTENTS

FIGURES

TABLES

APPENDIXES

1 SUMMARY OF RESULTS

Diatoms were analyzed in cores 25 and 33 (sections A and B) from Upton Slough (Nestucca Bay, Oregon) for two primary purposes: (1) to reconstruct the depositional environments indicated by different lithologic units in the cores, and particularly to evaluate abrupt lithologic changes between buried soils and overlying mud or sandy mud (contacts N4-N7); and (2) to provide additional insight into possible tsunami deposition associated with each buried soil event.

I used a 2-tier approach to analyzing diatoms in the Upton Slough cores: an initial analysis at high-magnification (1250x) under oil immersion to evaluate the paleoecology for each sample; and a second analysis for select samples at low magnification (500x) to look for possible supporting evidence for tsunami deposition. High-magnification analyses are necessary for differentiating different paleoenvironments, and were informative for most samples in the 2 cores. However, these data alone are not entirely reliable for differentiating possible tsunami deposits from other kinds of deposits, particularly sandy tidal flats. Therefore, I also diatom evaluated larger diatoms at low magnification (500x) in select samples above contacts N4-N7 to look for evidence of differential fragmentation or inland transport of larger coastal planktonic or benthic taxa.

For each of the buried soil contacts in both cores, the diatom data show a distinct and lasting change from either a freshwater or salt marsh environment near of above mean higher high water to a brackish lower intertidal or shallow subtidal setting. The 2 buried soils in core 25 (contacts N4 and N5) were both high salt marshes prior to burial. In core 33, which includes 4 buried soils (contacts N4-N7), peat N7 was probably a high salt marsh, and peat N6 was a low or high salt marsh. Peat N5 in core 33 was a wet freshwater marsh or swamp: the diatoms consist of fresh to fresh-brackish taxa, and suggest at least periods of standing water. The top of peat N4 in core 33 (at 64.5-65.5 cm) contains a diatom assemblage consistent with a high salt marsh, but diatoms lower in the peat (70-71 cm) show that the site had previously been a freshwater marsh or meadow. Therefore, over time the site became more saline, but still remained a marsh environment.

To evaluate possible tsunami deposition, the results from the high-magnification analysis were supplemented with additional observations at low magnification of diatom characteristics in the first 2 or 3 samples above each buried soil contact. The diatom criteria used to attempt to differentiate tsunami from non-tsunami deposits include:
1. Severe fragmentation of pennate diatoms > 100 µm long;
2. Relatively high fragmentation of all diatom valves larger than 40 µm, particularly pennate valves > 40 µm long;
3. Relatively higher frequency of coastal marine planktonic and tychoplanktonic taxa;
4. Relatively high frequency of exceptionally large, benthic epipsammic diatoms;
5. Relatively high frequency of small epipsammic diatoms, ± evidence for enhanced preservation.

Items 1-4 are based on low-magnification counts, and item #5 is from the high-magnification counts because the smaller epipsammic diatoms are not possible to adequately document without

an oil immersion lens.

Using the criteria listed above, the diatom data suggests that there is evidence for tsunami deposition associated with contacts N4 and N5 in both cores 25 and 33, and for the single observation of contact N7 in core 33 (Table 3). There is no evidence for tsunami deposition for contact N6. Strong evidence for tsunami deposition is particularly significant for contact N5 in core 33 because the site is beyond the upvalley extent of visibly sandy, mappable deposits. The weaker, but plausible, evidence for a tsunami associated with contact N7 shows the potential for evaluating possible tsunami events in older, less well-preserved deposits.

Finally, the diatom data show that different tsunami events produce different combinations of supporting evidence. For example, diatom assemblages in both cores 25 and 33 associated with the N4 tsunami are similar to one another, but have characteristics that differentiate them from assemblages associated with the N5 tsunami. This may prove useful for correlating the same event in different locations. It is possible that different compositions of tsunami-associated assemblages from the same site can provide insight into changes in the coastal area over time; for example, whether there may have been less open connection with the ocean (as may be the case for N4) or more open connection (as possibly for N5).

2 TECHNIQUES FOR SAMPLE PROCESSING AND DATA COLLECTION

Diatom samples were processed for this study following established techniques (Hemphill-Haley, 1996; Hemphill-Haley and Lewis, 2003). The basic steps for processing sediment samples and producing diatom slides are as follows:

1. About 1 cc of sediment is soaked in approximately 10-20 ml of 30% H_2O_2 to digest organic matter, and rinsed several times with distilled water.
2. The cleaned material is then transferred to a graduated centrifuge tube, where the volume is measured.
3. The sample is diluted 10x in distilled water, and an aliquot of the suspension is transferred to a glass coverslip with a mechanical pipette.
4. The aliquot is evenly dispersed on the coverslip and allowed to dry.
5. The coverslip is then permanently affixed to a glass slide using a mounting medium designed for diatom studies (in this case, Hyrax mounting medium).

The purpose for evaluating diatoms in the Upton Slough samples was two-fold: (1) to use occurrences of paleoecologically significant diatom taxa to identify environmental changes in the stratigraphic record; and (2) to ascertain if changes in diatom assemblages could provide insight into whether or not deposits capping buried soils represented tsunami deposits. In order to accomplish this "two-fold" study, I determined that a "two-tiered" approach to analyzing diatoms would be required. First, a basic paleoenvironmental analysis would require counting diatoms at high magnification (1250x, with an oil-immersion objective) in order to accurately identify all of the most paleoenvironmentally useful taxa, many of which are quite small (most < 40 µm along their greatest axis).[1] This high-magnification analysis would also provide information about occurrences and preservation of small epipsammic diatoms, which can provide significant evidence for possible tsunami deposition (Hemphill-Haley, 1995a, 1996; Sawai et al., 2009). Following the high-magnification paleoecological analysis, a second analysis at low magnification (500x on the Olympus microscope I use) would be required to examine larger diatoms in suspect tsunami and post-tsunami samples as a means of determining if there was evidence for accumulation under turbulent (tsunami) or non-turbulent depositional processes.

For the high-magnification paleoecological analysis, I counted diatoms at 1250x along random traverses of the slide. With the exception of 2 samples with sparse, poorly preserved valves (core 25: 106 cm; core 33: 179.5 cm), I counted at least 100-150 valves in addition to the ubiquitous, heavily silcified, centric species *Paralia sulcata*. *Paralia sulcata* is very useful for recognizing marine incursions into non-marine environments (Dawson et al., 1996), but minimally informative for differentiating different kinds of estuarine deposits (Vos and de Wolf, 1993; Robinson, 1993; Atwater and Hemphill-Haley, 2000). Including *P. sulcata*, diatom counts for diatomaceous samples ranged from 107 to 547 valves. Abundance data and observations for *P. sulcata* in the Upton Slough samples are provided in Appendix 1.

For the low-magnification analysis, I focused on the possible tsunami samples and immediately

[1] Diatoms in the Upton Slough samples range in size from ~5 µm to ~280 µm, with most measuring about 10-40 µm along their greatest axis (diameter for centric valves; pervalvar (longest) axis for pennate valves). High magnification is necessary to even distinguish smaller taxa on the slide, as well as to identify most taxa to species level with any confidence.

superjacent muddy deposits. I scanned the slides at 500x, counting all intact and broken diatoms larger than 40 µm for a total of at least 100 valves per sample. The reason for focusing on larger valves, and excluding valves < 40 µm, is that many smaller diatoms (especially epipsammic taxa) form sturdy valves resilient to abrasion and breakage, as compared to many kinds of larger diatoms that are relatively more delicate and susceptible to breakage during turbulent flow. I counted both pennate and centric diatoms > 40 µm, initially to determine if there was evidence for preferential fragmentation of pennate valves over centric valves, as has been reported from other studies concerning diatom fragmentation under conditions of turbulent flow (Dawson et al., 1996) or shear stress (Scherer et al., 2004). However, these earlier studies primarily reported preferential preservation of *P. sulcata* relative to pennate diatoms, which, as noted above, is prevalent in most core samples (Appendix 1), and minimally useful for this study.[2] But occurrences of large, centric, planktonic marine diatoms in the Upton Slough samples, which were more readily observed at lower magnification, provide valuable information about the influx of marine water and have been shown to be important components of tsunami deposits (Sawai et al., 2009).

Some estuarine benthic and planktonic diatoms form narrow, elongate valves exceeding 100 µm in length, such as species of *Gyrosigma*, *Nitzschia*, and *Synedra*. Because of their large length-to-width ratios (many exceeding 20:1), they would be exceptionally prone to breakage during turbulent flow. Conversely, when they are found intact, it is good evidence for the deposit having accumulated in a relatively quiet depositional setting. Therefore, I also recorded occurrences and relative preservation of pennate diatoms > 100 µm, in order to evaluate these as a separate subset of total pennate diatoms > 40 µm. As shown below, preferential preservation of taxa > 100 mm long seems to be a significant tool for contrasting tsunami from non-tsunami estuarine deposits.

3 DATA ORGANIZATION FOR PALEOECOLOGICAL ANALYSES

For the high-magnification paleoecological analyses, the diatom data were first organized based on general salinity tolerances or preferences, and secondly subdivided by general preferences (where possible) for different coastal and estuarine environments.

3.1 General salinity groups

Diatoms tallied for the high-magnification paleoecological analyses were assigned to 1 of 3 general salinity groups based on standard references (e.g., Krammer and Lange-Bertalot, 1986, 1988, 1993a, b; Vos and de Wolf, 1993; Snoeijs, 1993; Snoeijs et al., 1994, 1995, 1996, 1998; Witkowski et al., 2000) and my own professional experience working with diatoms from numerous coastal localities in California, Oregon, Washington, and Alaska.

General salinity groups used for this study are: (1) Fresh or fresh-brackish diatoms; (2) Brackish-fresh diatoms; and (3) Brackish-marine or marine diatoms (Appendix 2).

[2] It is possible that abundant, well-preserved valves of *P. sulcata* in sandy mud capping peat N4 is evidence for rapid burial and preservation, which is also supported by superior preservation of other benthic diatoms in the sample (see also Appendix 1).

Group 1 diatoms (fresh or fresh-brackish) include species that would be found in freshwater marshes or other wet environments protected from salt water or tidal influence.

Group 2 diatoms (brackish-fresh) are oligohalobous ("indifferent") taxa, meaning they can tolerate a wide range of salinities from fresh to strongly brackish. Some species in this group are particularly indicative of high marshes, which, in addition to being able to tolerate a wide range of salinities (due to more or less frequent tidal inundation), commonly have sturdy valves to allow them to survive subaerial exposure.

Group 3 diatoms (brackish-marine or marine) are coastal and estuarine taxa that are indicative of:
(a) lower intertidal or shallow subtidal settings that experience higher average salinities and more reworking by tidal action than would occur on high marshes (tidal flats, shallow channels, low marshes)
(b) coastal marine planktonic or tychoplanktonic environments. *Tychoplanktonic* refers to taxa that are primarily benthic, but are easily suspended and therefore also commonly found in the plankton.

3.2 Paleoenvironmental groups

In additional to general salinity groups, diatoms were assigned to general paleoenvironmental groups when possible, based on the standard references noted above plus published and unpublished empirical data showing the preferences for some taxa to thrive in certain environmental settings in the Pacific Northwest (McIntire and Overton, 1971; Whiting and McIntire, 1985; Hemphill-Haley, 1993a, b; 1995b; 2006; and unpublished data; Nelson and Kashima, 1993; Hemphill-Haley and Lewis, 1995; Nelson et al., 2000; Sawai and Nagumo, 2003). The paleoenvironmental groups used for this study are: (1) freshwater marsh or swamp; (2) high salt marsh; (3) low salt marsh; (4) sandy or muddy tidal flat/shallow channel; (5) brackish-marine planktonic or tychoplanktonic; (6) Miscellaneous – not assigned to any empirical group (Appendix 3). Note that the environments easiest to differentiate based on diatoms are freshwater marshes swamps, and high salt marshes. In contrast, the low marsh environment is very difficult to differentiate from tidal flats because of the amount of tidal mixing, and for this reason some researchers don't attempt to subdivide the two intertidal environments (e.g., Nelson et al. 2000)

4 RESULTS PART I: PALEOENVIRONMENTAL EVALUATION BASED ON DIATOM ANALYSES COMPLETED AT HIGH-MAGNIFICATION

4.1 Core 25

Core 25 was collected at the northwestern margin of Upton Slough approximately 0.85 km from Nestucca Bay and the Little Nestucca River. The section of core evaluated for diatoms is 0.5 m long, showing the subsurface stratigraphy from about 64 cm to 112 cm below the modern surface. Core 25 includes 2 bold, buried peats (contacts N4 and N5). The top of peat N4 is at about 72 cm; the top of peat N5 is at approximately 105.5 cm. Both peats N4 and N5 show

abrupt upper contacts with overlying sandy mud. Diatom analyses for core 25 are summarized in Figures 1-4 and Table 1.

4.1.1 Core 25: diatom abundance

Diatoms are abundant and diverse in all of the core 25 samples with the exception of the sample from peat N5 at 106-107 cm (Figure 1). The other samples in the core, including peat N4, contain more than 2 million diatom valves per cc of sediment, but diatoms in peat N5 peat are rare and poorly preserved (showing evidence for dissolution, as further discussed below).

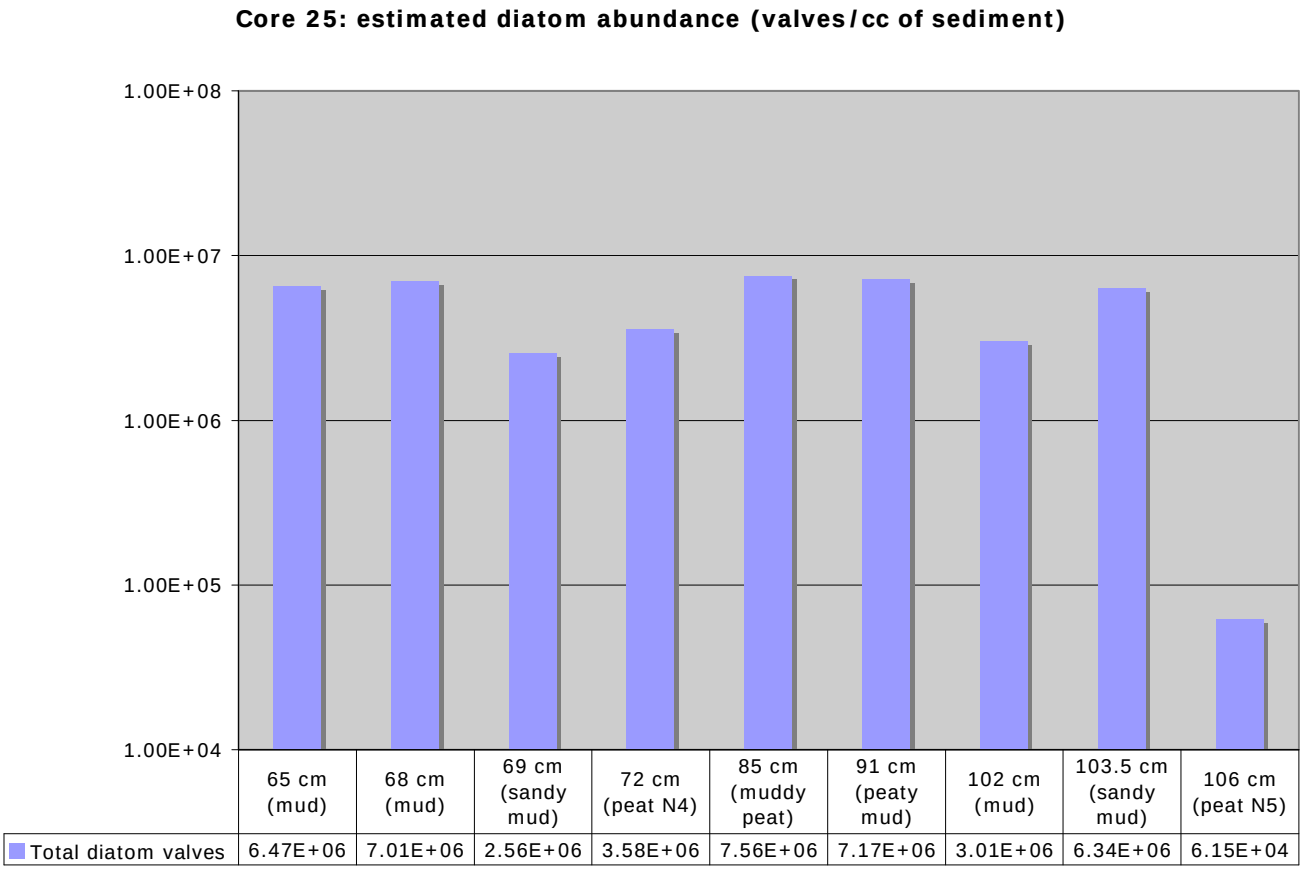

Figure 1. Core 25: estimated diatom abundances (valves/cc of sediment).

4.1.2 Core 25: salinity groups

In general, the results for core 25 show that Group 2 diatoms (brackish-fresh) dominate in peaty samples, supporting accumulation in a brackish marsh setting, and Group 3 taxa (brackish marine or marine) dominate in muddy samples, consistent with accumulation in a lower intertidal depositional environment (Figure 2). Group 1 (freshwater) taxa occur in small numbers in all samples, but there is no evidence for an established freshwater environment at any sampled horizon in the core.

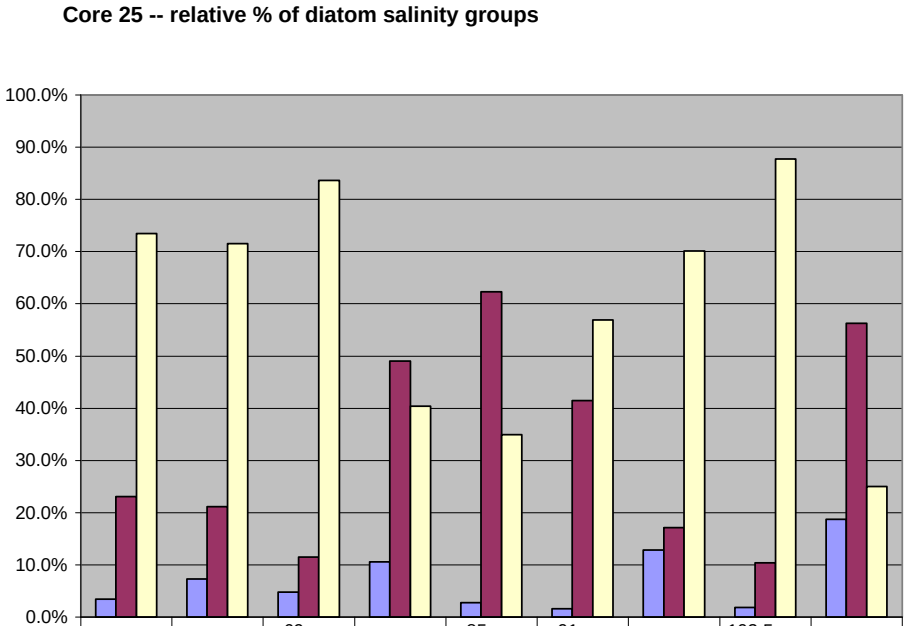

	65 cm (mud)	68 cm (mud)	69 cm (sandy mud)	72 cm (peat N4)	85 cm (muddy peat)	91 cm (peaty mud)	102 cm (mud)	103.5 cm (sandy mud)	106 cm (peat N5)
GROUP 1 Fresh or fresh-brackish diatoms	3.4%	7.3%	4.8%	10.6%	2.7%	1.6%	12.8%	1.9%	18.8%
GROUP 2 Brackish-fresh diatoms	23.1%	21.2%	11.5%	49.0%	62.3%	41.5%	17.1%	10.4%	56.3%
GROUP 3 Brackish-marine or marine diatoms	73.5%	71.5%	83.7%	40.4%	34.9%	56.9%	70.1%	87.7%	25.0%

Figure 2. Core 25: relative % of general diatom salinity groups.

4.1.3 Contact N4 in core 25

Contact N4 in core 25 is an abrupt boundary between a well-developed peat (peat N4) and overlying sandy mud inferred to be a possible tsunami deposit (Figure 3). The top of peat N4 is visible in core 25 at about 72 cm. The well-developed peat is about 10 cm thick, grading downward to muddy peat at about 82-83 cm, which then grades to less organic mud at about 90 cm. The muddy peat and peat are dominated by brackish-fresh diatoms (Figure 2), and diatoms from a sample near the top of the peat at 72-73 cm indicate a high salt marsh environment (Figure 3). Possible frequent tidal inundation of the marsh surface is suggested by common occurrences of lower intertidal taxa mixed with high marsh taxa. Diatoms in mud at 91-92 cm indicate a muddy estuarine tidal flat, and the assemblage at 85-86 cm may indicate a transitional low to high marsh, evidenced by a mix of both well preserved marsh taxa and tidal flat taxa. Based on the diatom data, the transition up-section from mud at 92 cm to the top of the peat at 72 cm is consistent with transition over time from a lower intertidal flat to a salt marsh near or above mean higher high water.

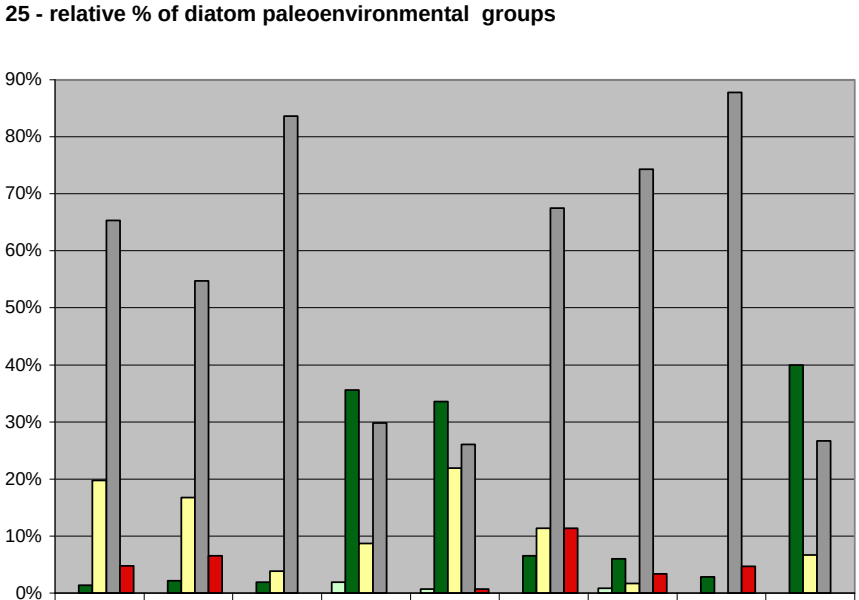

	65 cm (mud)	68 cm (mud)	69 cm (sandy mud)	72 cm (peat N4)	85 cm (muddy peat)	91 cm (peaty mud)	102 cm (mud)	103.5 cm (sandy mud)	106 cm (peat N5)
Fresh wetland taxa	0.0%	0.0%	0.0%	1.9%	0.7%	0.0%	0.9%	0.0%	0.0%
Mid to high marsh (less saline)	1.4%	2.2%	1.9%	35.6%	33.6%	6.5%	6.0%	2.8%	40.0%
Lower marsh (more saline)	19.7%	16.8%	3.8%	8.7%	21.9%	11.4%	1.7%	0.0%	6.7%
Sandy or muddy tidal flat/channel	65.3%	54.7%	83.7%	29.8%	26.0%	67.5%	74.4%	87.7%	26.7%
Brackish/marine planktonic or tychoplanktonic	4.8%	6.6%	0.0%	0.0%	0.7%	11.4%	3.4%	4.7%	0.0%

Figure 3. Core 25: relative % of diatom paleoenvironmental groups.

At a minimum, diatoms in the sandy mud and mud above peat N4 in core 25 indicate an abrupt and lasting transition from a high salt marsh to a lower intertidal or shallow subtidal environment (Figure 3). Tsunami deposition for the sandy mud immediately above the soil (69-70 cm) is suggested by relatively abundant and unusually well-preserved benthic tidal flat diatoms, including diverse small epipsammic species (Figure 4). Additional evidence for tsunami deposition, as further described in Section 5, includes fragmentation of larger pennate valves and influx of well-preserved specimens of exceptionally large epipsammic taxa.

Diatoms in muddy samples overlying the tsunami layer (at 65-66 cm and 67-68 cm) are consistent with deposition on a muddy estuarine tidal flat. Presence of well-preserved elongate taxa (*Nitzschia sigma*, *Gyrosigma wansbeckii*) suggests a relatively quiet depositional setting with minimal reworking. Other prominent taxa, including *Caloneis westii* and *Navicula digitoradiata*, are common in both low marsh and tidal flat environments.

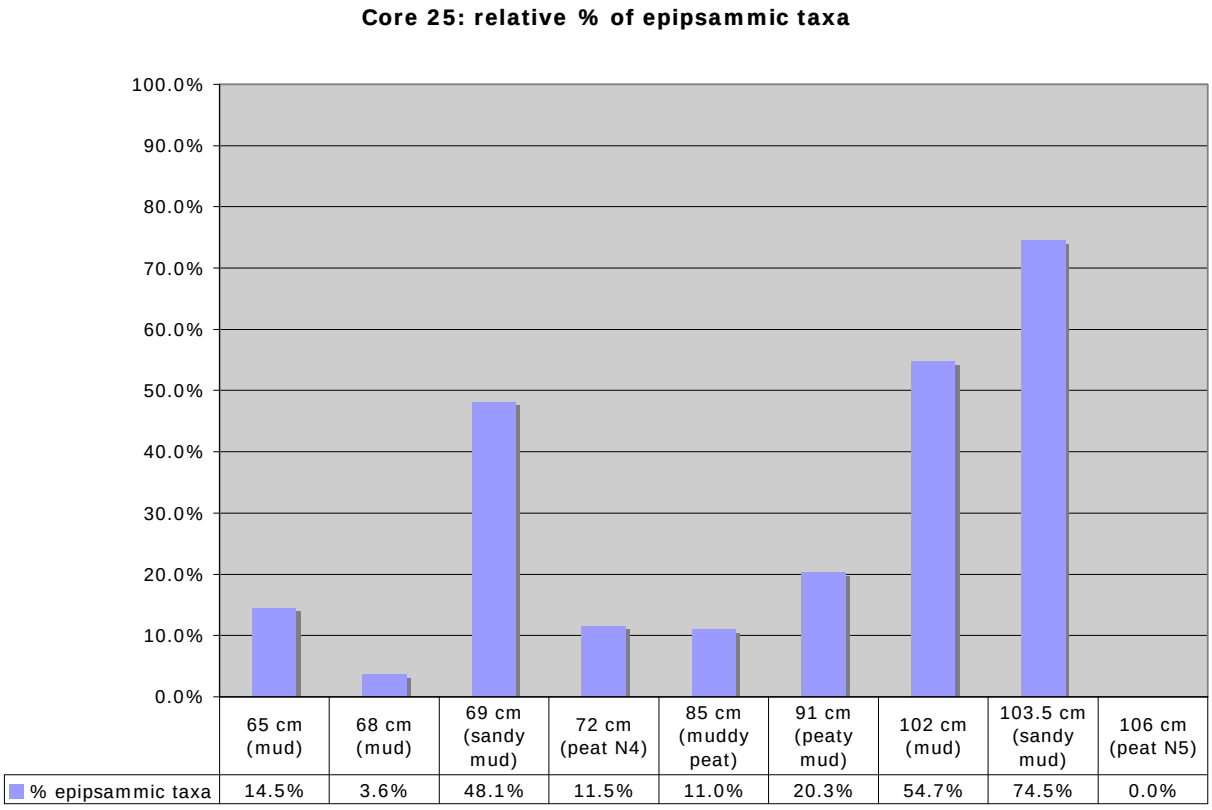

Figure 4. Core 25: relative % of epipsammic diatoms.

4.1.4 Contact N5 in core 25

Contact N5 in core 25 is a sharp contact between a well-developed peat (peat N5) and a superjacent deposit of sandy mud inferred to be a possible tsunami deposit. Peat N5 extends from the base of the core at 112 cm to about 105.5 cm. Based on diatoms observed near the top of the peat at 106-107 cm, the peat likely developed in a salt marsh environment. Diatoms are very rare in the sample (Figure 1), but primarily include taxa common to salt marshes (Figure 3). These results are a bit tenuous as the interpretation is based on a count of only 17 diatoms, but the absence of freshwater taxa supports a brackish rather than freshwater environment during the soil development.

The poor diatom preservation in peat N5 is the result of severe valve dissolution. Rather than showing evidence for mechanical breakage, the diatom valves show loss of silica around the edges, and in some cases only the most heavily silicified, central raphe areas are still intact. Strong diatom dissolution is not typical for well-preserved buried soils in Pacific Northwest coastal deposits, and in fact similar dissolution is not evident in peat N4 in core 25, or in 4 buried peats examined in core 33 (Section 6). Therefore, the condition of the diatoms in peat N5 in core 25 is atypical, and may provide additional insight into the paleoecology of the deposit.

Diatoms dissolve most readily in alkaline conditions, and in environmental settings in which there is an undersaturation of silica. Alkaline conditions can be ruled out for the organic-rich

buried soil, so silica undersaturation is the likely cause for diatom dissolution in peat N5. Based on work by Andrejko and Cohen (1984) on diatoms in peats from the Okefenoke swamp/marsh, the severe dissolution in peat N5 could be the result of utilization of available silica by organisms in the marsh soil. Andrejko and Cohen showed that in soils with persistent atmospheric exposure but limited minerogenic inputs – as would be the case for a marsh that became isolated from regular tidal inundation to deliver new sources of silica, including mineral particles and transported diatoms – silica utilization by biological organisms leads to silica undersaturation and accelerated diatom dissolution. It is possible, therefore, that prior to subsidence and burial of peat N5, the marsh had built up above the reach of tides, or was otherwise blocked by regular tidal or other flooding. The fact that diatoms are not similarly dissolved in the sandy mud and mud overlying peat N5 suggests that the valve dissolution was part of the processes taking place in the soil prior to subsidence and burial of the marsh.

Above peat N5, diatoms were analyzed in sandy mud at 103.5-104.5 cm and mud at 102-103 cm (Figure 3). The diatom assemblage in the sandy mud is dominated by taxa found on sandy tidal flats/channels (Figure 3). Small epipsammic species compose 74.5% of the assemblage (Figure 4). The epipsammon are relatively well preserved (including many examples of taxa < 10 µm long still attached to sand grains), but otherwise preservation is poor with abundant broken diatom valves. At a minimum, the diatom results show that:
1. there was a distinct change in environment from a high marsh (or possibly supratidal marsh/meadow, based on evidence for silica leaching and dissolution of diatom valves) to a lower intertidal flat or subtidal zone;
2. the sandy deposit is inconsistent with with downstream (freshwater) flooding;
3. the sand originated in a brackish-marine aquatic setting capable of supporting diatom populations (i.e., is inconsistent with beach backshore or dune origin, where high concentrations of pristine epipsammic diatoms would not be found).

A tsunami origin for the sandy mud is supported by the diatom data. In addition to excellent preservation of dominant epipsammic taxa, which suggests rapid redeposition and burial of a modern assemblage (Hemphill-Haley, 1995, 1996; Sawai et al., 2006), there is evidence for severe fragmentation of larger benthic diatoms and frequent occurrences of large planktonic taxa, which supports turbulent redeposition of material from a marine source, rather than *in situ* accumulation on a sandy tidal flat. These observations are further explained in Section 5.

In contrast to the sandy mud, the overlying mud sample at 102-103 cm more likely represents an *in situ* tidal flat deposit, based on occurrences of large, elongate tidal flat diatoms that would not survive turbulent transport intact. The sample also contains abundant “background” diatom fragments, typical of tidal flat material, and small epipsammic diatoms remain prominent (about 55%; Figure 4).

4.1.5 Paleoenvironmental summary for core 25

Inferred paleoenvironments for core 25 samples are shown in Table 1.

Table 1. Core 25: inferred paleoenvironments based on high-magnification diatom analyses**.**

Depth in core (cm)	Lithology	Inferred paleoenvironment	Comments
65-66	Mud	Muddy tidal flat	Well preserved large valves of elongate diatoms (*Nitzschia sigma, Gyrosgima wansbeckii*) suggests relatively quiet depositional setting with minimal reworking
68-69	Mud	Muddy tidal flat	*Navicula digitoradiata* common as below, plus common *Caloneis westii*.
69-70	Sandy mud	Tsunami	Well-preserved sandy tidal flat material; consistent with tsunami deposition. Diatom preservation unusually good, with common intact frustules of taxa indicative of brackish marine sandy environments: *Navicula digitoradiata, Catenula adhaerens, Dimmeragramma minor, Plagiogramma staurophorum, Trachysphenia australis, Coccoenis neothumensis*. Also, a few large intact valves of *Cerataulus turgidus* (large centric epipsammic diatom).
72-73	Peat (N4)	High marsh	Well preserved high marsh taxa are prominent (*Cosmioneis pusilla, Pinnularia lagerstedtii*).
85-86	Muddy peat	Low to high marsh	Includes mix of well-preserved high marsh spp. (e.g. *Cosmioneis pusilla, Pinnularia lagerstedtii, Diploneis pseudovalis*) and common low marsh taxa (particularly *Diploneis interrupta*, plus *Caloneis westii, Diploneis smithii* v. *rhombica*).
91-92	Peaty mud	Muddy tidal flat or marsh/tidal flat transition	Diatoms abundant and well preserved, and consistent with deposition in a lower intertidal environment. Common taxa include: *Navicula* cf. *vaneei*, plus prominent *Thalassiosira* spp., *Tryblionella* spp., *Actinoptychus senarius, Melosira moniliformis*. Marsh-related taxa are much less frequent than in the overlying muddy peat sample.
102-103	Mud	Tidal flat	Assemblage includes prominent small pennate taxa indicative of sandy environments. Relatively quiet depositional setting indicated by occurrences of large, well preserved diatoms with elongate valves, particularly *Gyrosigma peisonis*. In contrast to some well-preserved valves, diatom fragments compose a large percentage of background sediment.
103.5-104.5	Sandy mud	Tsunami	Sample dominated by well-preserved epipsammic diatoms; no large intact pennate diatoms observed.
106-107	Peat (N5)	High marsh	Diatoms very rare, but included poorly preserved salt marsh taxa (no freshwater taxa observed).

4.2 Core 33 (sections A and B)

Cores 33A and 33B are each about 0.5 m long, and show the subsurface stratigraphy down to about 190 cm (core 33A extends from 0.54 cm to 154 cm; core 33B extends from about 140 cm to 190.5 cm). Each core includes 2 bold peats: section A includes peats N4 and N5; section B contains peats N6 and N7. Of the 4 buried soil contacts, sand is only visible above peat N4. Core 33B also includes a muddy peat zone at 170 cm that was evaluated as a possible, additional marsh deposit. Diatom analyses for core 33 are summarized in Figures 5-10 and Table 2.

4.2.1 Core 33: diatom abundance

Diatoms are present in all samples in core 33, and relatively abundant (exceeding 1 million valves/cc of sediment) with the exception of the assemblage in the muddy sample capping peat N7 at 179.5-180.5 cm (Figures 5a, 5b). Diatoms are relatively rare in this sample (~5.5 x 10^5 valves/cc of sediment), and show evidence for dissolution in addition to fragmentation. Of interest, however, is that although diatoms in this sample are rare overall, there are a few well-preserved marine planktonic species (*Actinocyslus* sp., *Thalassionema nitzschioides*, *Thalassiosira* cf. *pacifica*). Other diatoms are poorly preserved, showing strong valve dissolution, including *Paralia sulcata* and lower intertidal benthic taxa including *Caloneis westii*. Three of the core 33 samples have greater than 10 million diatom valves/cc of sediment, including the sandy mud sample capping peat N4. Estimated diatom abundance for this sample is > 1.9 x 10^7 valves/cc of sediment, and it contains abundant well-preserved diatoms—particularly small epipsammic taxa—consistent with rapid entrainment and burial by a tsunami.

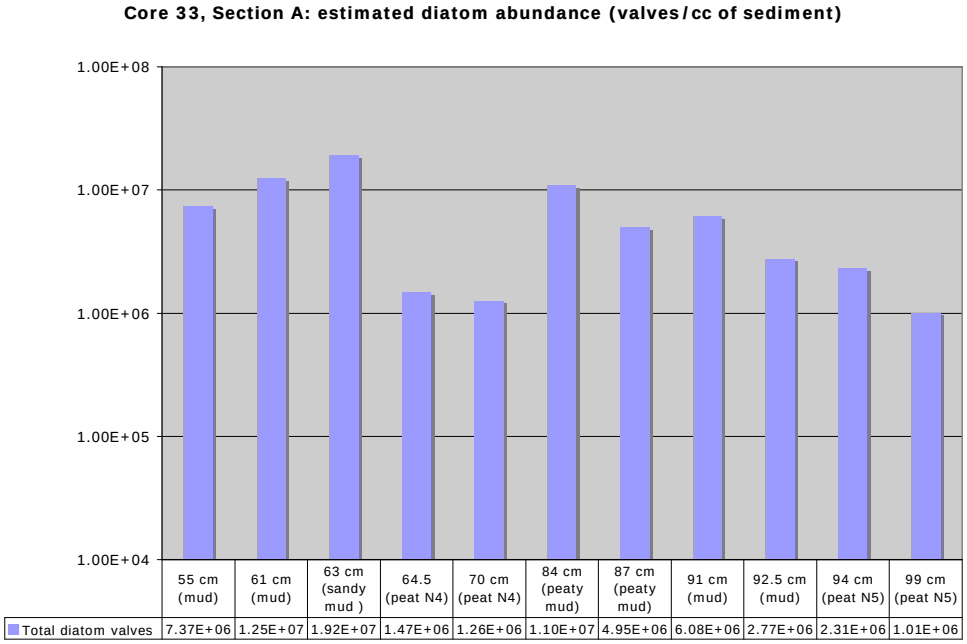

Figure 5a. Core 33A: estimated diatom abundances (valves/cc of sediment).

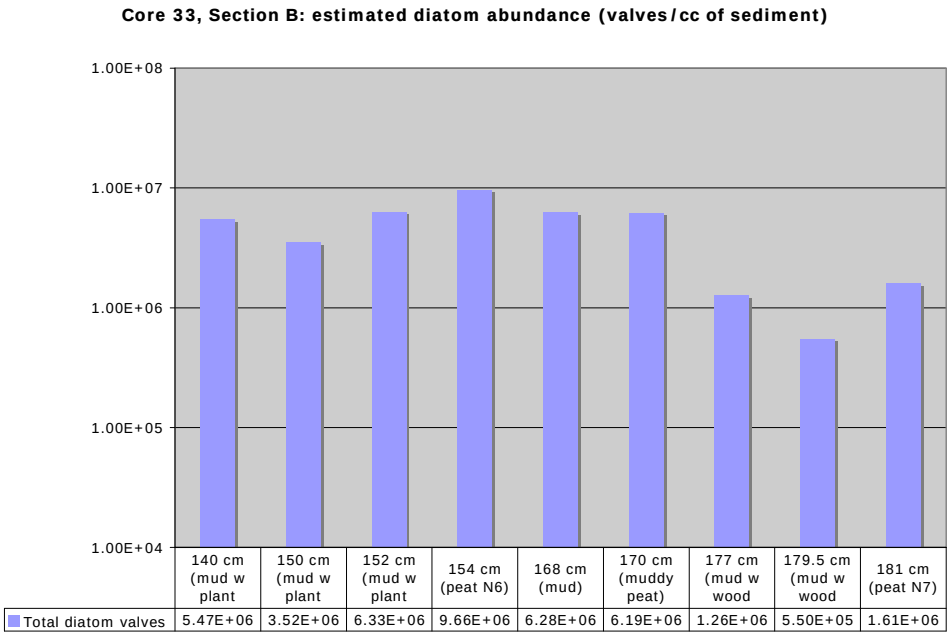

Figure 5b. Core 33B: estimated diatom abundances (valves/cc of sediment).

4.2.2 Core 33: salinity groups

In contrast to core 25, diatoms in core 33 show that there were 2 periods of relatively freshwater conditions during peat accumulation: peat N5 (94 and 99 cm) and the middle part of peat N4 at 70 cm (Figures 6a, 6b). Otherwise, Group 2 diatoms (brackish-fresh) dominate in peaty samples (top of peat N4, plus peats N6 and N7), indicating salt marsh conditions, and Group 3 taxa (brackish marine or marine) dominate in muddy samples, consistent with accumulation in a lower intertidal or shallow subtidal depositional environment. As in core 25, Group 1 (freshwater) taxa occur in small numbers in all samples, but only dominate in the three sample horizons noted above.

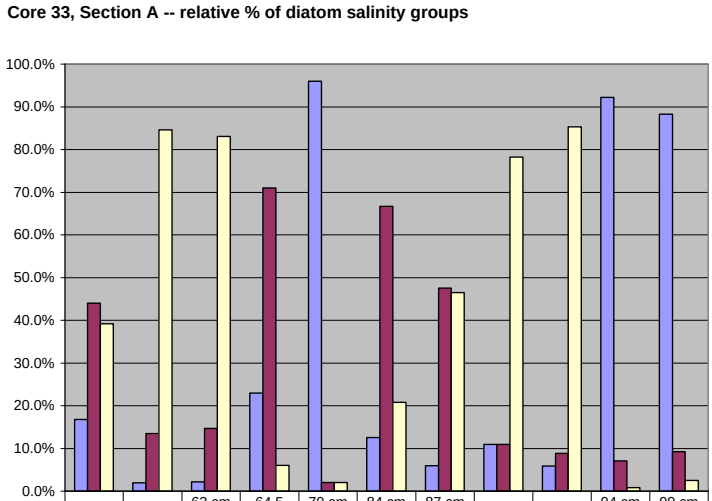

	55 cm (mud)	61 cm (mud)	63 cm (sandy mud)	64.5 (peat N4)	70 cm (peat N4)	84 cm (peaty mud)	87 cm (peaty mud)	91 cm (mud)	92.5 cm (mud)	94 cm (peat N5)	99 cm (peat N5)
GROUP 1 Fresh or fresh-brackish diatoms	16.8%	1.9%	2.2%	23.0%	96.0%	12.5%	5.9%	10.9%	5.9%	92.2%	88.2%
GROUP 2 Brackish-fresh diatoms	44.0%	13.5%	14.7%	71.0%	2.0%	66.7%	47.5%	10.9%	8.8%	7.0%	9.2%
GROUP 3 Brackish-marine or marine diatoms	39.2%	84.6%	83.1%	6.0%	2.0%	20.8%	46.5%	78.2%	85.3%	0.8%	2.5%

Figure 6a. Core 33A: relative % of general diatom salinity groups.

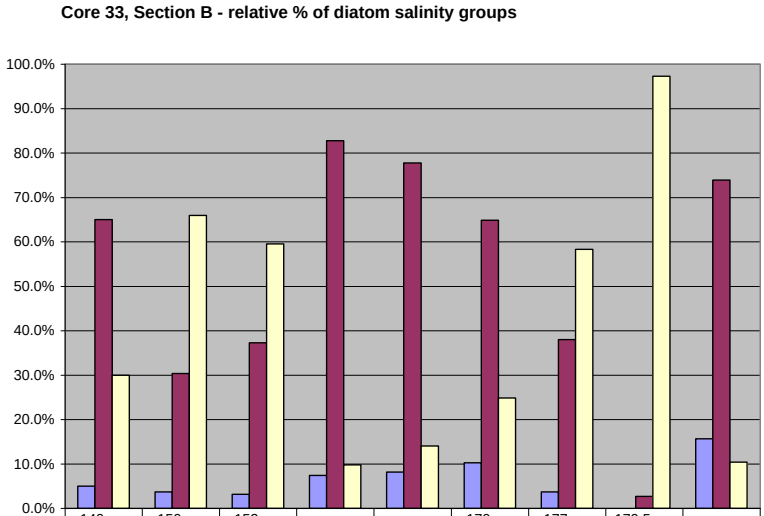

	140 cm (mud w plant frags)	150 cm (mud w plant frags)	152 cm (mud w plant frags)	154 cm (peat N6)	168 cm (mud)	170 cm (muddy peat)	177 cm (mud w wood	179.5 cm (mud w wood	181 cm (peat N7)
Fresh or fresh-brackish diatoms	5.0%	3.7%	3.2%	7.4%	8.1%	10.3%	3.7%	0.0%	15.7%
Brackish-fresh diatoms	65.0%	30.4%	37.3%	82.8%	77.8%	64.8%	38.0%	2.7%	73.9%
Brackish-marine or marine diatoms	30.0%	65.9%	59.5%	9.8%	14.1%	24.8%	58.3%	97.3%	10.4%

Figure 6b. Core 33B: relative % of general diatom salinity groups.

4.2.3 Contact N4 in core 33A

Peat N4 is visible in the core 33A photo between about 64 and 80 cm, with a zone of brown-gray peaty mud between about 80 cm and 90 cm. Two samples from the peaty mud (84 cm and 87 cm) contain diatoms consistent with a salt marsh environment, including *Cosmioneis pusilla*, *Pinnularia lagerstedtii*, and *Luticola mutica*. A high marsh is also indicated for the uppermost

peat sample at 64.5 cm (Figure 7). The intervening peat sample, at 70 cm, is anomalous because it includes species that are indicative of fresher conditions than indicated in the samples above and below. Whereas the sample in the uppermost peat contains diatoms that can tolerate fluctuating salinities in an estuarine environment, the sample at 70 cm suggests an environment protected from the influx of salt water.

Diatoms in the sandy mud and mud above peat N4 suggest a transition from a high salt marsh to a tidal flat or shallow subtidal environment (Figure 7). Supporting evidence for the sandy mud at 63 cm representing a tsunami deposit is suggested by relatively abundant and unusually well-preserved benthic tidal flat diatoms. Small epipsammic diatoms account for 69.1% of the assemblage (Figure 8), and are very well preserved with some valves still attached to sand grains.

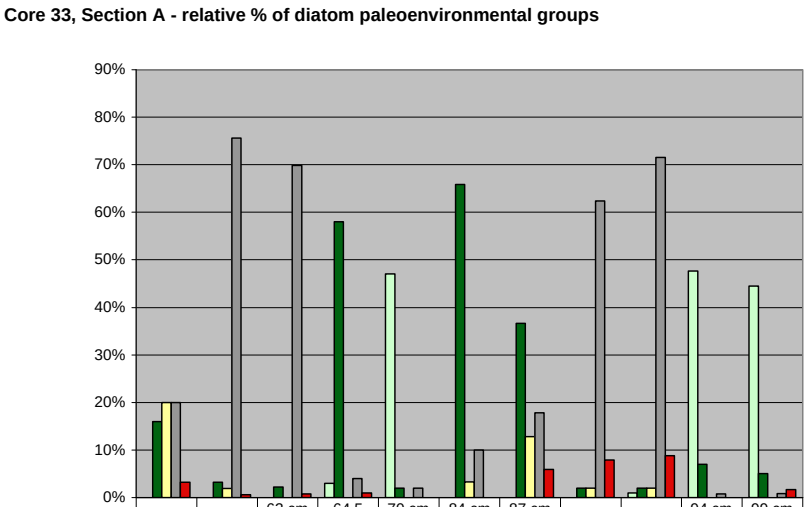

	55 cm (mud)	61 cm (mud)	63 cm (sandy mud)	64.5 (peat N4)	70 cm (peat N4)	84 cm (peaty mud)	87 cm (peaty mud)	91 cm (mud)	92.5 cm (mud)	94 cm (peat N5)	99 cm (peat N5)
Fresh wetland taxa	0.0%	0.0%	0.0%	3.0%	47.0%	0.0%	0.0%	0.0%	1.0%	47.7%	44.5%
Mid to high marsh (less saline)	16.0%	3.2%	2.2%	58.0%	2.0%	65.8%	36.6%	2.0%	2.0%	7.0%	5.0%
Lower marsh (more saline)	20.0%	1.9%	0.0%	0.0%	0.0%	3.3%	12.9%	2.0%	2.0%	0.0%	0.0%
Sandy or muddy tidal flat/channel	20.0%	75.6%	69.9%	4.0%	2.0%	10.0%	17.8%	62.4%	71.6%	0.8%	0.8%
Brackish/marine planktonic or tychoplanktonic	3.2%	0.6%	0.7%	1.0%	0.0%	0.0%	5.9%	7.9%	8.8%	0.0%	1.7%

Figure 7. Core 33A: relative % of diatom paleoenvironmental groups.

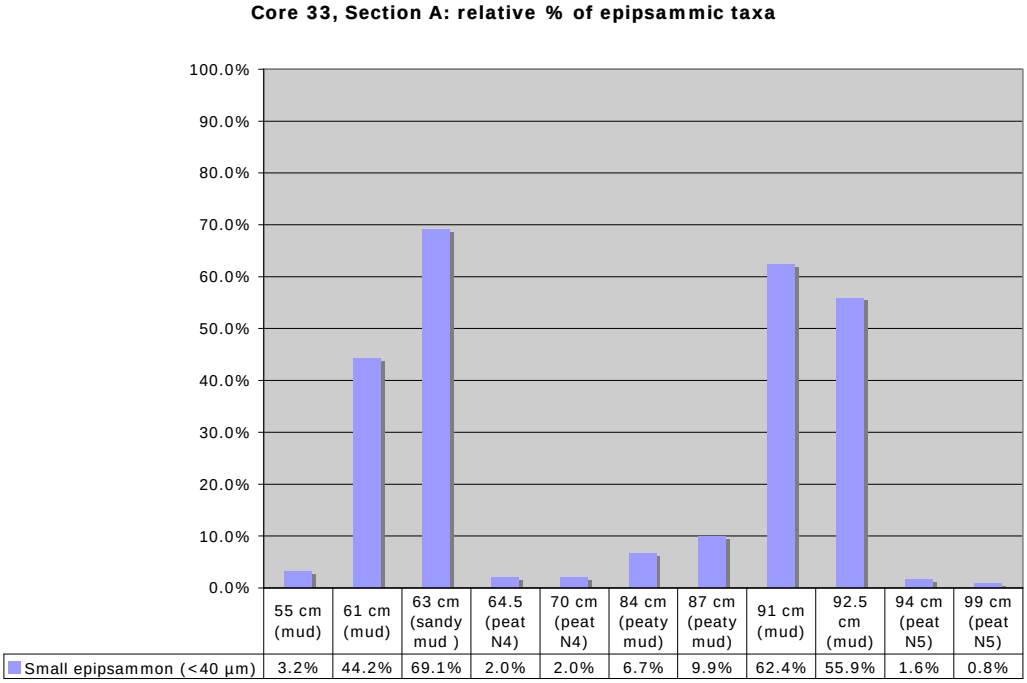

Figure 8. Core 33A: relative % of epipsammic diatoms.

4.2.4 Contact N5 in core 33A

Peat N5 is visible in core 33A (in the core photo) from the base of the core at 105 cm to an angular but fairly sharp upper boundary at about 94.5 cm. The 2 diatom samples in peat N5, at 94-95 cm and 99-100 cm, show that the peat accumulated in a wet freshwater marsh or swamp, probably with periods of standing water or frequent flooding by freshwater (Figure 7). Prominent diatoms consist of species of *Pinnularia, Eunotia*, and *Gomphonema* that would not be found in saline environments. The environment indicated by the diatoms is different from that in peat N4 (70 cm), which was more likely a drier freshwater marsh or meadow.

The mud capping peat N5 dominantly contains brackish-marine tidal flat species, indicating, at a minimum, an abrupt change from a freshwater environment to a brackish-marine lower intertidal or shallow subtidal environment. Tsunami deposition seems plausible when all diatom evidence is considered (Section 5), but the results are equivocal when based solely on the high-magnification analysis. Diatoms in the mud immediately above the peat (92.5 cm) are diverse and relatively frequent, and diatom preservation is poor overall because of fragmentation. Comparable to contact N5 in core 25, small epipsammic diatoms are prominent in the capping mud at both 91 cm and 92.5 cm (Figure 8), but are not as noticeably well preserved as in core 25. Without obvious evidence for excellent preservation, which can be attributed to rapid redeposition and burial, there is little supporting evidence to differentiate a possible tsunami deposit from a tidal flat/shallow subtidal deposit.

The high-magnification analysis is certainly useful in this case, however, because it shows how prominent the tiny epipsammon are in the sample, even though the deposit isn't visibly sandy.

This shows that diatoms may be useful for distinguishing tsunami deposits beyond the inland extent at which they can be identified based grain size.

4.2.5 Contact N6 in core 33B

The diatom results show that peat N6 formed in a high salt marsh (Figure 9). Diatoms in peat N6 include taxa typical of high marshes (*Cosmioneis pusilla*, *Pinnularia lagerstedtii*), plus common valves of *Luticola mutica*. *L. mutica* is only moderately helpful as an ecological indicator because it can tolerate a very wide range of salinities, and is often found in fresh as well as brackish areas of estuaries, and on both high and low marshes. It is an epiphyte, and therefore commonly abundant on riverbanks. Unlike *C. pusilla* and *P. lagerstedtii*, it's not as likely to be found in dry aerophile conditions (in high marshes above MHHW), so it's possible that peat N6 developed in a marsh setting was fairly wet, rather than a drier, grassy high marsh. Overall, the diatom assemblage in peat N6 supports a brackish environment, as opposed to freshwater conditions observed for peat N5 and part of peat N4.

Peat N6 is capped by mud with abundant organic fragments: diatoms were analyzed in samples at 152 cm, 150 cm, and 140 cm. Diatoms in the mud at 152 and 150 cm show a transition to a lower intertidal/subtidal brackish marine deposit. Pertinent taxa include species common on tidal flats (*Nitzschia sigma, N. fasciculata, Scoliotropis tumida*, *Gyrosigma peisonis*, *Tryblionella* spp.) as well as coastal planktonic/tychoplanktonic species (*Actinoptychus senarius*, *Coscinodiscus* spp., *Thalassionema nitzschioides*). In addition, large valves of *Paralia sulcata* are particularly prominent in this sample (Appendix 1), which further supports a brackish-marine environmental setting.

There is no obvious evidence from the diatoms for tsunami deposition. Small epipsammic diatoms are present but not abundant (Figure 10), and there is no evidence for enhanced preservation of small valves from rapid burial. Further, the occurrences of in the sample of large, intact elongate diatom valves (*Gyrosigma)* are inconsistent with turbulent flow.

Diatoms in the mud at 140 cm are dominated by well-preserved taxa common to low salt marshes, including *Caloneis westii* and *C. bacillum*. The overall assemblage is consistent with a quiet depositional setting, either a low marsh or tidal flat/marsh transition.

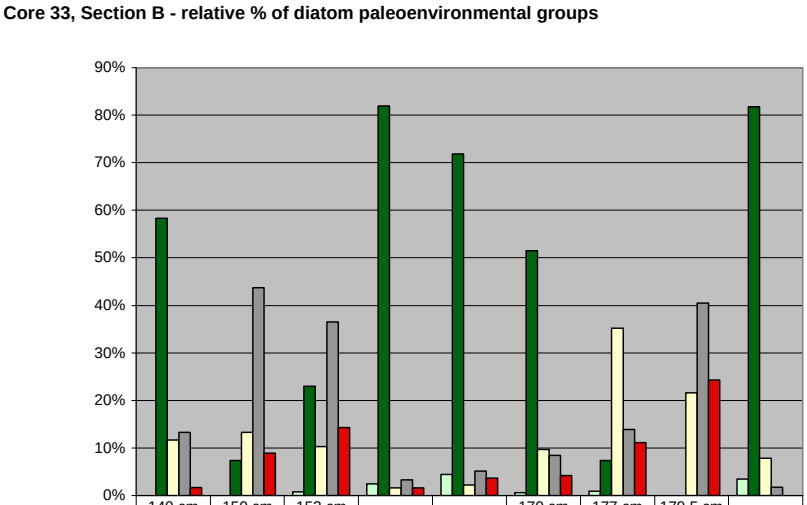

	140 cm (mud w plant	150 cm (mud w plant	152 cm (mud w plant	154 cm (peat N6)	168 cm (mud)	170 cm (muddy peat)	177 cm (mud w wood	179.5 cm (mud w wood	181 cm (peat N7)
Fresh wetland taxa	0.0%	0.0%	0.8%	2.5%	4.4%	0.6%	0.9%	0.0%	3.5%
Mid to high marsh (less saline)	58.3%	7.4%	23.0%	82.0%	71.9%	51.5%	7.4%	0.0%	81.7%
Lower marsh (more saline)	11.7%	13.3%	10.3%	1.6%	2.2%	9.7%	35.2%	21.6%	7.8%
Sandy or muddy tidal flat/channel	13.3%	43.7%	36.5%	3.3%	5.2%	8.5%	13.9%	40.5%	1.7%
Brackish/marine planktonic or tychoplanktonic	1.7%	8.9%	14.3%	1.6%	3.7%	4.2%	11.1%	24.3%	0.0%

Figure 9. Core 33B: relative % of diatom paleoenvironmental groups.

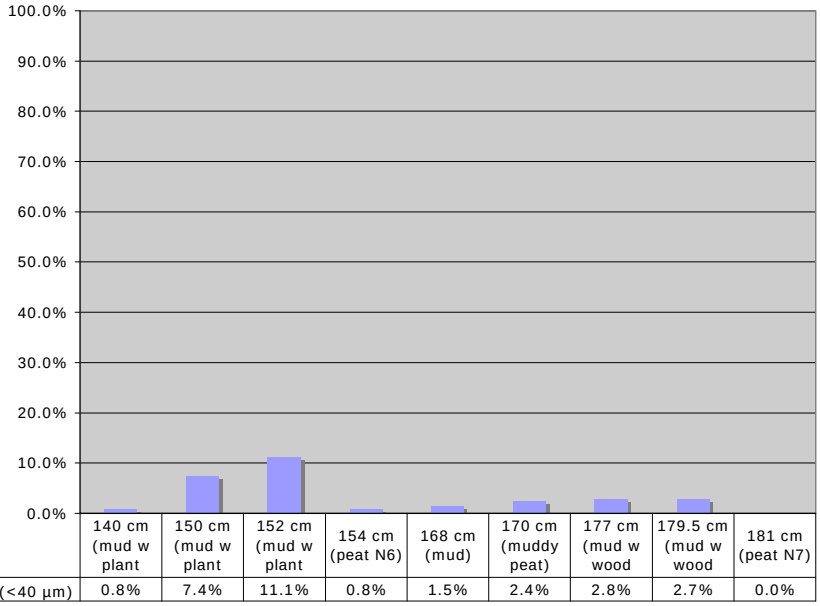

	140 cm (mud w plant	150 cm (mud w plant	152 cm (mud w plant	154 cm (peat N6)	168 cm (mud)	170 cm (muddy peat)	177 cm (mud w wood	179.5 cm (mud w wood	181 cm (peat N7)
Small epipsammon (<40 µm)	0.8%	7.4%	11.1%	0.8%	1.5%	2.4%	2.8%	2.7%	0.0%

Figure 10. Core 33B: relative % of epipsammic diatoms.

4.2.6 Contact N7 in core 33B

Contact N7 is visible in core 33B (at 181 cm) as a sharp boundary between a bold peat (peat N7) and superjacent massive gray mud containing woody fragments. Diatoms from the uppermost 1 cm of the peat (181-182 cm) are indicative of a high marsh environment (Figure 9). Pertinent taxa include well-preserved *Cosmioneis pusilla*, *Nitzschia terrestris*, and *Diadesmis contenta*, all of which are indicative of aerophile conditions in high salt marshes. Compared to diatom abundances in the other muddy samples in cores 33A and 33B (Figures 5a, 5b), diatoms are relatively rare in the sample immediately above peat N7 (179.5-180.5 cm) as well as in the next superjacent mud sample at 177 cm. Both samples contain noticeably large specimens of centric (marine planktonic) and pennate (benthic) taxa. This is unlike a typical tidal flat deposit, and may be more indicative of a marine coastal deposit or possibly a winnowed (channel?) deposit. The overall evidence for tsunami deposition is possible but weak for N7, as further discussed in Section 5.

4.2.7 Evaluation of possible additional buried soil between contacts N6 and N7

Diatoms were examined in muddy peat (170-171 cm) and mud (168-169 cm) about halfway between contacts N6 and N7 to determine if the peaty mud/mud transition might represent an additional buried soil in the stratigraphic record. The results are equivocal, with the best explanation that both deposits are strongly reworked, and don't represent a buried peat/mud couplet caused by earthquake subsidence. For both samples, diatom preservation is poor with severe fragmentation, and the most abundant diatoms in both samples consist of the same dominant marsh species that comprise the assemblage in peat N6 (*Luticola mutica*, *Cosmioneis pusilla*, and *Pinnulaira lagerstedtii*). Significantly, whereas the marsh diatoms are well preserved in peat N6, the diatoms in the peaty mud and mud are poorly preserved with fragmented valves. The diatom data show that there is a lack of evidence for a stable marsh horizon (with well-preserved, *in situ* diatoms) giving way to a lower intertidal/shallow subtidal environment. Instead, both samples appear to be composed of reworked marsh material.

4.2.8 Paleoenvironmental summary for core 33

Inferred paleoenvironments for core 33 (sections A and B) samples are shown in Table 2.

Table 2. Core 33: paleoenvironments inferred from high-magnification diatom analyses.

Depth in core (cm)	Lithology	Inferred paleoenvironment	Comments
Core 33A			
55-56	Mud	Tidal flat / shallow subtidal channel	Diverse assemblage consistent with lower intertidal/shallow subtidal environment.
61-62	Mud	Tidal flat / shallow subtidal channel	Diverse assemblage consistent with lower intertidal/shallow subtidal environment. Epipsammon common; large valves of *P. sulcata* are prominent.
63-64	Sandy mud	Tsunami	Consistent with tsunami deposition based on unusually well preserved brackish marine diatoms, including rare, very-well preserved large marine centric species (*Actinoptychus splendens*, a tychoplanktonic species; and *Ceratulus turgidus* a large benthic species) and common small epipsammic diatoms still attached to sand grains. *Paralia sulcata* is unusually well preserved in this sample, with common large valves still connected in chains.
64.5-65.5	Peat (N4)	High salt marsh	Assemblage dominated by taxa commonly found on high salt marshes (including *Cosmioneis pusilla*, *Navicula cincta*)
70-71	Peat	Fresh to fresh-brackish marsh	Sample dominated by taxa commonly found in freshwater marshes or meadows, including *Eunotia minor*, *E. pectinalis*, *Navicula rhyncocephala*, *Stauroneis obtusa* (freshwater aerophile species). Valve preservation poor overall.
84-85	Peaty mud	Brackish marsh? Reworked?	Sample contains common well-preserved high salt marsh diatoms (particularly *Pinnularia lagerstedtii*, *C. pusilla*) associated with abundant reworked woody material.
87-88	Peaty mud	Incipient marsh?/tidal flat-marsh transition?	Contains mix of taxa found on intertidal muddy flats as well as salt marshes.
91-92	Mud	Tidal flat / shallow subtidal channel (weak evidence for tsunami)	Diatoms not abundant, but epipsammon common. Prominent benthic taxa include *Rhaphoneis psammicola*, *Delphineis surirella*, *Cocconeis scutellum*. Occurrences of large centrics may indicate open connection with deeper marine water.
92.5-93.5	Mud	Tidal flat / shallow subtidal channel (weak evidence for tsunami)	Diatoms relatively sparse, and fragmentation severe. Wide range of sizes, tidal flat/channel species prevalent (*D. surirella*, *S. fasciculata*), but also occurrences of rare, large planktonic species. Epipsammon common, but not as pristine as in sandy mud (inferred tsunami) sample at 63-64 cm. Evidence for tsunami is equivocal, but possible supporting evidence is overall poor preservation, frequency of epipsammon, and prominent occurrences of marine planktonic taxa.
94-95	Peat (N5)	Wet freshwater marsh or swamp	Diatoms diverse and common, dominated by large *Pinnularia* spp. and *Eunotia* spp., consistent with wet, fresh environment.

Table 2. Core 33: paleoenvironments inferred from high-magnification diatom analyses.

Depth in core (cm)	Lithology	Inferred paleoenvironment	Comments
Core 33A			
99-100	Peat	Wet freshwater marsh or swamp	Prominent diatoms include species of *Pinnularia*, *Eunotia*, and *Gomphonema.* Also frequent *Tabellaria flocculosa*, probably indicative of standing water or flooding by freshwater.
Core 33B			
140-141	Mud	Low marsh or tidal flat/marsh transition	Diatoms include well-preserved taxa common on low salt marshes, including *Caloneis westii* and *C. bacillum*. The overall assemblage is consistent with a quiet depositional setting.
150-151	Mud w/ plant fragments	Tidal flat / shallow subtidal zone	Prominent tidal flat/shallow subtidal taxa as for 152-153 cm.
152-153	Mud w/ plant fragments	Tidal flat / shallow subtidal zone	Pertinent taxa include species common on tidal flats (*Nitzschia sigma, N. fasciculata*, *Scoliotropis tumida*, *Gyrosigma peisonis, Tryblionella* spp.) as well as coastal planktonic/tychoplanktonic species (*Actinoptychus senarius*, *Coscinodiscus* spp., *Thalassionema nitzschioides*). Large valves of *Paralia sulcata* also prominent.
154-155	Peat (N6)	Low to high salt marsh	Pertinent diatoms include well-preserved high marsh taxa (*C. pusilla, P.* lagerstedtii) and taxa found in high and low marshes (*Luticola mutica*).
168-169	Mud	Reworked marsh material?	Diatoms mostly consist of poorly preserved, fragmented valves of the same high marsh taxa observed in peat N6 (*Luticola mutica, P. lagerstedtii, C. pusilla*).
170-171	Muddy peat	Reworked marsh material?	Diatoms mostly consist of poorly preserved, fragmented valves of the same high marsh taxa observed in peat N6 (*Luticola mutica, P. lagerstedtii, C. pusilla*).
177-178	Mud with wood fragments	Equivocal (marine deposit?)	Diatoms rare, consisting of large planktonic marine diatoms and rare, poorly preserved, rare, large benthic estuarine diatoms. P. sulcata is rare. Winnowed channel sample?
179.5-180.5	Mud w/ plant fragments	Equivocal (marine deposit?)	Diatoms rare, consisting of large planktonic marine diatoms and rare, poorly preserved, rare, large benthic estuarine diatoms. Winnowed channel? Nearshore marine?
181-182	Peat (N7)	High salt marsh	Pertinent taxa include well-preserved *Cosmioneis pusilla*, *Nitzschia terrestris*, and *Diadesmis contenta*, all of which are indicative of drier aerophile conditions in high salt marshes.

5 RESULTS II: EVALUATION OF POSSIBLE TSUNAMI DEPOSITS BASED ON DIATOM ANALYSES COMPLETED AT LOW MAGNIFICATION

5.1 Overview

Most diatoms are too small to be observed in detail unless at high magnification with an oil immersion objective. For this reason, diatom counts are typically completed at magnifications of 1000x-1250x in order to adequately identify ecologically significant taxa of all sizes, many of which are quite small (< 40 µm). During the course of this study, however, it became apparent that, although high-magnification counts are imperative for collecting paleoecological information on a complete assemblage, the effects of turbulent (tsunami) flow on diatom preservation is best evaluated by examining larger taxa over a greater portion of the sample at low magnification. For this reason, in addition to counting diatoms at 1250x with an oil immersion lens (including documenting abundance and relative preservation of small epipsammic diatoms), I also counted at least 100 diatoms larger than 40 µm at low magnification (500x) in select samples to look for possible evidence for tsunami deposition. Based on these preliminary analyses, I used the following criteria to designate possible paleo-tsunami deposits based on entrained diatoms:

1. Severe fragmentation of pennate diatoms > 100 µm long;
2. Relatively high fragmentation of all diatom valves larger than 40 µm, particularly pennate valves > 40 µm long;
3. Relatively higher frequency of coastal marine planktonic and tychoplanktonic taxa;
4. Relatively high frequency of exceptionally large, benthic epipsammic diatoms;
5. Relatively high frequency of small epipsammic diatoms, ± evidence for enhanced preservation.

Items 1-4 are based on low-magnification counts, and item #5 is from the high-magnification counts because the smaller epipsammic diatoms are not possible to adequately document without an oil immersion lens.

Using the criteria listed above, the diatom data suggests that there is evidence for tsunami deposition associated with contacts N4 and N5 in both cores 25 and 33, and for the single observation of contact N7 in core 33 (Table 3). There is no evidence for tsunami deposition for contact N6.

Table 3. Diatom evidence used to differentiate tsunami and non-tsunami deposits above buried soil contacts N4-N7. (Cores 25 and 33, Upton Slough, Nestucca Bay, Oregon).

Buried soil contact ID	Core ID	Depth in core (cm)	[1] % intact pennate diatom valves > 100 µm long	[2] % intact pennate diatom valves > 40 µm long	[3] % coastal marine diatoms (planktonic + tychoplanktonic species	[4] # of large epipsammic taxa observed in 10 traverses (400 mm^2 area of slide)	[5] % well-preserved epipsammic diatoms [high mag counts]	Lithology	Evidence for tsunami
Contact N4	**25**	68-69	31.7%	70.8%	7.5%	4	3.6%	Mud	–
		69-70	1.0%	50.0%	7.7%	9	48.1%	Sandy mud	1, 2, 4, 5
	33	61-62	20.2%	71.6%	1.8%	9	44.2%	Mud	–
		63-64	4.9%	30.4%	9.8%	19	69.1%	Sandy mud	1, 2, (3), 4, 5
Contact N5	**25**	102-103	23.8%	52.4%	14.3%	4	54.7%	Mud	–
		103.5-104.5	2.9%	27.2%	31.1%	9	74.5%	Sandy mud	1, 2, 3, 4, 5
	33	87-88	23.3%	65.8%	4.8%	1	9.9%	Peaty mud	–
		91-92	0.8%	41.7%	30.8%	12	62.4%	Mud	1, 2, 3, 4, 5
		92.5-93.5	0.0%	39.3%	29.9%	8	55.9%	Mud	1, 2, 3, 4, 5
Contact N6	**33**	150-151	21.7%	51.7%	5.8%	1	7.4%	Mud	–
		152-153	13.9%	51.1%	8.0%	1	11.1%	Mud	–
Contact N7	**33**	177-178	1.0%	43.8%	7.6%	0	2.8%	Mud	–
		179.5-180.5	3.0%	26.7%	19.8%	0	2.7%	Mud	2, 3

Characteristics of diatoms in tsunami samples as compared to non-tsunami samples:
[1] Severe fragmentation of large, narrow pennate diatoms > 100 µm long.
[2] Fewer intact specimens of all diatom valves > 40 µm long.
[3] Greater frequency of coastal marine planktonic and tychoplanktonic taxa.
[4] Greater frequency of exceptionally large, robust epipsammic diatoms (*Cerataulus turgidus*, *Campylodiscus echeneis*).
[5] Greater frequency of small epipsammic diatoms, including evidence for enhanced preservation.

5.2 Diatom criteria for tsunami deposition

5.2.1 Criterion #1: severe fragmentation of pennate diatoms > 100 µm long

A few diatom species observed in the Upton Slough samples have narrow, elongate valves exceeding 100 µm in length, including *Gyrosigma peisonis*, *G. wansbeckii*, *Nitzshcia sigma*, and *Synedra fasciculata*. For both contacts N4 and N5 in cores 25 and 33, diatom taxa with valves > 100 µm long are present in both possible tsunami and post-tsunami deposits, but frequent intact valves are only present in post-tsunami deposits (Figure 1). The tsunami deposits contain valve fragments, the likely result of abrasion during turbulent flow.[3] For contact N6, frequent occurrences of intact valves in both samples analyzed suggest that neither was deposited by a tsunami.

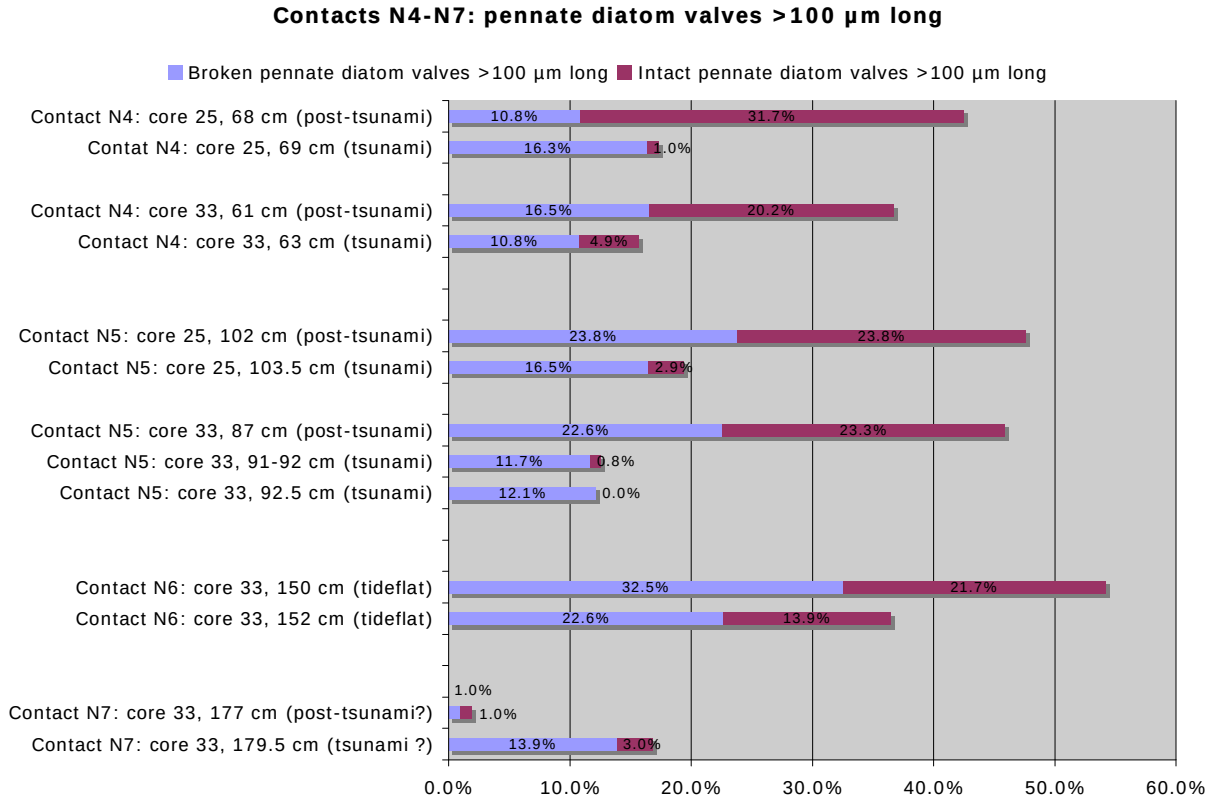

Figure 11. Diatom criterion #1 for tsunami deposition: severe fragmentation of diatom valves > 100 µm long.
[Question: What do the percentages reflect? Are these percentages of the entire sample counted?]

5.2.2 Criterion #2: relatively high fragmentation of all diatom valves > 40 µm

In addition to evidence for poor preservation of diatoms with easily fragmented valves > 100 µm long, there is evidence for overall greater fragmentation of both pennate and centric diatoms

[3] Note that this evidence also shows (as does subsequent evidence), that the likely tsunami deposit above contact N5 in core 33 is thicker than had been expected. This may be because the tsunami deposit accumulated in a swale or depression, which is supported by the diatoms in the underlying peat that indicate periods of standing water.

larger than 40 µm in possible tsunami deposits.[4] Compared to evidence for fragmentation of elongate valves > 100 µm, however, the fragmentation of all pennate diatoms > 40 µm provides less compelling evidence for turbulent flow because most have smaller length-to-width ratios (e.g., 4:1 as compared to 20:1) and are generally more resistant to breakage. Examples of common taxa > 40 µm long found on marshes and tidal flats species of *Navicula*., *Caloneis westii*, *Scolioneis tumida*, and *Diploneis interrupta*. Centric diatoms > 40 µm in diameter in the Upton Slough samples include marine planktonic (e.g., *Coscinodiscus* spp., *Thalassiosira* spp., *Actinocyclus* spp.) and tychoplanktonic (*Actinoptychus* spp., *Stephanodiscus* spp.) taxa. The centric diatom *Paralia sulcata* was excluded from the basic analysis, as previously discussed.

The results show that intact valves of all diatoms larger than 40 µm are less frequent in several of the suspect tsunami deposits in cores 25 and 33, but relative preservation of pennate diatoms is more informative than preservation of centric diatoms, and there is no evidence for preferential preservation of centric over pennate valves (Figure 12). Greater fragmentation (fewer intact specimens) of pennate taxa is evident for tsunami deposits in cores 25 and 33 for contacts N4, N5, and N7. For contact N6, intact pennate valves exceed 50% for both samples, showing that both samples were likely deposited under relatively quiet depositional conditions.

[4] Evaluating fragmentation for diatoms smaller than 40 µm is less useful than focusing on larger valves, because many small pennate diatoms found in estuarine marshes and tidal flats have heavily silicified valves resistant to breakage. This is particularly true for small epipsammic taxa that have adapted to survival in abrasive sediment environments such as sandy intertidal flats, surf zones, or shallow subtidal areas.

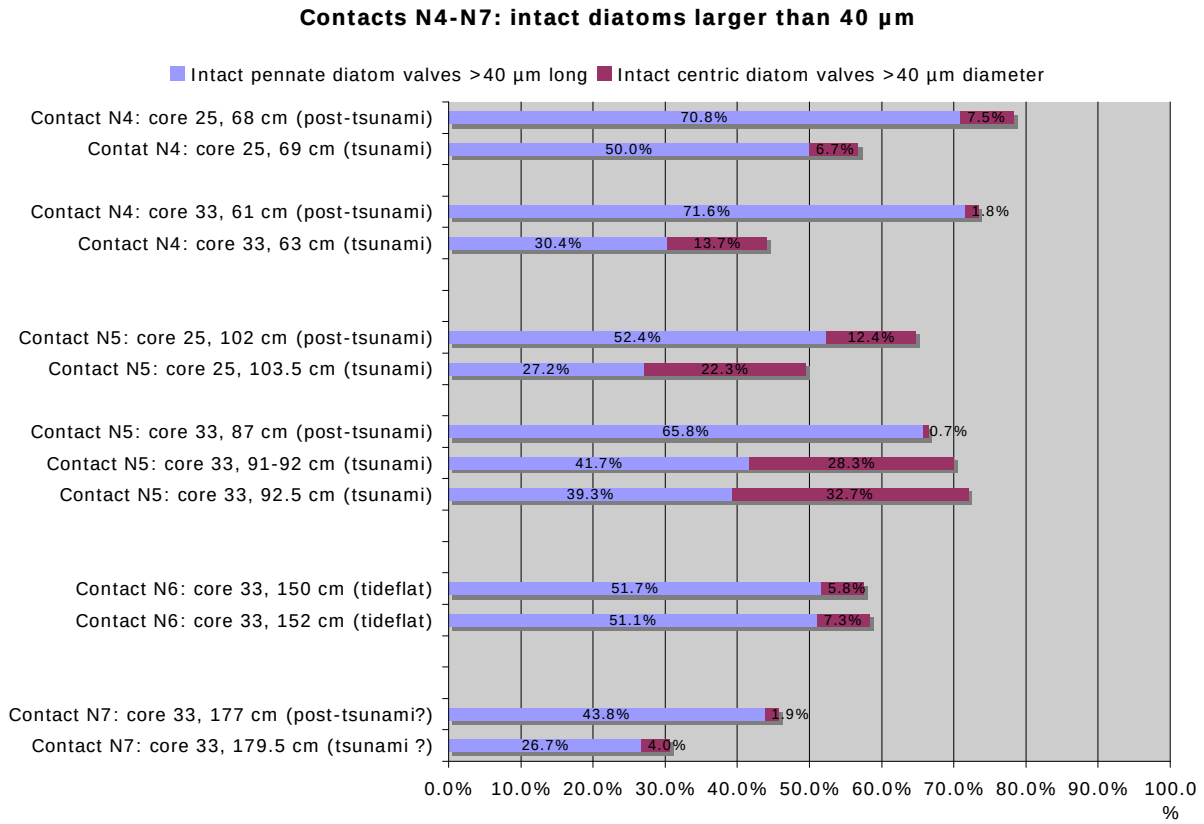

Figure 12. Diatom criterion #2 for tsunami deposition: fewer intact valves (relatively greater fragmentation) of all diatom valves larger than 40 µm, but particularly pennate valves > 40 µm long.

5.2.3 Criterion #3: relatively higher frequency of coastal marine planktonic and tychoplanktonic taxa

Marine planktonic and tychoplanktonic diatoms observed in the Upton Slough samples primarily consist of taxa with centric valves (e.g., *Coscinodiscus* spp., *Thalassiosira* spp.), but also include the pennate diatoms *Thalassionema nitzschioides* and *Delphineis karstenii*. Up-estuary deposition of marine planktonic/tychoplanktonic diatoms is most obvious for possible tsunami deposits above contact N5 in both cores 25 and 33 (Figure 13). Prominent occurrences of these taxa provide evidence for an influx of marine water, and also help correlate the same tsunami event in both cores. In contrast to N5, planktonic/tychoplanktonic diatoms are not strongly associated with possible tsunami deposits above contact N4. In core 25, frequencies are roughly equal in tsunami and post-tsunami deposits. In core 33, there is a small but noticeable difference in frequency between the lower and upper samples, but overall a strong signal of incursion and deposition of planktonic taxa is lacking. For contact N6 in core 33, the relatively low frequency of planktonic/tychoplanktonic taxa in both samples is consistent with tidal flat deposition, as planktonic taxa are commonly a minor component of tidal flat deposits. It is possible, therefore, that the N4 samples also indicate resuspension and redeposition of shallow estuarine benthic deposits as compared to possibly deeper water deposits. Finally, although coastal diatoms are not as prominent above contact N7 in core 33 as above contact N5 in both cores, there is some

evidence for marine incursion for this event. For the most, diatom preservation is moderate to poor in samples above N7, primarily the results of post-deposition dissolution. However, in addition to containing more than twice the number of coastal taxa than the possible post-tsunami deposit, the tsunami deposit contains very well-preserved specimens of large marine taxa not observed in the post-tsunami deposit, including *Actinocyclus octonarius*, *Coscinodiscus radiatus*, and also *Lyrella amphioroides*, which is exclusive to this sample.

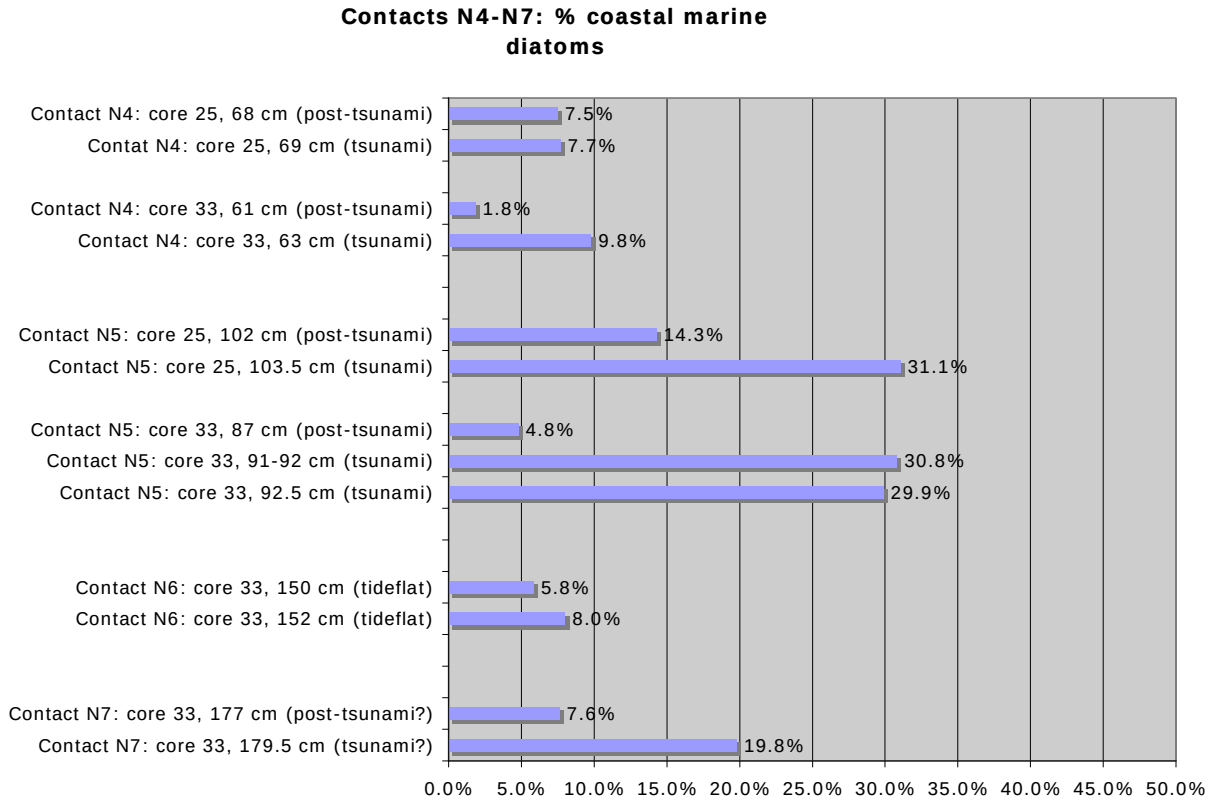

Figure 13. Diatom criterion #3 for tsunami deposition: relatively more frequent occurrences of coastal marine planktonic and tychoplanktonic taxa as compared to non-tsunami deposits.

5.2.4 Criterion #4: relatively high frequency of exceptionally large, benthic epipsammic diatoms

Up-estuary occurrences of large epipsammic diatoms (e.g., *Ceratalus turgidus*, *Campylodiscus echeneis*) may also be evidence for resuspension and transport by a tsunami. Both *C. turgidus* and *C. echineis* form heavily silicified valves: *C. turgidus* has a globular valve, and *C. echineis* forms a squarish valve folded over on itself. Both are associated with sandy coastal and estuarine deposits, but because of their larger size, aren't easily observed at high magnification, and may be under-represented in diatom slides specifically processed to identify the diverse numbers of small taxa. Because of the possibility that the large epipsammon were under-represented as a result of the standard sample processing technique used for the Upton Slough samples, I used a different counting technique for them: identifying the total number of valves encountered on a 400 mm^2 area of the slide rather than including them as part of the counts for the first 100 valves

larger than 40 µm. The results of the counts show that the large epipsammon are more frequent in the possible tsunami deposits above contacts N4 and N5 in as compared to the post-tsunami deposits (Figure 14). They are rare for deposits above contact N6, which is consistent with a fine-grained tidal flat environment. Interestingly, they are absent from the N7 samples, even though other relatively large coastal diatoms are present. This seems to indicate that the source of the deposits above N7 was not conducive to high production of large epipsammon.

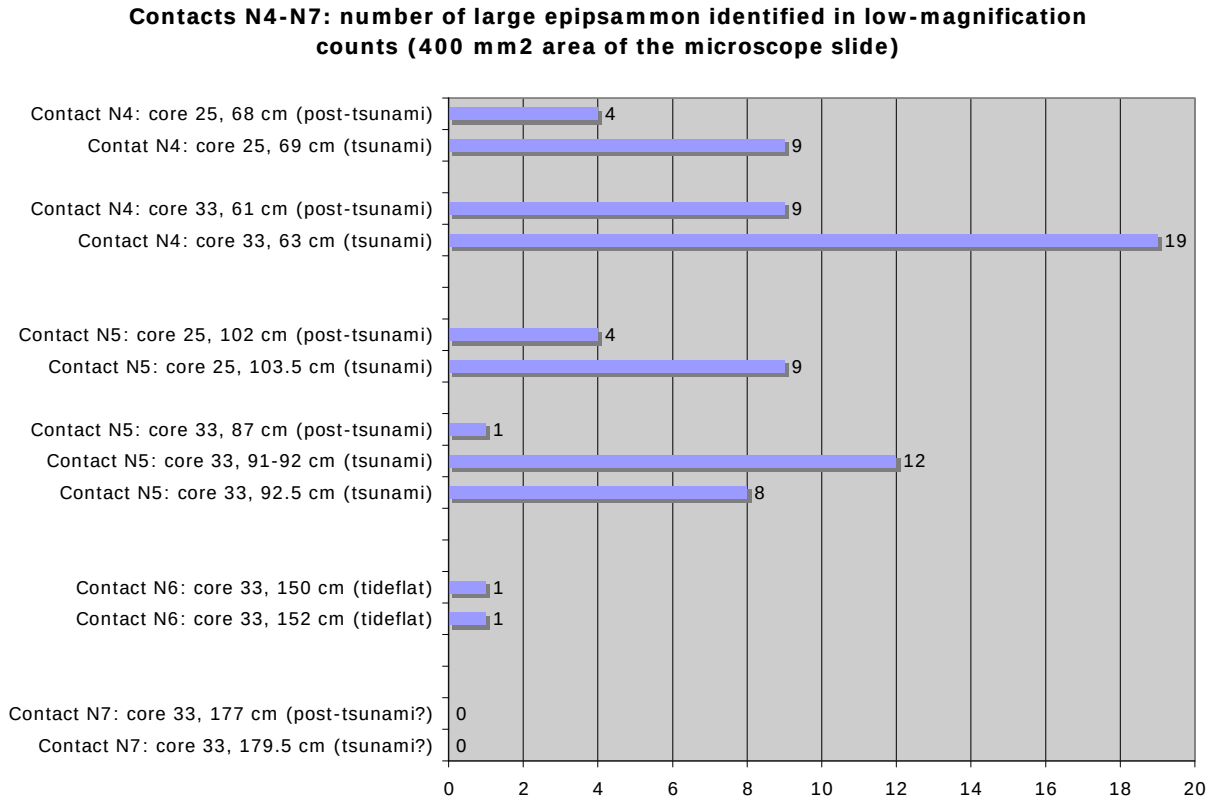

Figure 14. Diatom criterion #4 for tsunami deposition: relatively high frequency of exceptionally large, benthic epipsammic diatoms.

5.2.5 Criterion #5: relatively high frequency of small epipsammic diatoms, ± evidence for enhanced preservation

In contrast to the very large epipsammic diatoms listed above, tiny epipsammic diatoms must be evaluated at high magnification. Abundant occurrences of brackish-marine epipsammic diatoms can be used to show incursion from coastal sources, and evidence for good valve preservation (including tiny valves still attached to sand grains) can be used to infer rapid redeposition and burial of modern deposits. Furthermore, as most of the sand-associated diatoms are actually the size of silt particles, they can be used to show a farther inland extent of a tsunami deposit than is possible by mapping the deposit based on coarse grain size.

Small epipsammon are prominent in the possible tsunami samples above contact N4 in both cores 25 and 33 (Figure 15). Both samples are visibly sandy in cores, and the preservation of

epipsammic diatoms is very good with instances of complete frustules and tiny valves still attached to sand grains. Epipsammon are still common, though less frequent, in post-tsunami mud in core 33, and dramatically less frequent in post-tsunami mud in core 25.

Contact N5 is interesting because epipsammic diatoms are prominent in tsunami deposits in both cores, but whereas the sample in core 25 is visibly sandy, the samples in core 33 are not. The epipsammon in core 33 are not as pristine as in the sandier deposits, but they are a significant proportion of the overall assemblage. They help to clearly differentiate the tsunami deposits from the post-tsunami sample in core 33, an show a possible correlation to the sandy deposit in core 25. For contact N6, low numbers of small epipsammic diatoms are consistent with tidal flat deposition. For contact N7, very rare occurrences of small epipsammon is in line with the absence of large epipsammon (Figure 14), indicating fundamental differences in the deposits above N7 as compared with N5 or N4.

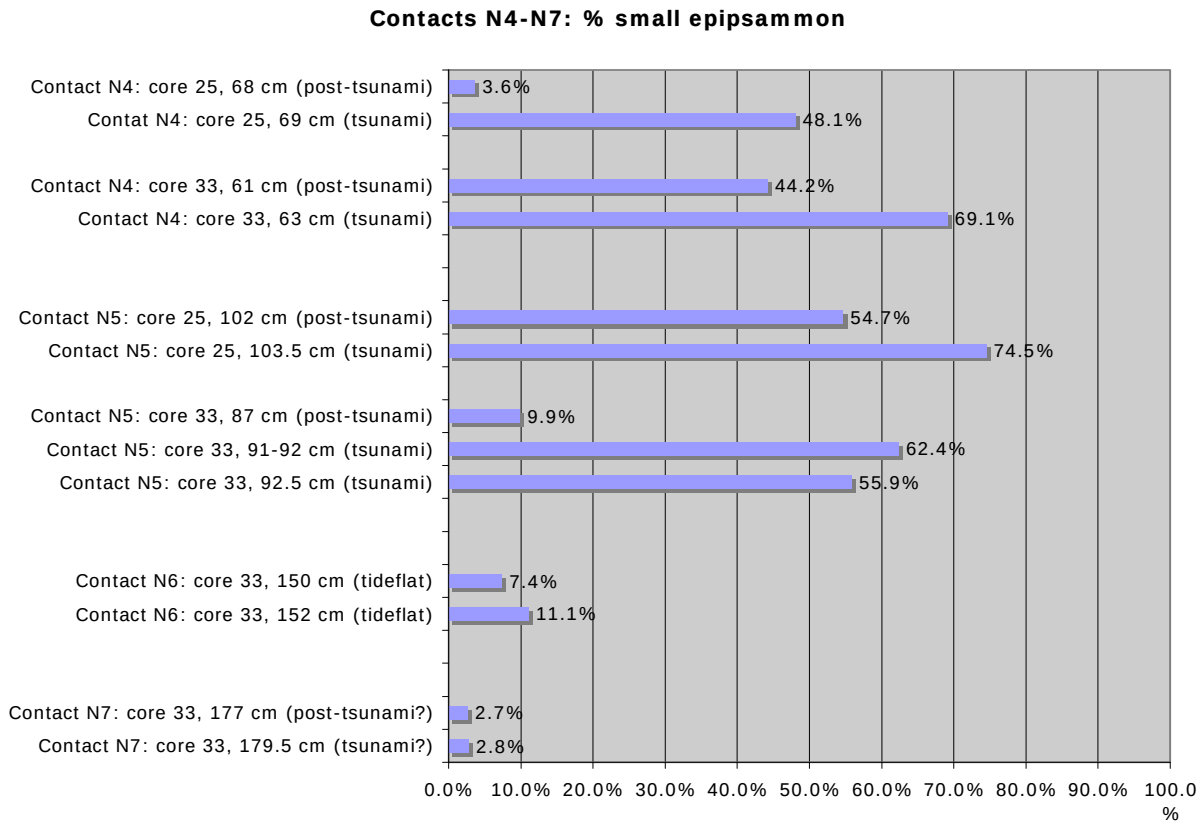

Figure 15. Diatom criterion #5 for tsunami deposition: relatively high frequency of small epipsammic diatoms.

6 DISCUSSION

1. For this study, thorough high-magnification diatom analyses proved useful for identifying past depositional environments, particularly the likely environments for the buried soils prior to submergence. The paleoenvironmental settings for some of the samples were not possible to differentiate with any certainty, possibly because the material was too reworked (e.g., by tidal action, or small channels cutting across the marsh). Under high magnification it's possible to identify even smaller taxa to the species level, and also get a good look at overall preservation of most diatoms in an assemblage.

2. At high magnification, however, it's not possible to evaluate the presence and relative preservation of larger diatoms over a greater proportion of the sample, which can provide additional useful information about suspect tsunami deposits. A breakthrough for this study was the recognition that there is additional insight to be gained by completing systematic counts focusing on the larger diatoms in an assemblage. This seems like an obvious approach, but to my knowledge no one has evaluated diatoms in tsunami samples like this before. Important references by Dawson et al. (1996) and Sawai et al. (2009), for example, mention counting diatoms under oil immersion, which implies high magnification. Inferences about relative amounts of fragmentation in these studies also appear to be based on observations during high-magnification counts. The benefit of also looking at samples under low magnification is that it's easier to document occurrences of larger diatoms, particularly pennate taxa > 100 µm long, which seem especially useful for differentiating an *in situ* benthic (tidal flat/shallow subtidal) sample from one that has been resuspended and transported under turbulent flow conditions. Lower-magnification analyses also help to identify the larger marine planktonic diatoms that might accompany a landward surge by a tsunami.

3. The diatom criteria for identifying tsunami deposits seem to apply well to the Upton Slough samples, but this is a preliminary study, and those criteria may not apply everywhere, or additional criteria may become evident if this technique is continued elsewhere. It is clear from the Upton Slough samples that the criteria that support tsunami deposition for one event do not perfectly coincide with another event. For example, the tsunami deposit above contact N5 in both cores shows as strong incursion of coastal marine taxa (prominent planktonic diatoms), but these taxa are not important in the N4 deposits. Instead, the N4 deposits contain a greater number of especially long, relatively delicate taxa. Elongate taxa are also present in N5, but they are not as prominent nor consist of the same species as for N4. These results may show that the cores sites had more direct access to the open ocean at the time of N5 (prominent planktonics) as compared to the period of deposition for N4 (prominent benthic tidal flat taxa). It is possible that these kinds of evaluations will provide general insight into changes in coastal morphology of the study area over time, and that the different characteristics of diatom assemblages in different tsunami deposits will help to correlate coeval units at different locations.

7 REFERENCES

Andrejko, M.J, and Cohen, A.D., 1984 Scanning electron microscopy of silicophytoliths from the Okefenoke swamp-marsh complex, *in* Cohen, Casagrande, Andrejko, and Best (eds), The Okefenokee Swamp: Its natural history, geology and geochemistry: Los Alamos, Wetland Surveys, p. 466-491.

Atwater, B.F., and Hemphill-Haley, E., 1997, Recurrence Intervals for Great Earthquakes of the Past 3500 Years at Northeastern Willapa Bay, Washington: USGS Professional Paper 1576, 108 p.

Dawson, S., Smith, D.E., Ruffman, A., and Shi, S., 1996, The diatom biostratigraphy of tsunami sediments: examples from Recent and Middle Holocene events: Physics and Chemistry of the Earth, v. 21, no. 12, p. 87-92.

Hemphill-Haley, E., 1993a, Occurrences of recent and Holocene intertidal diatoms (Bacillariophyta) in northern Willapa Bay, Washington: U.S. Geological Survey Open-File Report 93-284, 94 p.

Hemphill-Haley, E., 1993b, Taxonomy of recent and fossil (Holocene) diatoms (Bacillariophyta) from northern Willapa Bay, Washington: U.S. Geological Survey Open-File Report 93-289, 151 p.

Hemphill-Haley, E., 1995a, Diatom evidence for earthquake-induced subsidence and tsunami 300 years ago in southern coastal Washington: Geological Society of America Bulletin, v. 107, no. 3, p. 367-378.

Hemphill-Haley, E., 1995b, Intertidal diatoms from Willapa Bay, Washington: Application to studies of small-scale sea-level changes: Northwest Science, v. 69, no. 1, p. 29-45.

Hemphill-Haley, E., 1996, Diatoms as an aid in identifying late Holocene tsunami deposits.: The Holocene, v. 6, no. 4, p. 439-448.

Hemphill-Haley, E., 2006, Diatoms (Bacillariophyta) from salt marshes and intertidal flats of Tomales Bay, California. A report to the National Park Service Tomales Bay Biodiversity Inventory (TBBI), 30 pp., 17 plates. Available from: http://www.tomalesbaylife.org

Hemphill-Haley, E., and Lewis, R.C., 1995, Distribution and taxonomy of diatoms (Bacillariophyta) in surface samples and a two-meter core from Winslow Marsh, Bainbridge Island, Washington: U.S. Geological Survey Open-File Report 95-833, 103 p.

Hemphill-Haley, E., and Lewis, R.C., 2003, Diatom data from Bradley Lake, Oregon: Downcore analyses: U.S. Geological Survey Open-File Report 03-190, 138 p.

Krammer, K., and Lange-Bertalot, H., 1985, Naviculaceae, Bibliotheca Diatomologica, Band 9, J. Cramer: 230 pp.

Krammer, K., and Lange-Bertalot, H., 1986, Bacillariophyceae 1, Naviculaceae. In Ettl, H., Gerloff, J., Heynig, H., and Mollenhauer, D., (eds), Süsswasserflora von Mitteleuropa, vol. 2, no. 1. Fischer, Stuttgart.

Krammer, K., and Lange-Bertalot, H., 1988, Bacillariophyceae 2, Epithemiaceae, Bacillariaceae, Surirellaceae. In Ettl, H., Gerloff, J., Heynig, H., and Mollenhauer, D., (eds), Süsswasserflora von Mitteleuropa, vol. 2, no. 2. Fischer, Stuttgart.

Krammer, K., and Lange-Bertalot, H., 1991a, Bacillariophyceae 3, Centrales, Fragilariaceae, Eunotiaceae. In Ettl, H., Gerloff, J., Heynig, H., and Mollenhauer, D., (eds), Süsswasserflora von Mitteleuropa, vol. 2, no. 3. Fischer, Stuttgart.

Krammer, K., and Lange-Bertalot, H., 1991b, Bacillariophyceae 4, Achnanthaceae. In Ettl, H., Gerloff, J., Heynig, H., and Mollenhauer, D., (eds), Süsswasserflora von Mitteleuropa, vol. 2, no. 4. Fischer, Stuttgart.

McIntire, C.D., and Overton, W.S., 1971, Distributional patterns in assemblages f attached diatoms from Yaquina Estuary, Oregon: Ecology, v. 52, no. 5, p. 758-777.

Nelson, A.R., and Kashima, K., 1993, Diatom zonation in southern Oregon tidal marshes relative to vascular plants, Foraminifera, and sea level: Journal of Coastal Research, v. 9, no. 3, p. 673-697.

Nelson, Alan R., Jennings, Anne E., Gerson, Linda D., Sherrod, Brian L., 2000, Differences in great-earthquake rupture extent inferred from tsunami-laid sand and foraminiferal assemblages beneath tidal marshes at Alsea Bay, Oregon: Geological Society of America Abstracts with Programs, v. 32, no. 7.

Robinson, M., 1993, Microfossil analyses and radiocarbon dating of depositional sequences related to Holocene sea-level changes in the Forth Valley, Scotland: Transactions of the Royal Society of Edinburgh, Earth Sciences, Vol. 84, p. 1-60.

Sawai, Y., Jankaew, K., Martin, M.E., Prendergast, A., Choowong, M., Charoentitirat, T., 2009, Diatom assemblages in tsunami deposits associated with the 2004 Indian Ocean tsunami at Phra Thong Island, Thailand: Marine Micropaleontology, v. 73, p. 70-79.

Sawai, Y., and Nagumo, T., 2003, Diatoms from Alsea Bay, Oregon: Diatom, v. 19, p. 33-46.

Vos, P., and de Wolf, H., 1993, Diatoms as a tool for reconstructing sediment environments in coastal wetlands – methodological aspects: Hydrobiologia, v. 269/270, p. 285-296.

Whiting, M.C., and McIntire, C.D., 1985, An investigation of distributional patterns in the diatom flora of Netarts Bay, Oregon, by Correspondence Analysis: Journal of Phycology, v. 21, no. 4, p. 665-661.

Witkowski, A., Lange-Bertalot, H., and Metzeltin, D., 2000, Diatom flora of marine coasts: Iconographica Diatomologica, v. 1, 925 p.

APPENDIX A
Counts data and concentration estimates for *Paralia sulcata*.

Core 25: number of P. sulcata counted

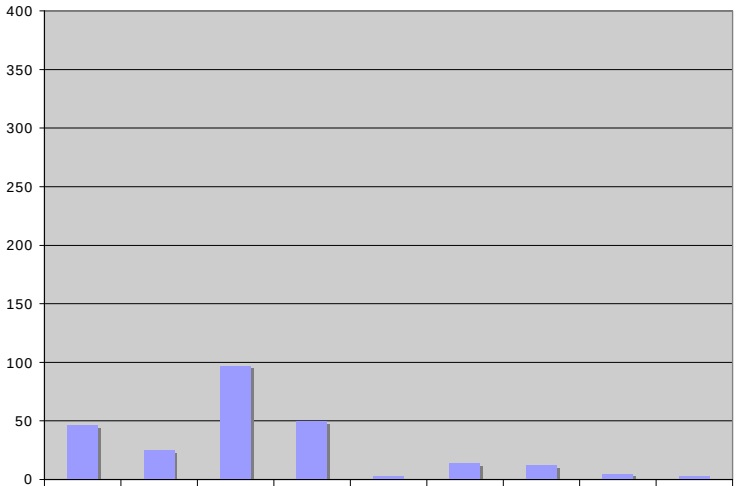

	65 cm (mud)	68 cm (mud)	69 cm (sandy mud)	72 cm (peat N4)	85 cm (muddy peat)	91 cm (peaty mud)	102 cm (mud)	103.5 cm (sandy mud)	106 cm (peat N5)
Number of P. sulcata counted	46	25	97	50	3	14	12	5	3

Core 25: estimated abundances of Paralia sulcata (valves/cc of sediment)

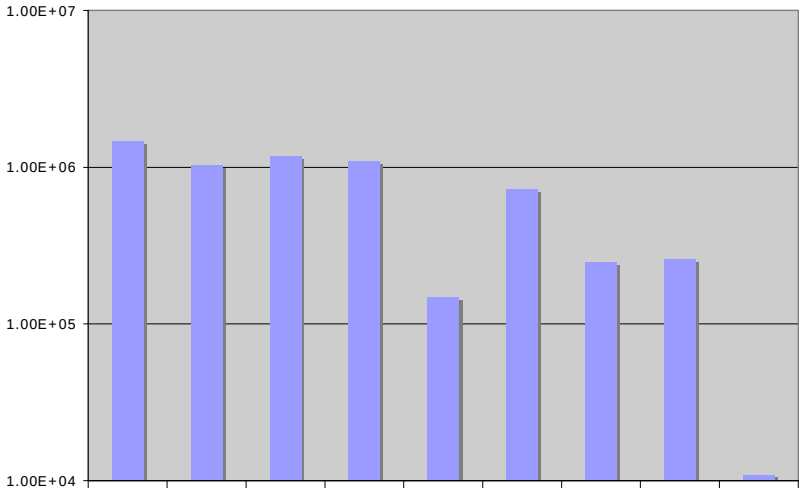

	65 cm (mud)	68 cm (mud)	69 cm (sandy mud)	72 cm (peat N4)	85 cm (muddy peat)	91 cm (peaty mud)	102 cm (mud)	103.5 cm (sandy mud)	106 cm (peat N5)
Concentration of P. sulcata	1.46E+06	1.03E+06	1.18E+06	1.09E+06	1.47E+05	7.22E+05	2.48E+05	2.58E+05	1.09E+04

Core 25: *P. sulcata* is present in all core samples samples, and most prevalent in samples in and above peat N4. Diatoms are very rare overall in peat N5 at 106 cm.

Core 33A: number of P. sulcata counted

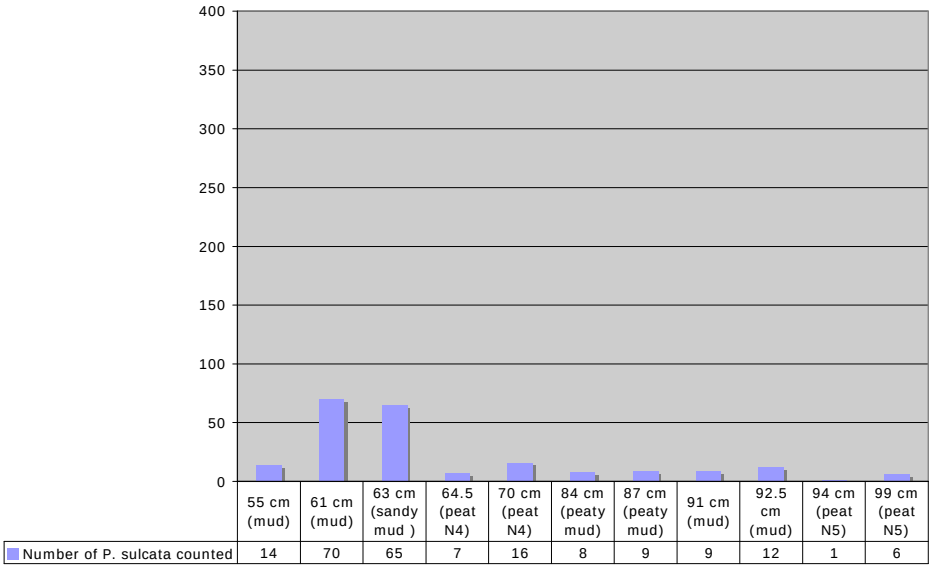

	55 cm (mud)	61 cm (mud)	63 cm (sandy mud)	64.5 (peat N4)	70 cm (peat N4)	84 cm (peaty mud)	87 cm (peaty mud)	91 cm (mud)	92.5 cm (mud)	94 cm (peat N5)	99 cm (peat N5)
Number of P. sulcata counted	14	70	65	7	16	8	9	9	12	1	6

Core 33A: estimated abundance of Paralia sulcata (valves/cc of sediment)

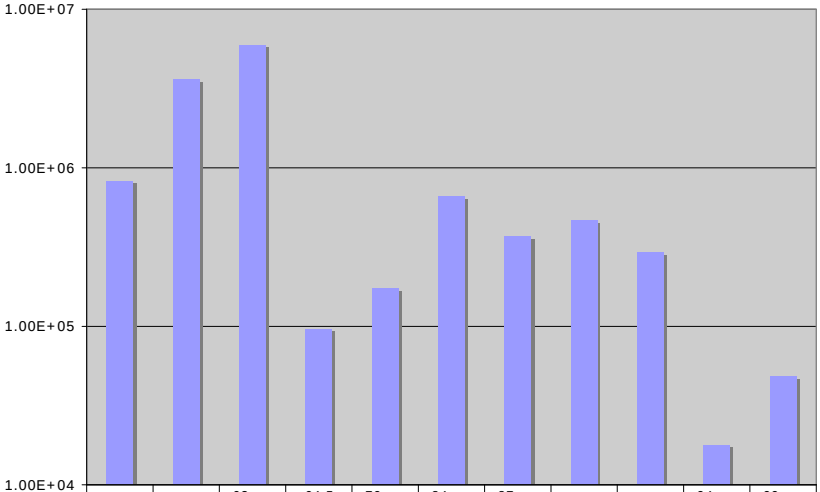

	55 cm (mud)	61 cm (mud)	63 cm (sandy mud)	64.5 (peat N4)	70 cm (peat N4)	84 cm (peaty mud)	87 cm (peaty mud)	91 cm (mud)	92.5 cm (mud)	94 cm (peat N5)	99 cm (peat N5)
Concentration of P. sulcata	8.25E+05	3.61E+06	5.96E+06	9.63E+04	1.74E+05	6.60E+05	3.71E+05	4.64E+05	2.91E+05	1.79E+04	4.85E+04

Core 33A: *P. sulcata* is present in all samples, and because it is so resistant to dissolution, also provides remnant valves in freshwater deposits at 70 cm, 94 cm, and 99 cm. It is possible that occurrences of abundant, very well-preserved valves in sandy mud at 63 cm, including numerous occurrences of multiple valves still attached in chains, may be evidence for rapid deposition and preservation by the N4 tsunami.

Core 33B: number of P. sulcata counted

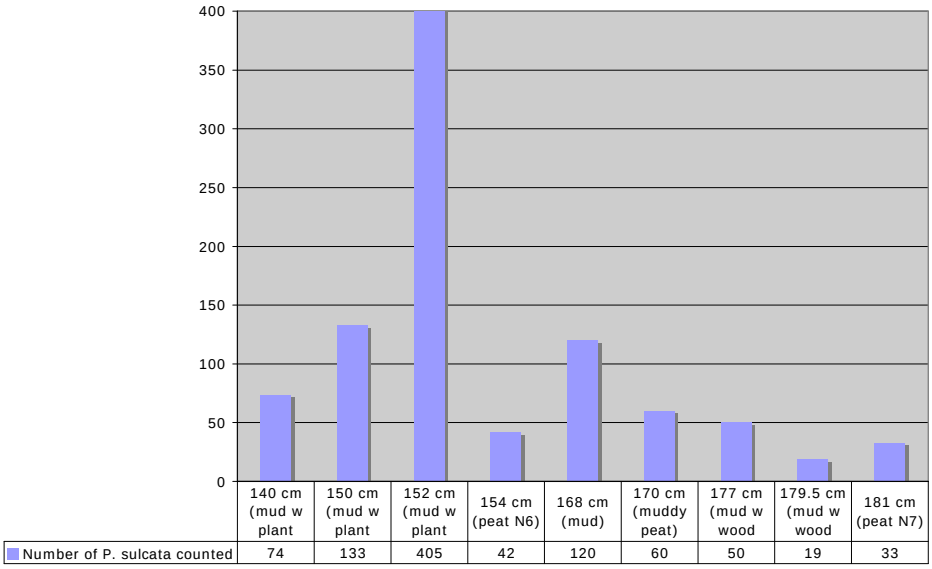

	140 cm (mud w plant	150 cm (mud w plant	152 cm (mud w plant	154 cm (peat N6)	168 cm (mud)	170 cm (muddy peat)	177 cm (mud w wood	179.5 cm (mud w wood	181 cm (peat N7)
Number of P. sulcata counted	74	133	405	42	120	60	50	19	33

Core 33B: estimated abundance of Paralia sulcata (valves/cc of sediment)

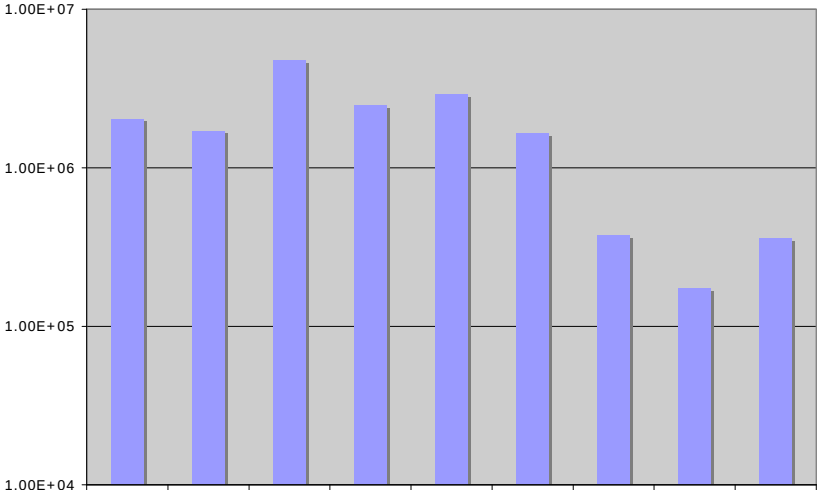

	140 cm (mud w plant frags)	150 cm (mud w plant frags)	152 cm (mud w plant frags)	154 cm (peat N6)	168 cm (mud)	170 cm (muddy peat)	177 cm (mud w wood frags)	179.5 cm (mud w wood frags)	181 cm (peat N7)
Concentration of P. sulcata	2.04E+06	1.71E+06	4.77E+06	2.48E+06	2.91E+06	1.65E+06	3.75E+05	1.74E+05	3.58E+05

Core 33B: *P. sulcata* is present in all samples. The count of 405 valves at 105 cm, in the mud capping peaet N6, shows that *P. sulcata* is substantially more common than other diatoms in the sample (that is, 405 *P. sulcata* valves were counted before a total of at least 100 other diatoms were counted). Specimens of *P. sulcata* are mostly represented by large valves in this sample, as well as the next higher mud sample at 150 cm. In contrast, although *P. sulcata* is also a prominent component in the underlying peat N6, it is mainly represented by <u>small</u> valves (< 15 µm diameter). The significance of this is equivocal, but perhaps warrants further investigation.

APPENDIX B
Diatom taxa organized into general salinity groups.
Upton Slough Cores 25 and 33 (sections A & B)

Group 1: fresh or fresh-brackish diatoms

Achnanthes hungarica
Amphora libyca
Aulacoseira italica (planktonic)
Cocconeis placentula
Cymbella affinis
Cymbella aspera
Cymbella elginensis
Cymbella pusilla
Cymbella silesiaca
Cymbella sinuata
Cymbella sp.
Denticula subtilis
Diadesmis contenta
Diploneis ovalis
Eunotia formica
Eunotia minor
Eunotia pectinalis
Fragilaria construens
Fragilaria martyi
Fragilaria pinnata
Gomphonema acuminatum v. turris
Gomphonema angustatum
Gomphonema parvulum
Gomphonema pseudoaugur
Navicula lapidosa
Navicula perminuta
Navicula rhyncocephala
Navicula vaneei
Nitzschia aff. Pusilla
Nitzschia palea
Nitzschia pusilla
Nitzschia terrestris
Pinnularia borealis
Pinnularia gibba
Pinnularia major
Pinnularia microstauron
Pinnularia viridis
Placoneis elginensis
Placonneis elginensis v. cuneata
Planothidium lanceolata
Rhoicosphenia abbreviata
Sellaphora americana
Sellaphora bacillum
Stauroneis obtusa
Synedra ulna
Tabellaria flocculosa (planktonic)

Group 2: brackish-fresh diatoms

Amphora coffeiformis
Caloneis bacillum
Cocconeis neothumensis
Cosmioneis pusilla
Diploneis interrupta
Diploneis pseudovalis
Diploneis smithii rhombica
Epithemia turgida
Fragilaria subsalina
Frustulia rhombica
Frustulia vulgaris
Gyrosigma spenceri
Luticola mutica
Luticula muticoides
Navicula cincta
Navicula cryptocephala
Navicula meniscus
Navicula peregrina
Navicula peregrinopsis
Navicula phylleptosoma
Nitzschia capitellata
Nitzschia commutata
Nitzschia commutoides
Nitzschia fasciculata
Nitzschia inconspicua
Nitzschia scapelliformis
Nitzschia sigma
Nitzschia sp. Cf. Dissipata
Pinnularia aff. C. bacillum
Pinnularia lagerstedtii
Planothidium delicatula
Planothidium haukiana
Pseudostaurosira perminuta
Rhopalodia brebissonii
Tryblionella debilis

APPENDIX B
Diatom taxa organized into general salinity groups.
Upton Slough Cores 25 and 33 (sections A & B)

Group 3: brackish-marine or marine diatoms

Achnanthes brevipes v. intermedia
Actinocyclus sp.
Actinoptychus senarius
Actinoptychus splendens
Amphora marina
Bacillaria paradoxa
Biddulphia aurita
Biremis lucens
Caloneis aemula
Caloneis brevis
Caloneis westii
Campylodiscus bicostatus
Campylodiscus clypeus
Catenula adhaerens
Ceratalus turgidus
Chaetoceros spp.
Chamaepinnularia clamans
Cocconeis distans
Cocconeis peltoides
Cocconeis scutellum
Coscionodiscus sp.
Delphineis karstenii
Delphineis surirella
Dimeregramma minor
Diploneis bombus
Endictya hendeyi
Fallacia cryptolyra
Fallacia forcipata
Fallacia pygmaea
Fragilaria investiens
Gyrosigma balticum
Gyrosigma eximium
Hyalodiscus scoticus
Mastogloia exigua
Navicula digitoradiata
Navicula normalis
Navicula ramosissima
Nitzschia bilobata
Nitzschia dissipata
Nitzschia dubia
Nitzschia frustulum
Nitzschia lanceola
Nitzschia sigma
Opephora guenter-grassi
Opephora olsenii/mutabilis
Opepora marina
Paribellus berkeleyi
Parlibellus delognei
Pinnuavis (Navicula) elegans
Plagiogramma staurophorum
Planothidium delicatula
Planothidium haukiana
Rhabdonema arcuatum
Rhaphoneis psammicola
Scoliotropis tumida
Seminavis sp. "Atwaterii"
Stephanodiscus spp.
Synedra fasciculata
Thalassionema nitzschioides
Thalassiosira cf. Pacifica
Thalassiosira eccentrica
Trachysphenia aspera
Tryblionella coarctata
Tryblionella granulata
Tryblionella levidensis
Tryblionella littoralis
Tryblionella panduriformis
Tryblionella vexans

APPENDIX C
Diatom taxa assigned to general paleoenvironmental groups based on empirical observations of modern taxa in estuaries of the Pacific Northwest.
Upton Slough Cores 25 and 33 (sections A & B)

FW marsh/swamp diatoms

Eunotia formica
Eunotia minor
Eunotia pectinalis
Fragilaria construens
Pinnularia borealis
Pinnularia gibba
Pinnularia major
Pinnularia microstauron
Pinnularia viridis
Placoneis elginensis
Placonneis elginensis v. cuneata

Typical high salt marsh taxa

Cosmioneis pusilla
Denticula subtilis
Diadesmis contenta
Diploneis pseudovalis
Navicula cincta
Nitzschia terrestris
Pinnularia lagerstedtii

Typical low marsh taxa**

Caloneis bacillum
Caloneis westii
Diploneis interrupta
Diploneis smithii rhombica
Gyrosigma eximium
Luticola mutica
Mastogloia exigua
Navicula digitoradiata
Nitzschia fasciculata
Nitzschia scapelliformis
Tryblionella debilis

****Most taxa in the low marsh category are also commonly found on tidal flats; tube-dwelling taxa like G. eximium and M. exiqua probably most indicative of the low marsh.**

Planktonic and tychoplanktonic taxa

Actinocyclus sp.
Actinoptychus senarius
Actinoptychus splendens
Chaetoceros spp.
Coscionodiscus sp.
Delphineis karstenii
Odontella aurita
Stephanodiscus spp.
Thalassionema nitzschioides
Thalassiosira cf. decipiens
Thalassiosira cf. dacifica
Thalassiosira eccentrica

Tidal flat taxa (*=epipsammon)

Achnanthes brevipes
Achnanthes brevipes v. intermedia
Amphora marina
Bacillaria paradoxa
Campylodiscus bicostatus
Campylodiscus clypeus
*Catenula adhaerens**
*Ceratalus turgidus** (>40 µm)
*Cocconeis neothumensis**
*Cocconeis peltoides**
Cocconeis scutellum
Delphineis surirella
*Dimeregramma minor**
Endictya hendeyi
Fallacia cryptolyra
Fallacia forcipata
Fallacia pygmaea
*Fragilaria schulzii**
Fragilaria subsalina
Fallacia forcipata
Fallacia pygmaea
*Fragilaria schulzii**
Fragilaria subsalina
Gyrosigma peisonis
Hyalodiscus scoticus
Nitzschia sigma
*Opephora guenter-grassi**
*Opephora olsenii/mutabilis**
*Opepora marina**
Pinnuavis (Navicula) elegans
*Plagiogramma staurophorum**
*Planothidium delicatula**
Planothidium haukiana
*Rhabdonema arcuatum**
*Rhaphoneis psammicola**
Scoliotropis tumida
Synedra fasciculata
Trachysphenia aspera
Tryblionella coarctata
Tryblionella granulata
Tryblionella levidensis
Tryblionella littoralis